DEPARTMENT OF NATIONAL RESOURCES

BUREAU OF MINERAL RESOURCES, GEOLOGY AND GEOPHYSICS

Record 1978/32

PRECAMBRIAN GEOLOGY OF THE WESTMORELAND REGION, NORTHERN AUSTRALIA

PART III: NICHOLSON GRANITE COMPLEX AND MURPHY METAMORPHICS

by

C.M. Gardner

Record 1978/32

PRECAMBRIAN GEOLOGY OF THE WESTMORELAND REGION, NORTHERN AUSTRALIA
PART III: NICHOLSON GRANITE COMPLEX AND MURPHY METAMORPHICS

by

C.M. Gardner

CONTENTS

Tables

Figures

(iii)

Plate

4

SUMMARY

The Nicholson Granite Complex and Murphy Metamorphics, together with the Cliffdale Volcanics, form the Murphy Tectonic Ridge, an east-northeast-trending belt 150 km long and up to 25 km wide, which occupies part of the southern portions of the Calvert Hills and Westmoreland 1:250 000 Sheet areas. The Tawallah Group unconformably overlies the largely granitic basement ridge on its northwestern side, and the Fickling and South Nicholson Groups are faulted against its southern side.

Five major and two minor phases have been distinguished within the granite complex. The main phases are Egn_1, Egn_2, Egn_5, Egn_6, and Egn_8. Egn_1 and Egn_2 - which are coarse-grained prophyritic hornblende-microcline-albite and albite-microcline granites, respectively, and locally carry abundant mafic xenoliths - crop out in the central and southeastern parts of the complex. The albite-microcline granite is intruded in the north by Egn_5 and Egn_6, medium even-grained albite-microcline granites, and in the west by medium to fine even-grained muscovite granite, Egn_8. The minor phases are Egn_{3-4} and Egn_7. Egn_{3-4} includes granodiorite ring dykes and stocks, and Egn_7 is microgranite associated mainly with Egn_5.

Poor exposure and preservation of the granite and metamorphics make it difficult to establish contact relations, especially within the older parts of the Nicholson Granite Complex. Contacts of the younger, high-level granites of the complex, Egn_5, Egn_6, Egn_7, and Egn_8, with the Cliffdale Volcanics, are well exposed and are intrusive. Egn_{3-4} intrudes the Murphy Metamorphics. Contacts between Egn_1 and the Cliffdale Volcanics are poorly exposed, and, on the basis of geochronological data, Egn_1 is older than the volcanics. Although Egn_2 intrudes Cliffdale Volcanics, it is not geochronologically distinguishable from Egn_1, and may include rocks of various ages.

It is concluded that late-stage recrystallisation in the presence of an intergranular fluid, and extensive post-crystallisation silicification, have variably modified the texture of the granites - e.g., by producing K-feldspar phenocrysts and replacing feldspars and mafics with quartz.

Compared with average granites, all the granites of the Nicholson Granite Complex are distinguished by high K_2O, high total Fe, and low U, W, and Sn. Major and minor element chemical trends are consistent with increasing

5

degrees of fractionation from $Egn_{1,2}$ to $Egn_{5,6}$ - i.e., from the southeastern part of the Murphy Tectonic Ridge northwards and eastwards. Egn_8 is enriched in alkalis relative to normal granites, and to Egn_5 and Egn_6.

Metamorphism within the Murphy Tectonic Ridge is restricted to low-grade contact hornblende hornfels effects in the volcanics along some contacts between granite and Cliffdale Volcanics.

The structure of the granite complex is dominated by primary east-northeast trends running parallel to the northern boundary of the Murphy Tectonic Ridge and by younger northwest trends related to the Calvert Fault. These trends are defined by abundant airphoto-lineaments, quartz veins, quartz feldspar porphyry dykes, and faults; displacement along the faults appears to have been restricted largely to vertical movement. Points of intersection of the two structural systems connect and form north-south lineaments; the best-developed secondary trend runs through the Crystal Hill area, where the greatest concentrations of greisen zones, quartz veins, and Sn, W, U, and Cu mineralisation occur. Minor mineralisation is localised along the intersections of faults.

Extensive erosion has removed an estimated 10 000 m from above the upper part of the complex.

I INTRODUCTION

The Nicholson Granite Complex derives its name from the Nicholson River, which rises on the eastern side of the Barkly Tableland and flows across the northern end of the border between Queensland and the Northern Territory, and enters the Gulf of Carpentaria north of Burketown (see Fig. 2). The complex crops out in the southwestern corner of the Westmoreland 1:250 000 Sheet area and in the southeastern part of the adjacent Calvert Hills 1:250 000 Sheet area. The Nicholson Granite Complex, the Murphy Metamorphics, the Cliffdale Volcanics, and what has previously been known as the Norris Granite form the Murphy Tectonic Ridge (MTR). The MTR is basement to the sediments of the McArthur Basin, which overlies the MTR in the northwest, and to the sediments of the South Nicholson Basin and the Lawn Hill Platform, which overlie the MTR in the south. The stratigraphic relations are summarised in Figure 2. The ridge forms a belt trending east to northeast about 150 km long and up to 25 km wide.

The regional geology and the geology of the cover rocks of the MTR have been described by Sweet & Slater (1975); the Cliffdale Volcanics have been described by Mitchell (1976).

The MTR may be subdivided into three sections. A poorly exposed western inlier of granite and metamorphic rocks crops out within the Nicholson River and Coanjula 1:100 000 Sheet areas in a roughly circular area 25 km in diameter. The central section of the MTR crosses the Seigal and Hedleys Creek* 1:100 000 Sheet areas as far east as the Calvert Fault (see Plate 1): it consists of granite with some acid volcanics in the northern part and a few small roof pendants of Murphy Metamorphics in the southern part. The northeastern section of the MTR lies north of the Calvert Fault, and consists of acid volcanics and granite. This study is restricted almost entirely to the central and northeastern sections of the MTR.

Granite forms a topographic low between steep scarps of the Westmoreland Conglomerate to the north and ridges of the Fish River Formation and Fickling Group to the south. Outcrop ranges from poor to non-existent in the western part of the area - i.e., from the Sheet area boundary to around the Fish River (Plate 1). Exposure is generally restricted to silicified or contact zones, and the granite is invariably extremely weathered, occurring as bleached kaolinised hummocks. Most of the area is covered by a

thin loose granite gravel composed mainly of sericitised feldspar with minor quartz. The area between the Fish River and Pandanus Creek (Plate 1) is a nearly featureless plain covered by reddish-white coarse unconsolidated gravel consisting of feldspar and quartz. The grainsize of the gravel ranges from 0.2 to 4 cm; shallow soil profiles are developed in creek banks. Outcrop is scarce and apparently structurally controlled, occurring as discontinuous bouldery ridges along fault zones, as low benches, and as sporadic corestones. The corestones are usually quite fresh - e.g., in the Rocky Creek area; 6 km south of Crystal Hill; the area around the middle reaches of Pandanus Creek (Fig. 1a); and the area northeast of the confluence of the Fish River and Tin Hole Creek, where the granite is in contact with Cliffdale Volcanics and Murphy Metamorphics.

North of these areas - i.e., in the area shown on the Calvert Hills Sheet as Norris Granite (Roberts, Rhodes, & Yates, 1963) - relief is greater, and outcrop is much more common. A dense reticulate pattern of fault zones, alteration zones, quartz veins, porphyry dykes, and outcrops of volcanics has retarded erosion of the granite so that outcrop is usually more than about 60 percent. Much of this granite has been silicified by the replacement of primary minerals by quartz. The airphoto-pattern in this area is more typical of granite terrains: low, white, jointed, coarsely etched hummocks predominate.

The first geological investigations of the Calvert Hills and Westmoreland 1:250 000 Sheet areas were made by Gregory (1861), who noted the occurrence of granite and sandstone in the headwaters district of the Nicholson River. Jensen (1941) considered that the 'granite porphyries' near the Northern Territory/Queensland border were laccolithic intrusions into the Cliffdale Volcanics, with which they were comagmatic and coeval. The Westmoreland 1:250 000 Sheet area was mapped by joint Bureau of Mineral Resources (BMR) and Geological Survey of Queensland (GSQ) parties as part of the 1950-1954 program of systematic mapping of the mineral belt of northwestern Queensland. The results of this work are contained in Carter, Brooks, & Walker (1961), who considered the Nicholson Granite to be possibly Lower Proterozoic, intrusive into the Cliffdale Volcanics, and consisting of two

---

* Preliminary-edition 1:100 000 geological maps of the Seigal and Hedleys Creek Sheet areas are available on request at the Bureau of Mineral Resources, Canberra, for $1 each.

Fig. 1a Bgn$_2$ pavement near Pandanus Creek
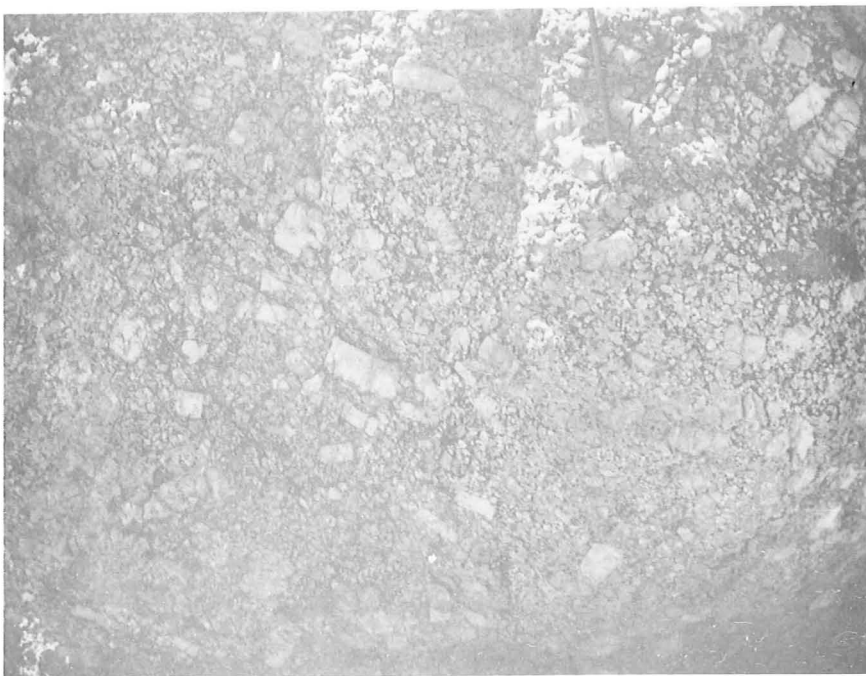
Fig. 1b. Subparallel alignment of K-feldspar phenocrysts in Bgn$_2$ boulder

lithologies - a coarse-grained pinkish-grey granodiorite and a massive porphyritic red quartz-mica diorite.

BMR started the systematic mapping of the Calvert Hills Sheet area in 1959, following an upsurge in interest in the area as a result of the discovery of uranium at Pandanus Creek in 1958. Firman (1959) described the Nicholson Granite from the Calvert Hills Sheet area as being intrusive into the Cliffdale Volcanics and including the following types: coarse-grained granite, biotite-actinolite tonalite, tin-bearing quartz-biotite greisen, biotite granite, and hornblende-biotite granite. These lithologies, as well as those given by Carter and others (1961), correspond roughly to some of the subdivisions recognised in the present work, but the relations among them were not clarified by Firman or Carter and others. Firman also noted the occurrence of roof pendants of quartz-plagioclase-biotite schist and of dacite xenoliths derived from the Cliffdale Volcanics.

Further mapping of the Calvert Hills Sheet area in 1961 as part of a BMR program to map the Carpentaria Upper Proterozoic Province (Roberts, unpubl. ms)*, led to the recognition that parts of the Nicholson Granite were probably older than the Cliffdale Volcanics, and to the subsequent subdivision into the Norris Granite (intruding the Cliffdale Volcanics) and the Nicholson Granite (overlain by the volcanics; Roberts and others, 1963). Roberts and others (1963) also named and described the Murphy Metamorphics - the roof pendants of schist previously described by Firman (1959). The main lithology of the Nicholson Granite was given as coarse-grained porphyritic biotite granite. Two phases were distinguished within the Norris Granite: an earlier medium-grained biotite granite/adamellite and a later finer-grained leucocratic granite. Differences in grainsize and lithology within the first phase were attributed to different cooling rates. Roberts and others (1963) considered the Norris Granite and the Cliffdale Volcanics to be comagmatic.

The Nicholson Granite Complex is bounded non-conformably in the north by the Westmoreland Conglomerate, which dips steeply (average 70°) to the northwest, and forms a sharp strike ridge called the China Wall (Plate 1). Along the contact the granite is exposed to within a few metres of the top of the scarp, indicating that the granite was extensively eroded both before and after the conglomerate was deposited. Farther to the northeast, the conglo-

---

* held in BMR by K.A. Plumb

merate unconformably overlies the Cliffdale Volcanics. At its southern margin the complex is faulted against the Fickling and South Nicholson Groups in the west, and is non-conformably overlain by the Wire Creek Sandstone.

II   FIELD RELATIONS AMONG THE MAJOR UNITS COMPRISING THE MURPHY TECTONIC RIDGE
(see rock relations diagram, Plate 1)

The oldest rocks in the MTR are schists and migmatites of the Murphy Metamorphics. Strongly cleaved and weakly to strongly foliated quartz-albite-muscovite-biotite schists crop out east of Fish River (e.g., S900230)*. The dip of the regional foliation ranges from vertical to steeply northwards; the strike is roughly east-west - i.e., it is slightly inclined to the major east-northeast faults in the granites.

The Murphy Metamorphics are intruded along their northern boundary by Pgn_{3-4}- coarse-grained porphyritic granodiorite. Within about 0.5 km of the contact the granodiorite carries abundant xenoliths of the metamorphics, and is foliated concordantly with them. The foliation is defined by the subvertical parallel alignment of red K-feldspar and plagioclase phenocrysts. Nearer the contact, the quartzofeldspathic minerals form even-grained bands, and the mafic xenoliths become more elongate and merge into continuous biotite-rich bands. Here migmatitic rocks, consisting of segregated muscovite, quartzofeldspathic, and biotite-rich bands, form the contact zone which gradually becomes more and more schistose as the granitic bands lens out - i.e., mafic bands of Murphy Metamorphics are progressively broken up into xenoliths, and then assimilated, as distance from the contact increases.

The uncontaminated granite Pgn_1 is a coarse-grained, biotite and hornblende-rich massive white granite containing xenoliths. It is apparently overlain by Cliffdale Volcanics in the Fish River area, and is intruded by a granite, Pgn_2, distinguished from Pgn_1 mainly by its significantly lower mafic mineral content; this granite crops out extensively in the southeastern and central parts of the MTR. The contact between Pgn_1 and Pgn_2 is not sharp, and the ranges of ages of the two overlap (see Table 1). However, an

---

*Such numbers are grid references based on grid lines at 1000 m intervals. S = Seigal 1:100 000 Sheet area. The first three digits are the easting; the last three are the northing.

*HC = Hedleys Creek 1:100 000 Sheet area
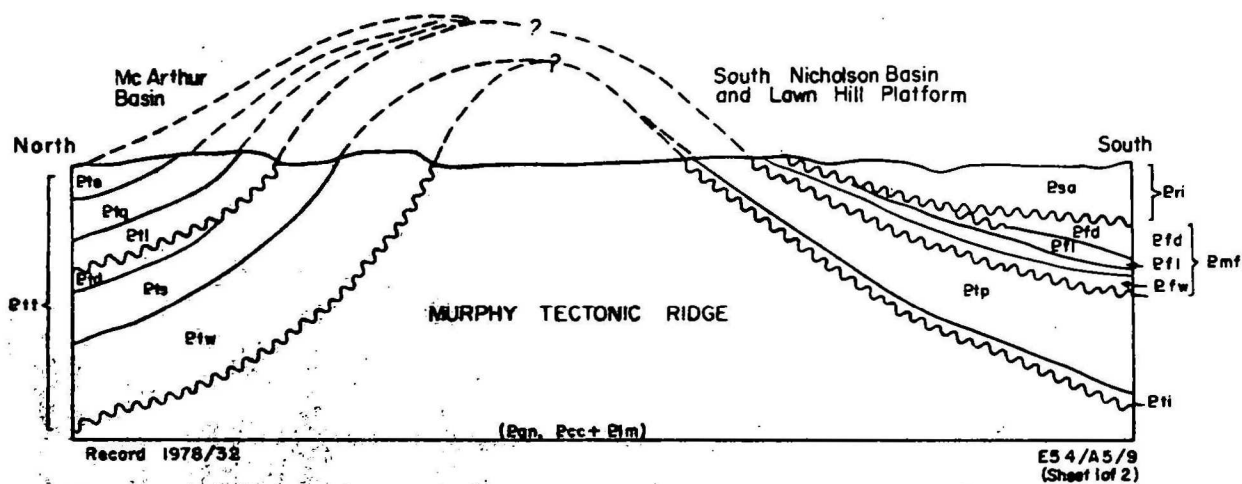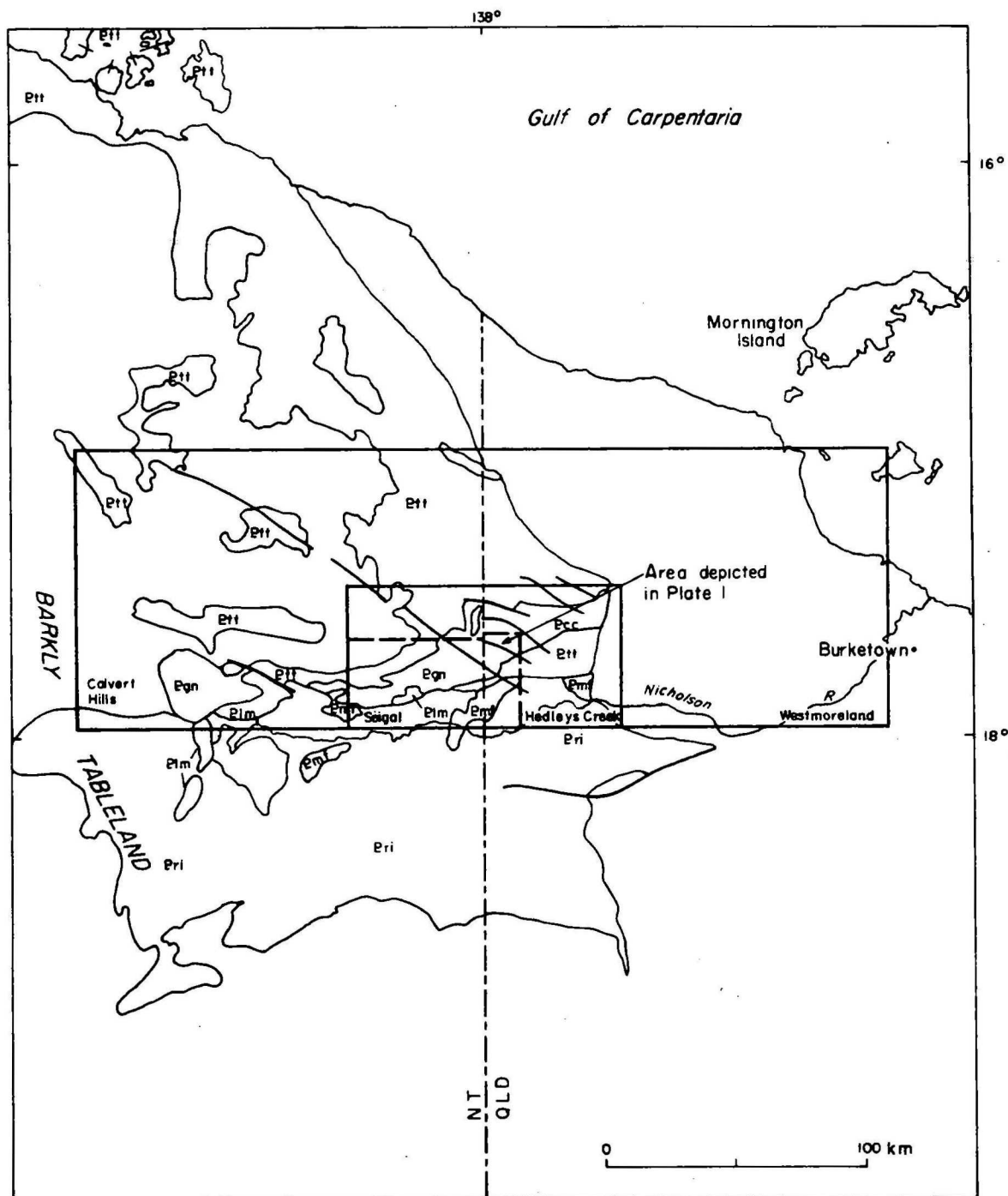
Fig. 2. Geology and diagrammatic relations between the Murphy Tectonic Ridge and overlying units

SOUTH NICHOLSON BASIN

SOUTH NICHOLSON GROUP (Pri)

Constance Sandstone
Psa

Adelaidean

McARTHUR BASIN

TAWALLAH GROUP (Ptt)

Masterton Fm Pth, Ptg

Wollogorang Fm Pto

Settlement Creek Volcanics
Pte

Aquarium Formation
Ptq

Sly Creek Sandstone
Ptl

McDermott Formation
Ptd

Seigal Volcanics
Pts

Westmoreland Conglomerate
Ptw

Murphy Tectonic Ridge

FICKLING GROUP (Pmf)

LAWN HILL PLATFORM

Doomadgee Formation
Pfd

Mount Les Formation Pfl

Walford Dolomite
Pfw

Fish River Formation
Ptf

Peters Creek Volcanics
Ptp

Wire Ceek Sandstone
Pti

Murphy Tectonic Ridge

Carpentarian

intrusive relation between them is deduced from the fact that Egn_2 intrudes recrystallised Cliffdale Volcanics in the Pandanus Creek area whereas Egn_1 is apparently overlain by Cliffdale Volcanics in the Fish River area.

Egn_1 and Egn_2 are intruded by red even-grained granites Egn_5 and Egn_6, microgranite Egn_7, and white muscovite granite Egn_8. Granodiorite and microgranodiorite ring dykes and stocks (Egn_{3-4}) of various ages intrude the older granites along their contacts with the younger phases.

Egn_5 is in contact with Cliffdale Volcanics along a boundary north of the abandoned tin-processing plant at S986377 eastwards to the Calvert Fault. This contact is well exposed, and appears to have been a passive intrusive contact, although field and petrographic characteristics of Egn_5 indicate that it is a high-level intrusion. The evidence for the high-level nature of Egn_5 is given in a later section, and is only summarised here. The association of dykes and volcanics with Egn_5, the absence of a metamorphic aureole, the abundance of microgranite, and the presence of graphic intergrowths, indicate that Egn_5 crystallised in a subvolcanic environment (Buddington, 1959). Typically, such granites intrude forcibly, and with considerable disruption to the country rock. The non-violent origin of this contact, however, is indicated by its subhorizontal, subconcordant disposition - bedding in the volcanics having been only slightly disturbed from horizontal - and the absence of volcanic xenoliths. This suggests that intrusion proceeded by means of laminar flow, rather than vertical injection (Mehnert, 1968). Very low-grade contact metamorphism is evident in the volcanics near the granite. The main contact effect was the recrystallisation and oxidation of the volcanic groundmass along a zone several metres wide; the latter effect is recognisable in the field as a change in colour in the volcanics from bluish black to reddish brown nearer the contact with the granite. The volcanics north of this contact crop out in a wedge-shaped area truncated on its northeastern edge by the Calvert Fault and overlain in the west by the Westmoreland Conglomerate. Several granite inliers occur within the wedge, usually as flat-topped pod-like masses, capped by volcanic rubble.

Similar contact relations are visible east of the Calvert Fault; only minor contact-metamorphic effects are obvious in the country rocks, and the narrow contact aureole is usually not evident. The contact is well exposed at S158365 where bluish-black ignimbrite is recrystallised, and xeno-

liths still recognisable as ignimbrite are common in the granite near the contact. Recrystallisation of the originally glassy groundmass and the development of biotite are the main contact effects; the presence of re-crystallised green-brown hornblende and biotite replacing dark brown micro-phenocrysts of these minerals indicates hornblende hornfels facies meta-morphism. Quartz veins and pegmatites are rare.

Volcanic xenoliths occur rarely in the granite. At HC965420*, blocks of grey medium-grained porphyritic acid volcanic within Pgn_2 contain feldspar phenocrysts, lithic fragments, and altered pumice. Minor quartz veins and bipyramidal quartz crystals stand out on pitted weathered surfaces, and a vague flow foliation also remains.

Contacts of the older part of the Nicholson Granite Complex with the Cliffdale Volcanics are poorly exposed, and the relations not clear. About 4 km north of the confluence of the Fish River and Tin Hole Creek, volcanics similar to the Cliffdale Volcanics unit 4c (red rhyolite) are in contact with Pgn_1 and Pgn_{3-4}. This contact was thought to be unconformable by Roberts and others (1963). The volcanics crop out as small isolated cappings of dense finely parallel-laminated red rhyolite within Pgn_{3-4}, which is contaminated as a result of intrusion into and part assimilation of mica schist of the Murphy Metamorphics. Contacts between granite and volcanics are exposed at several localities, and are generally subhorizontal, although some are steeper - e.g. at S917247 the contact dips south at about 75°.

The rhyolite is everywhere recrystallised in this area, possibly as a result of thermal metamorphism accompanying granite intrusion. If this interpretation is correct, the volcanics are older than the granite Pgn_1. The Fish River rhyolite is assigned to the Cliffdale Volcanics as it is similar to Pcc unit 4c. However, it may be the sole remaining exposed product of earlier extrusive activity intruded by Pgn_1 in the Fish River area. From the relative ages of the Cliffdale Volcanics (1770 m.y.) and Pgn_1 (1860 m.y.; Webb, 1975), the Cliffdale Volcanics, as defined from other areas, are assumed to be younger than Pgn_1.

---

* Pgn_{3-4} will be shown on the Seigal and Hedleys Creek 1:100 000 first-edition geological maps as Pgn_4.

III GEOCHRONOLOGY

The Nicholson and Norris Granites were isotopically dated as part of the Carpentaria Project (McDougall and others, 1965). Follow-up dating was done by Webb (1973, 1975) to clarify uncertainties in the earlier results. The data from the three projects are summarised in Table 1 and the sample localities are shown in Plate 1. The Cliffdale Volcanics are well dated at 1770 m.y. $\pm$ 20 m.y. (Webb, 1973).

McDougall and others (1965) determined the average age of Nicholson Granite samples as 1815 m.y., and of the Norris Granite samples as 1790 m.y. The authors pointed out, however, that the ranges of ages for the two granites overlap: Nicholson Granite ages range from 1790 m.y. to 1840 m.y., and Norris Granite ages range from 1760 m.y. to 1825 m.y. Furthermore the spread in measured age was greater than the experimental error. McDougall and others concluded that the average ages of the Nicholson and Norris Granites were experimentally indistinguishable.

The bimodal distribution of ages, with peaks at 1830 and 1770 m.y., indicated by this work, however, was shown to be real by Webb (1973), who determined two experimentally distinct whole-rock isochrons as listed in Table 1. Although the samples were initially divided into the Nicholson and Norris Granites as defined by Roberts and others (1963), the final isochrons have incorporated some regrouping in order to achieve the best experimental results. If the four Nicholson Granite samples (yielding an age of 1843 $\pm$ 83 m.y.) are included in the Norris Granite regression (1773 $\pm$ 24 m.y.) the isochron is greatly distorted; there is also a significant difference in initial Sr^{87}/Sr^{86} ratios between the two groups (see below).

Initial Sr^{87}/Sr^{86} ratios of the two isochrons are as follows:

Nicholson Granite: initial Sr^{87}/Sr^{86} = 0.7069 $\pm$ .0040

Norris Granite: initial Sr^{87}/Sr^{86} = 0.7178 $\pm$ .0038

The high initial Sr^{87}/Sr^{86} ratio of the Norris Granite relative to that of the Cliffdale Volcanics (0.7078 $\pm$ 0.0017; Webb, 1973) suggests that the two are not as closely genetically related as suggested by Roberts and others (1963).

Isotopic dating carried out in the course of the present investigation (Webb, 1975) confirms that there is granite older than the Cliffdale Volcanics, but indicates that not all of the granite mapped as Nicholson Granite by Roberts and others (1963) is older than the Volcanics.

The mapping shows that some areas mapped as Nicholson Granite by Roberts and others (1963) are now recognised as intrusive into Pgn_1 and Pgn_2, and are probably younger than the Cliffdale Volcanics. Thus the division into Nicholson and Norris Granites does not correspond to a division into older and younger granite. It is therefore proposed to discontinue the use of the term Norris Granite in favour of Nicholson Granite Complex to include both granites.

IV NOMENCLATURE

The granites of the Nicholson Granite Complex are classified according to their relative modal proportions of quartz (Q), albite + orthoclase (Ab + Or), and anorthite (An), using the terminology of Streckeisen (1973).

Although all the granites fall in two fields of Streckeisen's scheme - 'alkali-feldspar granite' and 'granite' - they show marked differences with respect to relative proportions of Ab and Or, and abundance and relative proportions of mafic minerals. Hence, where these features are considered significant, qualifiers have been added to the root name - e.g., granites containing at least 20 percent hornblende are referred to as hornblende granites.

The colour term used in the lithological descriptions refers to the hand specimen colour of the quartzofeldspathic minerals. The prefix 'leuco' indicates a colour index of less than 10% M, where M refers to the volume percent of mafic and related minerals (mica, amphibole, pyroxene, apatite, sphene, carbonate, etc.).

Grainsizes are determined from the following scheme:-

coarse-grained	:	> 3 mm average grain diameter
medium-grained	:	1-3 mm average grain diameter
medium-fine-grained	:	0.3 - 1 mm average grain diameter
fine-grained	:	0.05 - 0.3 mm average grain diameter

Table 1

Summary of geochronology of Nicholson Granite

Complex

Sample no.			Egn no.	Dating method	Age	Reference
72100025	)		6)			
0026	)		6)	Rb-Sr multiple rock	1843 ± 83 m.y.	Webb (1973)
0047	)		1)	isochron		
0046	)	same	1)			
GA 125[2]	)	locality[3]	1	K-Ar, biotite	1840	McDougall and others 1961
74760227			2	Rb-Sr[1]	1860 ± 103 m.y.	Webb (1975)
GA 159			2	K-Ar, biotite	(1820 ((1830	McDougall and others (1965)
GA 581			8	K-Ar, hornblende	1815	McDougall and others (1965)
GA 559			8	(K-Ar muscovite	1790	"
				((Rb-Sr	1770	"
74760226			8	Rb-Sr	1773 ± 56 m.y.	Webb (1975)
GA 484	)	same	2	)K-Ar, biotite	1780	McDougall and others (1965)
72100027	)	locality	2)			
0123	)		2)			
0020	)		5)			
				) Rb-Sr multiple rock	1773 ± 24 m.y.	Webb (1973)
0021	)		5)			
				) isochron		
0022	)		5)			
0045	)		5)			
0122	)		5)			
0024	)		5)			
GA 558	)		2)			
74760222			5	Rb-Sr	1776 ± 54 m.y.	Webb (1975)
GA 483 (same locality as 0122)			5	K-Ar, biotite	1760	McDougall and others (1965)
74760225			7	Rb-Sr	1705-1738 m.y.	Webb (1975)

1. Unless otherwise indicated, Rb-Sr isochrons are based on whole-rock data from a series of samples from a single locality.

2. Sample numbers prefixed GA are ANU sample numbers.

3. All sample localities are shown in Plate 1.

Other textural terms are used in the sense defined by Joplin (1971).

'Non-conformity' is used to express the relation between a sedimentary sequence overlying older igneous rocks (AGI, 1972).

V SUBDIVISION OF THE NICHOLSON GRANITE COMPLEX AND THE RELATIONS AMONG THE GRANITES

In this report, the Nicholson Granite Complex is subdivided into seven phases, Egn_1, Egn_2, Egn_{3-4}*, Egn_6, Egn_7, and Egn_8. The subdivision is mainly lithological and chemical, rather than geochronological, as age relations, particularly among the small intrusions, are uncertain. Thus, plutons separated from each other have been grouped on the basis of similar lithology and chemistry.

Distinguishing characteristics of each granite and the relations among them are summarised in Table 2.

Egn_1 is a white coarse-grained porphyritic hornblende-biotite-microcline-albite granite, distinctive in its high proportion of mafic minerals and in its euhedral K-feldspar phenocrysts. Egn_1 is probably overlain by the Cliffdale Volcanics, and is at least 1840 m.y. old. Egn_1 is thus one of the oldest phases of the complex.

Egn_2 is a porphyritic albite-microcline granite, but is younger and more fractionated than Egn_1. Egn_2 apparently intrudes the Cliffdale Volcanics along one of its contacts, but may include granite of a range of ages, some of which may be older than the Cliffdale Volcanics (see Geochronology).

Egn_1 and Egn_2 have similar textures, in which euhedral K-feldspars are surrounded by an hypidiomorphic granular groundmass of albite, quartz, and mafic minerals. This texture is contrasted with the texture of Egn_5 and Egn_6, in which K-feldspar does not form phenocrysts and is intergrown with the other minerals.

---

* Egn_{3-4} will be shown on the Seigal and Hedleys Creek 1:100 000 first-edition geological maps as Egn_4.

19

Egn_{3-4} is a grouping of lithologically and chemically identical hornblende granodiorites of different ages. Red coarse-grained granodiorites occur as ring dykes along margins of plutons, and are cut by smaller fine-grained melanocratic granodiorite dykes. The best-exposed dyke intrudes the Murphy Metamorphics, and is intruded by Egn_1. Other dykes intrude Egn_2, Egn_5, Egn_6, and the Cliffdale Volcanics, however, indicating that granodiorite ring dyke intrusion continued to at least 1770 m.y. Egn_{3-4} is petrographically similar to Egn_1 but is less fractionated.

Egn_5, Egn_6, Egn_7, and Egn_8 as a group are distinguished from Egn_1, Egn_2 and Egn_{3-4} by their more fractionated chemistry and absence of phenocrystic K-feldspar. All are coeval with or younger than the Cliffdale Volcanics. Egn_5 is red even-grained biotite-albite-microcline granite. Egn_6 is red even-grained albite-microcline leucogranite; Egn_7 is microgranite; and Egn_8 is white aplitic muscovite-bearing microcline-albite granite. The common occurrence of greisen and aplite dykes associated with Egn_5, Egn_6, and Egn_8 indicates high-level crystallisation for these younger granites. Muscovite pegmatites occur within Egn_8.

VI DESCRIPTION OF UNITS

MURPHY METAMORPHICS

The main exposures of the Murphy Metamorphics lie in the Nicholson River 1:100 000 Sheet area, immediately to the west of the Seigal 1:100 000 Sheet area. Exposure in both Sheet areas is too poor to permit determination of thickness of the unit or establishment of a type area.

Stratigraphic relations

The Murphy Metamorphics are the oldest rocks in the Westmoreland region; they are at least 1900 m.y. and possibly 2100 m.y. old (Plumb & Derrick, 1975). The Murphy Metamorphics are intruded by all members of the Nicholson Granite Complex, and are overlain by the Cliffdale Volcanics in the Fish River area. Unconformity between the Metamorphics and the Volcanics is inferred from the fact that the metamorphics have undergone regional deformation that has not affected the volcanics. In the Nicholson River 1:100 000 Sheet area the metamorphics are overlain by the Westmoreland Conglomerate and younger formations.

20

Table 2 . Distinguishing characteristics of Nicholson Granite Complex

	Pgn_1	Pgn_2	Pgn_{3-4}	Pgn_5	Pgn_6	Pgn_7	Pgn_8
Classification (Streckeisen, 1973)	Microcline-albite granite	Albite-microcline granite	Granodiorite	Albite-microcline granite	Albite-microcline leucogranite	Albite-microcline microgranite.	Microcline-albite granite
Lithology	White coarse-grained porphyritic; hornblende, biotite abundant; K-feldspar phenocrysts	White coarse-grained porphyritic; biotite but only tr hornblende; K-feldspar phenocrysts	Red coarse-grained porphyritic; hornblende, biotite abundant; mafic xenoliths; + recrystallised lenses, fine-grained, even-grained; melanocratic.	Red even-grained, medium-grained; some biotite	Red even-grained medium or coarse; rich in quartz	Red fine-grained	White, even medium grained to aplitic; no hornblende, minor biotite; muscovite-bearing; quartz-rich (40%)
Geochronology and field relations	1843 ± 83 m.y. over-lain by Cliffdale Volcanics; intrudes Murphy Metamorphics	1860 ± 103 - 1770 m.y.; composite? pluton; intrudes Cliffdale Volcanics	Ring dykes and stocks intrud-ing Murphy Metamorphics, $Pgn_{1,2,5,6}$, and Cliffdale Volcanics	1773 ± 24 m.y.; intrudes Cliffdale Volcanics with which it is coeval	1770? m.y.; related to Pgn_5	Microgranite and aplite dykes, chill zones, late-segregations of Pgn_2 and Pgn_5	1773 ± 56 m.y.; intrudes Murphy Metamorphics, Pgn_2, Pgn_6; ?youngest phase of granite intrusion
Petrography	Subsolvus granites:			Hypersolvus granites: - (Tuttle & Bowen, 1958)			

Subsolvus granites:

Two original feldspars:
K-feldspar carries inclusions
of all other minerals - it is possibly
partly a late-stage crystallisation
product.

Hypersolvus granites: - (Tuttle & Bowen, 1958)

Quartz and feldspars intergrown;
albite is exsolved from one original
alkali feldspar.

Distribution and exposure

In the Seigal 1:100 000 Sheet area, the Murphy Metamorphics crop out in two connected east-west belts around the confluence of the Fish River and Tin Hole Creek. Small isolated outcrops also occur in the area of the confluence of Pandanus and Little Dinner Creeks, and within an upfaulted block of granite adjacent to the Westmoreland Conglomerate, near the Fish River fork at S860295.

The formation forms low mounds of rubbly red-weathered schist.

Lithology and field occurrence

The western and northern parts of the Fish River exposures comprise red or black medium to fine (muscovite-epidote-) quartz-albite-biotite-chlorite schists tightly folded about an east-west axis. A wavy or parallel foliation defined by alignment of biotite flakes strikes between west and 10° north of west and dips vertically or steeply north.

Eastwards, the schists grade into massive medium to coarse granite-veined muscovite greiss. The gneiss consists of alternating bands of polygonal quartz-albite-muscovite rock, granite, and micaceous layers. The layer boundaries commonly follow irregular paths, so that bands bulge and pinch along their length. Band width ranges from less than a centimetre to about 20 cm.

Petrography

The mica schists are homogeneous or poorly segregated into bands of differing quartzofeldspathic content, possibly representing original sedimentary banding. The foliation is not well defined in thin section: broad chains of subparallel biotite with muscovite, chlorite, sericite, and equant quartz and albite form an irregular to polygonal aggregate. Slightly chloritised biotite flakes (25%) are associated with ragged muscovite (15%). Subhedral albite is antiperthitic and contains rare quartz inclusions. Anhedral aggregates of sericite and Fe-chlorite are alteration products of feldspar. Apatite and zircon are accessory minerals. The schists have been metamorphosed in the quartz-albite-epidote-biotite subfacies of greenschist-grade metamorphism (Turner & Verhoogen, 1960).

The micaceous layers of the gneiss consist of a medium to fine mosaic of equant quartz grains separated by chains of muscovite and red-brown biotite flakes. The micas are present in about equal proportions and total about 50 percent of the micaceous bands. Many of the quartz grains carry a nuclear goethite grain. Apatite and zircon are accessory minerals. The quartz-plagioclase-muscovite layers are coarser-grained than the micaceous parts, although similar in texture. An irregular mosaic of quartz grains comprising 60 percent of the bands is interrupted by patches of anastomosing strongly sericitised plagioclase. Muscovite, forming about 25 percent of these bands, occurs as radiating clumps. Accessory minerals are zircon, sphene, apatite, and goethite.

It can be seen from the above descriptions that muscovite is more abundant in the gneiss - i.e., near granite contacts - than it is in the schists.

Discussion

Despite the intense deformation that has affected the Murphy Metamorphics, and the resulting superimposition of foliation upon original bedding, which is no longer recognisable, the textural and compositional differences between the schists and the gneiss and the gneissic banding probably reflect primary sedimentary banding, as the temperature of metamorphism (greenschist) was not high enough for migmatite-style migration to occur; hence this is not a possible method of formation of the bands.

The increase in the proportion of muscovite in the metamorphics near granite contacts, however, suggests that some K_2O from the intruding granite has moved into the country rock.

The predominantly acid composition of the schists and gneiss of the Murphy Metamorphics points to parent material consisting of pelitic and quartzo-feldspathic sediments and volcanics. If, as suggested in a following section, the granite magmas were produced by anatexis of sediments at the base of the sequence now represented by the Murphy Metamorphics, the composition of the granites is such that the lower, unexposed parts of the pile must have included a significant proportion of basic material, probably volcanic, as well. Greenstone has been identified from the bases of a number of drill holes through the Murphy Metamorphics in the Nicholson River and Benmara 1:100 000 Sheet areas, to the west and southwest of Seigal (Nasca, 1972).

Although there is insufficient evidence to determine exactly the environment of deposition of the Murphy Metamorphics, the nature of the probable original sediments suggests geosynclinal deposition (Roberts and others, 1963).

The Murphy Metamorphics are similar in lithology and metamorphic grade to the Yaringa Metamorphics, the oldest rocks in the Mount Isa block. The two are probably tectonically equivalent. On a broader regional scale, both the Murphy and Yaringa Metamorphics have been tentatively tectonically correlated (Plumb & Derrick, 1975) with basement inliers in eastern Arnhem Land (Grindall Metamorphics, Bradshaw Granite, and Mirarrmina Complex) and the Pine Creek Geosyncline, with which they may be continuous in the sub-surface (Plumb & Derrick, 1975).

GRANITES

$$\underline{Pgn}_1$$

Field relations

Pgn_1, Pgn_2, Pgn_{3-4}, and parts of Pgn_6 and Pgn_8 constitute the Nicholson Granite as defined by Carter and others (1961).

A minimum estimate of the age of Pgn_1 is 1840 m.y. Pgn_1 intrudes the Murphy Metamorphics, and is itself intruded by younger phases of the complex. It is probably overlain by the Cliffdale Volcanics, and is non-conformably overlain by the Wire Creek Sandstone.

Distribution and exposure

Pgn_1 crops out in three areas in the southeastern and central parts of the MTR (Fig. 3a). It forms low hummocky ridges of weathered rubble along fault zones or flanking quartz veins. Fresh granite is exposed as isolated groups of corestones in or near creek banks - e.g., at S085310.

Elsewhere the area is covered by residual red sandy soil of K-feldspar tablets and subordinate quartz grains. Near the scree slopes of the scarp-forming Wire Creek Sandstone (at S115260) this soil also contains clasts derived from the sandstone. The granite was extensively eroded before the Westmoreland Conglomerate and Wire Creek Sandstone were deposited.

Lithology and field occurrence

Pgn_1 is a coarse-grained porphyritic granite, in which euhedral
pink K-feldspar phenocrysts commonly 8 cm across are set in subvertical
alignment in a groundmass of pale green euhedral plagioclase, quartz,
and roughly equal amounts of hornblende and biotite. Near its contacts
with the Murphy Metamorphics, Pgn_1 carries fine-grained xenoliths composed
of biotite and minor hornblende, plagioclase, and quartz. Away from the
contacts, xenoliths are coarser-grained, have hornblende granodiorite
mineralogy, and commonly grade into their host; they are probably more
assimilated inclusions of Murphy Metamorphics.

The granite is commonly altered as follows:

feldspars→sericite→clay) accompanied by release of
) silica and its deposition
biotite→chlorite→clay   ) as secondary quartz
hornblende→chlorite

The largest area of Pgn_1 lies south of the Calvert Fault between
Gorge and Pandanus Creeks. Pgn_1 is faulted against Peters Creek Volcanics
on its eastern border, and is mainly non-conformable against and locally
faulted against Wire Creek Sandstone along its southern boundary. To the
north, this area is separated from Pgn_2 by a granofelsic lenticular remnant
of Cliffdale Volcanics, recrystallised as a result of granite intrusion.
The contact between this lens of Cliffdale Volcanics with granite is nowhere
exposed; the northern boundary - against Pgn_2 - is assumed to be intrusive
as Pgn_2 clearly intrudes Cliffdale Volcanics elsewhere, whereas the southern
boundary - against Pgn_1 - is assumed to be non-conformable because Pgn_1 has
yielded isotopic ages older than those of the Cliffdale Volcanics. The
contact of Pgn_1 with Pgn_2 along the western boundary of this outcrop area is
also not exposed but is assumed to be intrusive, since Pgn_2 intrudes the
Cliffdale Volcanics, whereas Pgn_1 is apparently overlain by them.

A smaller area of Pgn_1 crops out at the intersection of the two
major structural trends of the MTR centred on SO35330; Pgn_1 is here in-
truded by Pgn_2, Pgn_5, and Pgn_6. The older granite is separated from Pgn_5
by a belt of foliated hornblende-rich granodiorite up to 1 km wide (SO41340).
Similar rocks are found along other contacts within the complex, and are
grouped and discussed under Pgn_{3-4}. They are emplaced as small stocks and
ring dykes along contacts between plutons, and are chemically similar to
the younger porphyry dykes that intrude the Cliffdale Volcanics. The
granodiorite dykes are probably forerunners of the porphyry dykes.

25

Fig 3a Distribution of Pgn₁

Fig 3b Distribution of Pgn₂ and Pgn₃₋₄

Fig 3c Distribution of Pgn₅, Pgn₆, and Pgn₇

Fig 3d Distribution of Pgn₈
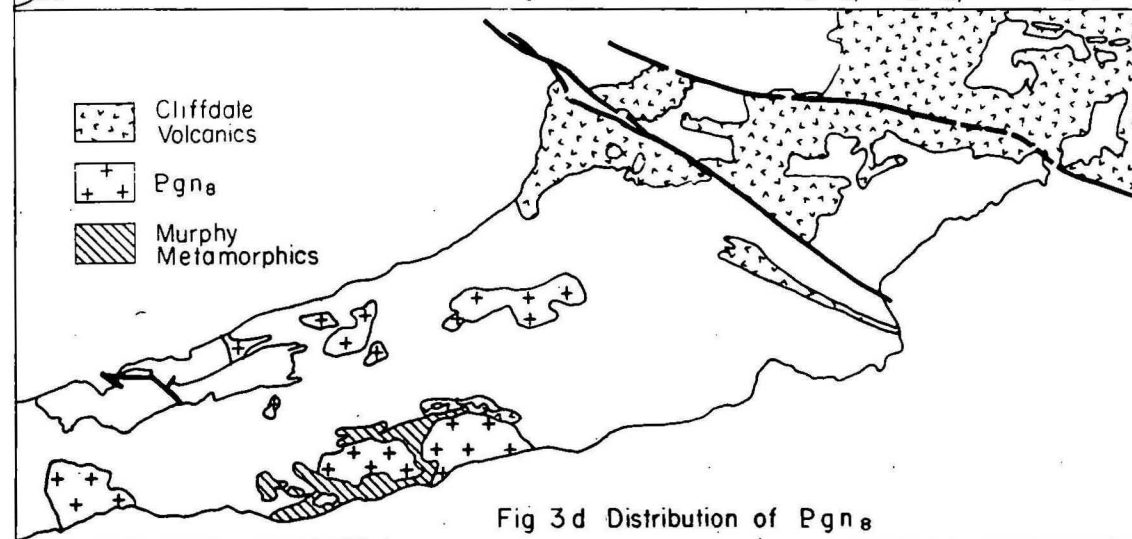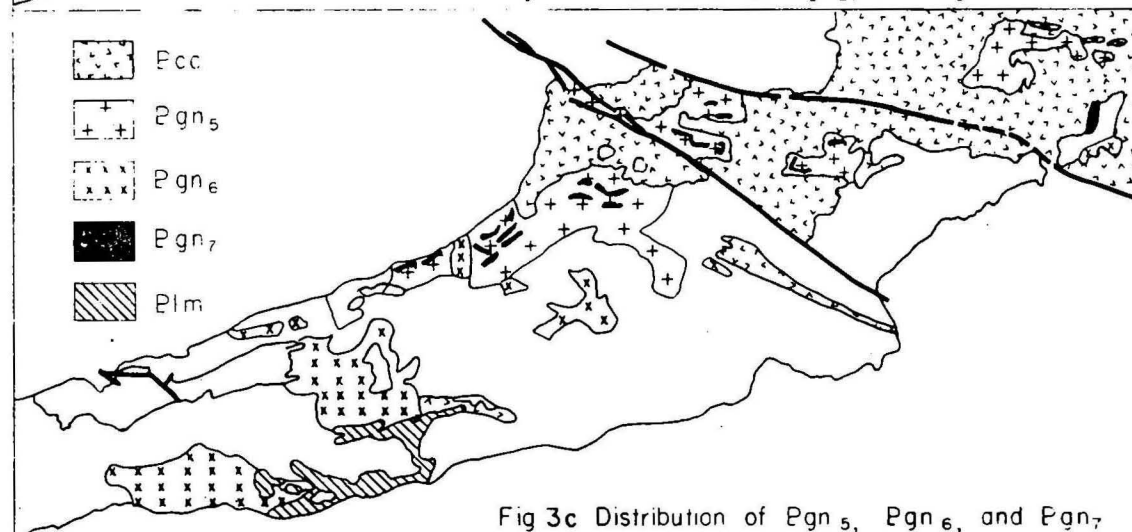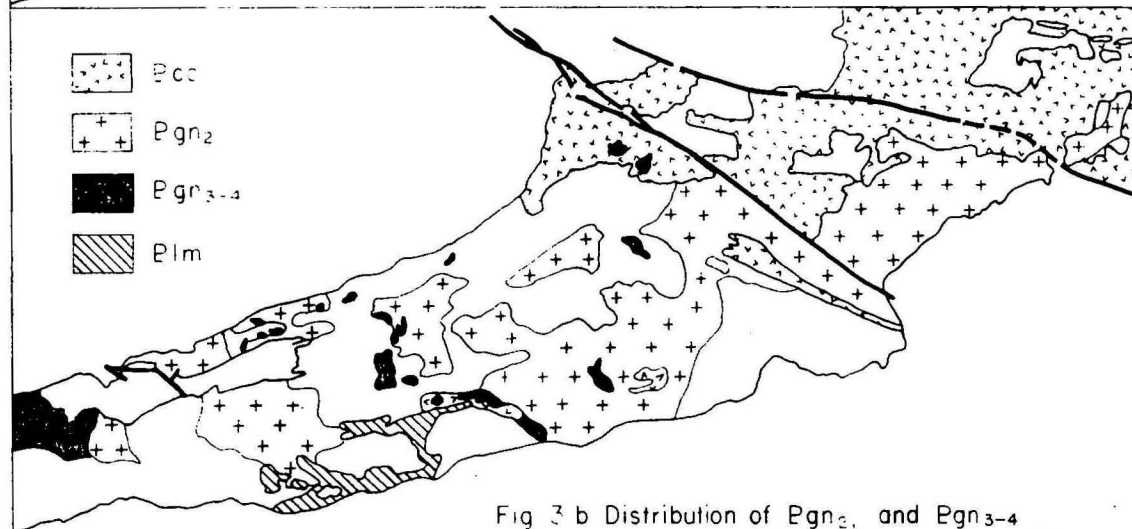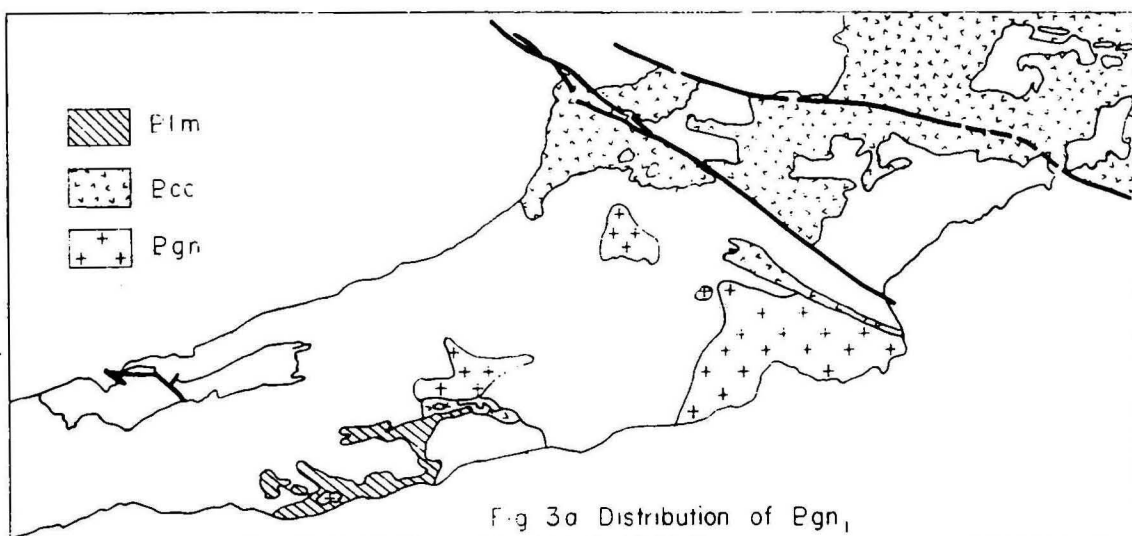
(a)
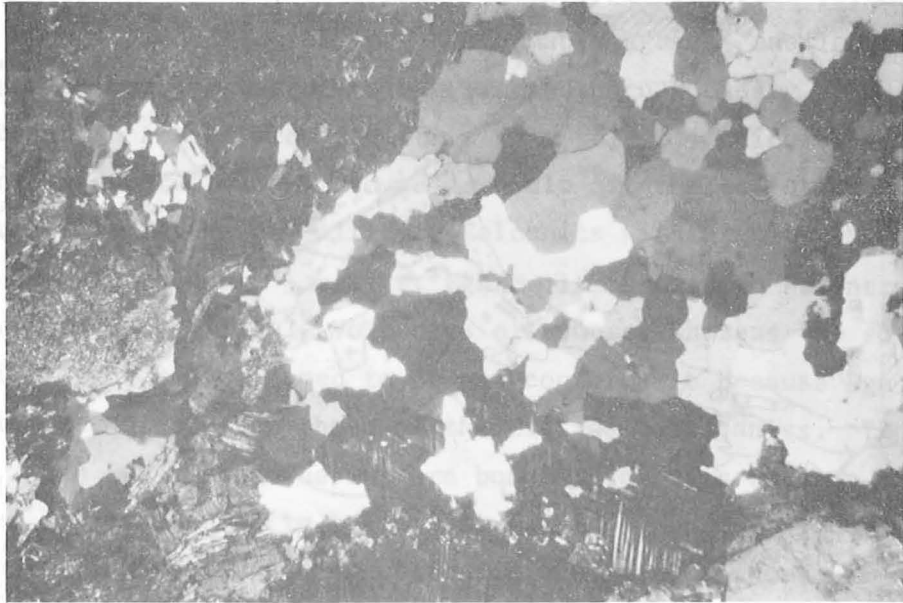
(b)

Fig. 4 Typical petrographic textures of Bgn₁.(a) hypidiomorphic granular
plagioclase (twinned, zoned, e.g. lower centre); biotite (mottled,
left of centre and upper right); K-feldspar (dark, upper left);
and quartz (pale, lower right). X20, crossed nicols,

(b) monomineralic area of recrystallized quartz surrounded by
biotite (left) and microcline (twinned, lower centre) X20,
crossed nicols.

Petrography (Table 3)

Bgn_1 is typically coarse-grained, but may be medium-grained, and inequigranular. Although K-feldspar is less abundant than plagioclase, it forms euhedral phenocrysts up to 7 cm long, whereas plagioclase grains are subhedral and generally less than 0.5 cm across. The concentration, shape, size, and orientation of the K-feldspar phenocrysts differ from locality to locality; phenocrysts nearer to pluton margins show a vague vertical foliation, whereas those away from margins are randomly oriented.

Texture is variable (see Fig. 4), but dominated by a tendency for each mineral to form monomineralic aggregates, indicating some recrystallisation of the groundmass minerals. Quartz and feldspar aggregates carry inclusions of hornblende-biotite chains. The K-feldspar phenocrysts (20%) show excellent microcline twinning, carry coarse perthite lamellae and abundant inclusions, and are densely invaded by trails of the groundmass minerals quartz, K-feldspar, plagioclase, and mafics. The crystallisation sequence deduced from the relative grainsizes and grain boundary relations is: K-feldspar, followed by plagioclase, joined by quartz. The inclusion of plagioclase and quartz in the K-feldspar phenocrysts, however, suggests that the K-feldspar phenocrysts crystallised later than the plagioclase and quartz. As the K-feldspars of several of the granites show distinctive textures similar to those in Bgn_1, the origin of the K-feldspar phenocrysts and their inclusions is discussed in a separate section, following the descriptions of the granites. Web-like grains of subhedral and anhedral twinned, sericitised plagioclase zoned from An_6 to An_0 form 30 percent of the section. Quartz (20%) occurs as recrystallised polygonal to amoeboid aggregates in which individual grains range from 0.2 - 3.0 mm in diameter. Hornblende (6%) and biotite (9%) occur as stumpy subhedral grains averaging 0.5 mm in length. Both have similar pleochroic schemes - the colours depart only slightly from olive-green. Very minor blue amphibole is also present. Opaque oxides are absent, but sphene forms 1-2 percent of the rock; other accessories are calcite, zircon, apatite, and epidote.

Elsewhere - e.g., around S950270 - Egn_1 is more even-grained, both feldspars occurring as subhedral phenocrysts. Patches of groundmass comprising plagioclase, quartz, hornblende, and biotite are scattered through the K-feldspar phenocrysts. In contrast, plagioclase is almost inclusion-free, carrying only rare epidote, biotite and sericite.

Egn_1 is the most 'basic' granite; other phases of the complex are characterised by successively lower plagioclase/total feldspar and hornblende/biotite ratios, lower mafic content, change from green to brown biotite paralleling increasing oxidation state of iron, gradual aggregation of mafic minerals, and replacement of calcic accessories by opaque oxides.

The relative depth of crystallisation of Egn_1 may be deduced from its field and petrographic characteristics. Egn_1 intrudes regionally metamorphosed rocks along contacts that are partly concordant and locally migmatitic. This relation implies relatively deep-seated intrusion. The absence of large-scale gneissic or flow structures in Egn_1, the presence of xenoliths, the low metamorphic grade of the country rock, and the development of a contact aureole, however, all indicate that Egn_1 migrated some distance from its site of melt formation before it crystallised. Egn_1 is thus an intermediate or mesozonal granite according to the classification of Buddington (1959). It was separated from its source region but crystallised under sufficient pressure to allow slow crystallisation and the formation of two separate euhedral or subhedral feldspar phases (Tuttle & Bowen 1958).

$$\underline{Egn_2 \quad Egn_{2a}, \quad Egn_{3-4}}$$

Field relations

Egn_2 includes most of the Nicholson Granite as shown on the Calvert Hills 1:250 000 Sheet. Egn_{3-4} includes marginal ring intrusions associated mainly with Egn_2.

Although the isotopic ages of Egn_1 and Egn_2 are not distinguishable within experimental error, ages of Egn_2 samples are consistently younger than those of Egn_1 samples; Egn_2 is therefore probably younger than Egn_1. Egn_2 intrudes the Cliffdale Volcanics along the contact through S113345, and is non-conformably overlain by the Westmoreland Conglomerate.

Table 3

Estimated volume percent of minerals and summary of salient petrographic features Bgn_1

Spec. no. [4]	0889	0924	0931
$Kspar$ [1]	30	20	20
	int. microcline & orthoclase, fine & coarse perthite		
Plag	30, An_6-An_0	35	35
Qtz	20	20	15
Biotite	8	9	12
Hblende	8	6	12
Muscovite	-	-	-
Access	Sphene[2], epidote, zircon, monazite, apatite, opaques, and calcite		
Grainsize scheme	Coarse but inequigranular; $Kspar_p$ > plag > qtz $\geqslant$ $Kspar_g$, hblende = biotite		
Texture	Hypidiomorphic granular, euhedral Kspar separated by subhedral to anhedral plag, qtz, biotite, hblende, small Kspars		
Inclusion scheme	Kspar carries aggregates identical to the groundmass, & individual plag, qtz, biotite, hblende		
Replacement scheme	Plag → sericite; all minerals → Kspar; hblende → uralite, epidote; all minerals → qtz		
Other features and comments	Silica & potash alteration extensive; probably proceeded immediately after crystallisation		
Xenoliths	Biotite-rich and biotite-hornblende-rich xenoliths common		
Classification[3]	Microcline-albite granite		

1. Abbreviations for Tables 3-7.

Kspar;	K-feldspar	Ab:	Albite
plag:	plagioclase	tr:	trace
qtz:	quartz	av:	average
hblende:	hornblende	incl:	inclusions
access:	accessories	gen:	generally
int:	intermediate	$Kspar_p$:	porphyritic K-feldspar
max:	maximum	$Kspar_g$:	groundmass K-feldspar
cts:	continuous		

30

2. Accessories are listed in order of decreasing abundance.
3. Classification according to Streckeisen (1973).
4. Specimen numbers are the last half of BMR registered numbers; e.g., first sample number is 73760889.

Granodiorite and microgranodiorite stocks and ring dykes (Bgn_{3-4}) were emplaced at various times in the history of the complex. The oldest stocks intrude the Murphy Metamorphics and are overlain by the Cliffdale Volcanics at S908239. Younger dykes intrude Bgn_2, Bgn_5, Bgn_6, and the Cliffdale Volcanics.

Distribution and exposure

Bgn_2 crops out more extensively than any other phase of the Nicholson Granite Complex (Fig. 3b). In the Hedleys Creek 1:100 000 Sheet area, Bgn_2 forms most of the southern part of the MTR. In the Seigal 1:100 000 Sheet area, Bgn_2 forms the south-central part of the complex as a U-shaped belt from around S050310 extending southwestwards to around S912294. Bgn_2 also forms a small northwest-trending lens east of an abandoned airstrip at S970340.

Ring dykes, from 0.1 to 1 km wide, form a discontinuous belt across the central part of the MTR. Stocks of Bgn_{3-4} crop out at S970230, S020260, and S045340.

Bgn_2 is also extensive west of the Fish River. It forms the strip of granite between the China Wall and the Tawallah Group inlier, and a slightly wider east-west strip south of this inlier. The southerly strip extends from near the western margin of the Sheet area eastwards to its contact with the Murphy Metamorphics and Bgn_6 west of the Fish River (S855226). Bgn_{3-4} occurs as dykes and stocks in these two areas (Fig. 3b); its extent near the western margin of the Sheet area may not be as continuous as shown on the map. A stock of porphyritic microgranodiorite intrudes Cliffdale Volcanics at S032398. Microgranodiorite dykes occur near or along contacts at S789280, S796287, S807290, S815295, S845310, S882305, S924334, and S953302 (Fig. 3b).

Bgn_{2a} is a body of altered Bgn_2, cropping out in the Hedleys Creek Sheet area, centred on HC980430.

A distinctive smooth-textured dark green and red airphoto-pattern can be correlated with areas of outcrop of Bgn_{3-4}. An east-southeast foliation, where developed, is easily discerned on the aerial photographs. The airphoto-pattern of Bgn_{3-4} is similar to that of Blm. The controlling factor in the two photo-patterns in the high proportion of biotite and hornblende in both rock types. The form and nature of outcrop of Bgn_2 and

Egn_{3-4} are similar to those of Egn_1: semi-continuous exposure is restricted
to fault zones, quartz veins, or jointed pavements in creek banks, but locally
abundant fresh exfoliated corestones form discontinuous outcrop over fairly
extensive areas - e.g., along the track between S115340 and S080377 and in
the areas around S768282 and S905315. Continuous outcrop of bleached
kaolinised Egn_2 forms smooth low-relief hummocks in its westernmost area of
outcrop, near the Sheet area boundary (S690220).

Lithology and field occurrence

Egn_2 is a medium or coarse white or white and green porphyritic
albite-microcline granite in which white euhedral K-feldspar phenocrysts,
differing in proportion and size from locality to locality, are set in
a granular groundmass of euhedral pale green plagioclase (30%), quartz (20%),
biotite (10-15%), and hornblende (10-15%). Where K-feldspar phenocrysts are
abundant, they are tabular rather than elongate and aligned. Micrograndiorite
xenoliths rich in biotite and hornblende are common throughout the granite.
The xenoliths in Egn_2 carry a higher proportion of plagioclase, which is
commonly phenocrystic, and are larger and more crowded than the xenoliths in
Egn_1. Pegmatoidal quartz-biotite veins up to 0.2 m wide are only rarely
observed. The occurrence of plagioclase phenocrysts in some of the inclu-
sions in Egn_2 suggests that the inclusions are early-crystallised products
of the Egn_2 melt, rather than relict solid material.

Egn_{3-4} is corestone-forming, usually foliated, medium or coarse
hornblende melagranodiorite. Microphenocrysts of white K-feldspar and red
plagioclase and mafic xenoliths are subvertically aligned in a dark ground-
mass. The groundmass is granular, medium to coarse, and even-grained, and
composed of plagioclase, hornblende, biotite, and minor K-feldspar. Adjacent
to contacts with the Murphy Metamorphics, grainsize and relative proportions
of these minerals differ, so that there is a continumm between the granitic
groundmass and mafic segregations, as described in Section II.

33

Both Egn_2 and Egn_{3-4} show weathering effects similar to those of Egn_1; the most notable features are the alteration of biotite to vermiculite rather than to chlorite, and the residual concentration of K-feldspar in the granite sand. Egn_{3-4} is generally less weathered than Egn_1 or Egn_2.

The southwestern part of the wedge-shaped outcrop in the Hedleys Creek 1:100 000 Sheet area is cut by numerous dykes. These range in size and composition from 10-cm veins of aplite to 10-m-wide vertical dykes of acid porphyry, some of which crop out - trending northwesterly - for up to 5 km. They have better topographic expression than the granites, and form blocky outcrops or corestones. Granophyric and microporphyritic chilled margins can be distinguished in the thicker dykes; these outer zones commonly display vertical flow banding or jointing.

Egn_{2a} is a small pod of distinctively altered Egn_2 forming the northeastern end of the Hedleys Creek outcrop area. Although the feldspars are sericitised, and the biotite is chloritised and sericitised, the granite is still well-consolidated. The sericitisation and extensive hematite and limonite staining in fractures give the rock a mottled appearance. Vertical veins of limonite-stained milky quartz from 1 to 2 m wide form north-north-west trending swarms up to 1 km long (av. 0.5 km) across the granite. The veins are restricted to altered granite. Rare porphyry dykes are also sericitised. Copper and tin mineralisation (see Section X) are associated with the altered granite.

Egn_2 between Little Dinner Creek and the Fish River is separated from Egn_8, Elm, and Egn_6 to the south and west, by ring intrusions of Egn_{3-4}. The ring intrusions are usually medium or coarse granodiorite, but are dense and fine-grained where recrystallised. Smaller aplitic and melanocratic microgranodiorite dykes are everywhere associated with the ring dykes. The cross-cutting melanocratic dykes contain about 25 percent modal hornblende and biotite. Where Egn_{3-4} occurs near the Murphy Metamorphics around S910240, it is foliated parallel to the schistosity in the metamorphics, and carries partly assimilated mafic schlieren derived from the schists. The narrow dykes intruding Egn_2 at S890300 are dense black recrystallised granodiorite, locally secondarily silicified. Red and purple aplites are abundant, and intrude the granite on both sides of the granodiorite dykes.

(a)
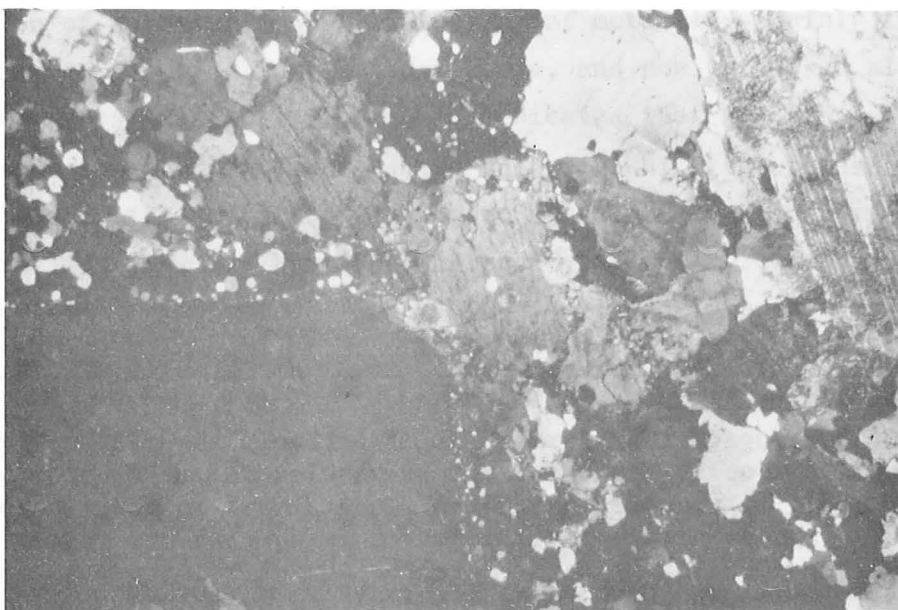
(b)

Fig. 5. Typical petrographic textures of Bgn$_2$ and Bgn$_{3-4}$.

    (a)   Bgn$_2$: hypidromorphic granular K-feldspar (perthitic, left and bottom); plagioclase (showing alteration to sericite, upper right); biotite (black, upper right of centre); and quartz (interstitial). X20, crossed nicols.

    (b)   Bgn$_{3-4}$: K-feldspar phenocryst (dark, lower left) rimmed by recrystallized matrix grading into coarser-grained biotite (mottled, centre); quartz (pale, upper right of centre); and plagioclase (twinned, upper right) X20, crossed nicols.

Fine-grained recrystallised granodiorites also intrude Egn_5, Egn_6, and Egn_8, but are restricted to areas in contact with Egn_1 or Egn_2. At S805295, S953302, S030270 and S045340, the black granodiorite grades locally into dark red granodiorite, the coloration having been produced by the high iron-oxide content of the feldspars.

The microgranodiorites are fine-grained and black or reddish black, and have red and brown weathered surfaces. The mafics impart a shiny surface to these massive, commonly recrystallised dykes. Volumetrically hornblende makes up 25 to 30 percent, biotite 10 percent, and quartz 10 percent, but the proportions of the feldspars vary among localities from 30 percent K-feldspar, 20 percent plagioclase to 10 percent K-feldspar, 40 percent plagioclase.

The intrusion at S032398 is a dark green to black medium-grained massive microgranodiorite which weathers to grey and white; it contains from 3 to 12 percent white to pale green plagioclase phenocrysts 3 to 4 mm long. Roughly equal amounts of biotite and hornblende make up about 40 percent of the rock; the remainder includes 10 percent each of quartz and K-feldspar.

The intrusion at S032398 is faulted against Cliffdale Volcanics along its eastern boundary. The body is sill-like in form, and has what appears to be a lateral extension in the form of an intermediate feldspar porphyry dyke. As the microgranodiorite is cut by dykes of microgranite and feldspar porphyry of more acid composition, it was probably emplaced before nearby masses of Egn_5 intruded.

Recrystallised microgranodiorite occurs as ring dykes along a zone 2 km long and up to 40 m wide between Egn_2 and Egn_6 at S885305. Plagioclase (30%) is fresh and dark red as a result of minute opaque oxide inclusions. Pale pink K-feldspar forms sporadic phenocrysts (2.5 cm long), but total K-feldspar is only about 10 percent. Biotite is greatly subordinate to hornblende, and both have been recrystallised to form equant, straight-sided or subspherical grains with triple grain-boundary junctions (Spry, 1969).

Similar but mineralogically more variable microgranodiorite crops out extensively at S815295 and S807290. These outcrops are richer in hornblende, and are cut by veins and dykes of leucogranite, quartz, and Egn_5. One dyke carries about 30 percent phenocrystic K-feldspar in the form of anhedral grains 0.5 cm across and not distinguishable in hand specimen because of the high concentration of dark euhedral poikilitic hornblende inclusions. Both quartz and K-feldspar are commonly poikilitic, but where K-feldspar is less abundant the concentration of inclusions is lower.

The dyke at S953302 is coarse-grained and extensively recrystallised, although original feldspar phenocrysts are unaltered and not poikilitic.

Gradations in weathering are well exposed at S743267 where porphyritic granite is thinly capped by ferricrete. Biotite is altered to a pale green mineral with optical characteristics intermediate between biotite and chlorite, which is in turn replaced by vermiculite. The heavy clouding of both feldspars, and the sericitisation of plagioclase, were followed by the removal of plagioclase and then of quartz to leave a lag gravel of K-feldspar tablets.

Petrography

Egn_2. (Table 4). Differences between Egn_1 and Egn_2 can be correlated with the more fractionated nature of Egn_2.

Egn_2 is also medium or coarse (average grain diameter 2 mm) and porphyritic, but the groundmass minerals are even-grained and not recrystallised to mono-mineralic aggregates as in Egn_1. The texture is hypidiomorphic granular (Fig. 5a) and dominated by individual grains of subhedral to euhedral K-feldspar and plagioclase. K-feldspar is the most coarse-grained (phenocrysts up to 3 cm) and the most nearly euhedral phenocryst mineral, incorporating quartz, biotite, plagioclase, and K-feldspar inclusions, generally within a restricted outer zone. Aggregates of phenocrysts are separated by narrow trails of groundmass or by cuspate quartz grains. Some subhedral plagioclase and a lesser proportion of quartz are also phenocrystic. Quartz phenocrysts carry plagioclase, biotite, and muscovite inclusions. The groundmass of irregular to polygonal grains of quartz, plagioclase, minor K-feldspar, biotite, and hornblende has a typical hypidiomorphic granular texture. K-feldspar in the groundmass and phenocrystic K-feldspar are both intermediate microcline. The subhedral K-feldspar phenocrysts carry abundant but patchily distributed inclusions. As in Egn_1, the order of crystallisation appears to have been: K-feldspar, joined by quartz, although the presence of inclusions in the K-feldspar suggests that the K-feldspar crystallised or recrystallised later than did the included minerals. This possibility is discussed in a later section.

Egn_2 apparently crystallised at a slightly shallower depth than Egn_1. Egn_2 shares the petrographic features of Egn_1 indicative of slow crystallisation from a relatively low-temperature melt: hypidiomorphic texture and the presence of two feldspars - albite and orthoclase, of which the orthoclase has inverted to microcline. In contrast to Egn_1, however, Egn_2 intrudes unmetamorphosed rocks along discordant contacts, indicating a higher level of

emplacement than that of Egn_1. No significance can be attached to the greater abundance of xenoliths in Egn_2 relative to Egn_1. It has been suggested that the xenoliths in Egn_1 are relict inclusions, and that most of those in Egn_2 are early-crystallised products of the Egn_2 melt.

$\underline{Egn_{3-4}}$. (Table 5). The texture of the porphyritic granodiorites ranges from interlocking granular to mosaic (see Fig. 5b). K-feldspar (15-20%) is subordinate to plagioclase with respect to abundance, grainsize, and grain boundary development. The microphenocrysts (2-5 mm diameter) are slightly perthitic euhedral or subhedral intermediate microcline carrying sporadic inclusions of biotite, plagioclase, quartz, and hornblende. Smaller K-feldspar grains show better-developed microcline twinning than the microphenocrysts. Plagioclase grains (20-30%) range from 0.4 to 4 mm across and are generally euhedral although in places are penetrated by other minerals. Although sericitised, plagioclase is clear rather than turbid. The red colour is due to exsolution of sub-microscopic inclusions of metallic - mainly iron - oxides originally in solution in the plagioclase, and now localised along twin and cleavage traces (Smith, 1974). This indicates that the Egn_{3-4} dykes crystallised at higher temperatures than Egn_1 and Egn_2, in which the feldspars are white or green, because the amount of iron oxide dissolved in feldspars at their time of crystallisation, and hence the intensity of their red colouration, increase with increasing temperature (Sen, 1960)*. Plagioclase carries sporadic biotite

---

1
Grey turbidity or clouding in feldspars is distinguished in this report from red colouration of feldspars, although both effects are due to the inclusion of iron or iron oxides, with minor amounts of other metals or metallic oxides. Clear red feldspars, as are characteristic of Egn_{3-4}, contain iron which was incorporated in the feldspar in solid solution during crystallisation. The amount of iron dissolved in the feldspar, and hence the intensity of the red colouration, increase with increasing temperature. Hence red fledspar granites crystallised at higher temperatures than white feldspar granites. With time, the iron exsolves to form submicroscopic grains of hematite, whose nucleation is controlled by the crystallographic planes of the host feldspar.

Microscopically distinguishable, randomly oriented inclusions of both trivalet and divalent iron oxides cause feldspar turbidity. Although some of the iron may have been exsolved from the feldspar, much of it probably came from outside the mineral and was introduced during deuteric alteration and/or weathering (Smith, 1974).

The extent of development of turbidity is not necessarily related to the intensity of red colouration. In the Nicholson Granite Complex, Egn_1, Egn_2, and Egn_8 have white, commonly turbid feldspars; Egn_{3-4} has red, clear feldspars; and Egn_5, Egn_6, and Egn_7 have pale red, commonly turbid feldspars.

and hornblende inclusions. The presence of possible grain boundaries within single microphenocrysts of plagioclase suggests that some of the plagioclase may be relict xenocrysts from the granite source material, possibly basic volcanics. Hornblende (up to 1 mm diameter) and slightly less abundant biotite (0.5-1 mm diameter) comprise about 30 percent of most samples, in the form of either mixed or monomineralic clots (3-5 mm diameter) or scattered euhedral or subhedral grains. The hornblende presents smooth boundaries to the other minerals, and carries sporadic inclusions of opaque oxides, apatite, biotite, and plagioclase. Brown biotite is also dotted with opaques and apatite. It is commonly warped and altered to opaques and green amphibole?, chlorite, or clay. Quartz (10-15%) is interstitial, and sphene, apatite, opaque oxides, calcite, and rare zircon are accessory.

The groundmass of the microgranodiorites has a foliated granoblastic polygonal texture in which the mafic minerals as well as the feldspars are parallel-aligned. Scattered sericitised euhedral plagioclase phenocrysts (up to 3 mm diameter) are set in parallel alignment in a fine-grained foliated hornblende-plagioclase groundmass which contains greenish brown biotite (15%), quartz (5-10%), microcline (5-10%), microcline (10%), and accessory sphene (1-2%), opaque oxides, apatite, chlorite, and zircon.

The microgranodiorite intruding the Cliffdale Volcanics contains euhedral hornblende pseudomorphs and plagioclase grains set in a granophyric intergrowth of orthoclase (25 to 30%), plagioclase (25%), and quartz (10 to 15%). The orthoclase is not perthitic, and contains abundant acicular apatite, opaque oxides, and minute hornblende grains. Both phenocrystic and groundmass plagioclase are normally zoned, but the less extensive sericitisation of the smaller grains is consistent with these grains' being less calcic than the phenocrysts (Table 5). Plagioclase is also saussuritised. The original mafic minerals are almost completely replaced by a mixture of uralite, Fe-rich chlorite, and opaque oxides. Minor pyroxene and about 2 percent each of sphene and opaque oxide spinel are accessory.

The microgranodiorite dykes near the Fish River are fine-grained (average grainsize 0.5 mm) and generally even-grained except for larger plagioclase grains, which reach 1-2 mm. Plagioclase is subhedral and more abundant than K-feldspar. Quartz, K-feldspar, hornblende, and biotite are all anhedral and interstitial; the quartz and K-feldspar are commonly graphically intergrown. Myrmekitic rims on plagioclase form plug-like protrusions into

39

(c)

(d)
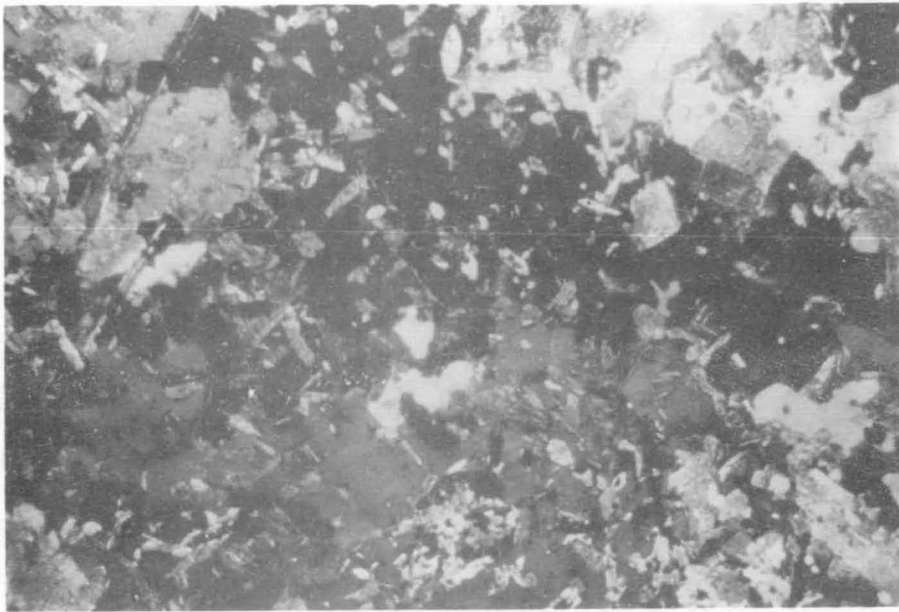
Fig. 5. (c) Bgn_{3-4}: recrystallised microgranodiorite showing
poikiloblastic quartz (black), and K-feldspar (grey)
carrying fine-grained inclusions of plagioclase, biotite,
hornblende and quartz. X20, crossed nicols.

(d) Bgn_{3-4}: recrystallised microgranodiorite showing hornfelsic
biotite (dark grey or black) with quartz K-feldspar and
plagioclase (all pale or grey) X20, crossed nicols.

K-spar. Although the proportions and total amount of mafics vary considerably hornblende is appreciably more abundant than biotite, and both occur as discrete subhedral grains rather than clots. Hornblende is partly replaced by mossy Fe-rich chlorite and opaque oxides, and biotite is partly chloritised.

Where dykes are recrystallised (see Fig. 5c,d), the interstitial minerals and the amphibole phenocrysts form a granoblastic mosaic; where large poikiloblastic K-feldspars occur, they have not been recrystallised. The possibility that the K-feldspars are postmagmatic crystallisation products is discussed in Section VI, "Origin of the K-feldspar phenocrysts'. The dykes are mineralogically similar to basic xenoliths in Pgn_2. As well as being closely spatially and temporally related, Pgn_{3-4}, Pgn_1, and Pgn_2 are also chemically closely related (see Section VIII), and so may be comagmatic.

$\underline{Pgn_5, \ Pgn_6, \ Pgn_7}$

Pgn_5, Pgn_6, and Pgn_7 are distinguished as a group from Pgn_1, Pgn_2, and Pgn_{3-4} in being red, even-grained, (biotite-) alkali feldspar granites. Pgn_5 and Pgn_7 correspond roughly to intrusions formerly known as Norris Granite; Pgn_6 corresponds to parts of what was previously known as the Nicholson Granite. Pgn_6 is free of mafic minerals, whereas Pgn_5 contains more than 5 percent biotite. Pgn_7 includes microgranite and aplite dykes, chilled zones, and late-stage segregations that occur throughout the Nicholson Granite Complex, but within Pgn_5 in particular. Pgn_5 has been dated at 1773 m.y. $\pm$ 24 m.y. by Webb (1973; see Table 1).

Field relations

Pgn_5, Pgn_6 and Pgn_7 intrude Pgn_2 and Cliffdale Volcanics (Pcc_1 and Pcc_2), and are non-conformably overlain by the Westmoreland Conglomerate. Pgn_5 also intrudes Pcc_4.

41

Table 4

Estimated volume percent of minerals and summary of salient

petrographic features of Bgn_2

Spec. no.	0875	0923A	0927	0880	0859A	1228	0840
Kspar	35	37	35	30	30	30	30
	(Int microcline & orthoclase, fine & coarse perthite)						
Plag	25	30	25: An_6-An_0	25	25	25	20
Qtz	30	20	25	35	20	30	35
Biotite	7	12	10	7	15	15	15
Hblende	-	-	tr	-	8	tr	tr
Muscovite	tr	tr	tr	2	-	-	-
Access	Apatite, zircon, monazite, fluorite, chlorite, calcite, opaques, and epidote						
Grainsize scheme	Medium or coarse, distinctly inequigranular; $Kspar_p$ $(>qtz_p)$ $\geqslant plag_p$ $> plag_g$ $\gg Kspar_g$ $\ggg qtz_g$						
Texture	Hypidiomorphic granular; euhedral Kspar separated by interlocking subhedral plag, qtz, biotite						
Inclusion scheme	Kspar carries qtz, plag, and biotite as single grains or as aggregated grains; plag carries rare qtz, biotite						
Replacement scheme	Biotite → qtz; plag, qtz → Kspar; (Kspar → qtz); biotite → Kspar; biotite → chlorite; plag → sericite						
Other features and comments	Patchy distribution of inclusions in Kspar, and their aggregated form, indicate metasomatic overgrowth to produce Kspar phenocrysts						
Xenoliths	Biotite xenoliths common, up to 15 cm across; larger ones carry Kspar phenocrysts, plag phenocrysts						
Classification	Albite-microcline granite						

Table 5
Estimated volume percent of minerals and summary of salient
petrographic features of Rgn_{3-4}

Spec. no.	1209	1218	1221	0860	1229	0827	0862	0850
Kspar (orthoclase & int microcline; sparsely developed perthite)	20	25	20	15	10	10	15	20
Plag	30	25	30	25; zoned An_{15} - An_0	20	45	50; An_{40} (phenocrysts) An_{20} (groundmass)	40
Quartz	15	10	10	10	10	15	5	15
Biotite	5	10	15	15	20	5	10	10
Hblende	25	30	25	20	30	20	20	15
Muscovite	-	-	-	-	-		-	

Access	Apatite, calcite, zircon, opaques, sphene, pyroxene, epidote, and fluorite
Grainsize Scheme	Granodiorites are coarse-grained with prophyritic plag $\pm$ porphyritic Kspar; $plag_p$ ($\geqslant Kspar_p$) $\geqslant plag_g \geqslant Kspar_g \geqslant$ qtz. Microgranodiorites are fine, even-grained or with porphyritic plag; $plag_p \gg plag_g \gg Kspar_g >$ qtz = hornblende $>$ biotite
Texture	Feldspar phenocrysts subhedral to euhedral; all grains present smooth subhedral boundaries; granophyric intergrowth of groundmass quartz and both feldspars common; microgranodiorites commonly recrystallised
Inclusion Scheme	Kspar rarely carries inclusions of plag, qtz, biotite, hblende; plag carries biotite, hblende, access
Replacement scheme	Biotite $\rightarrow$ chlorite + opaques $\rightarrow$ clay, plag $\rightarrow$ sericite, hblende $\rightarrow$ uralite
Other features	Foliated, contaminated by mica-bearing and hblende-bearing rocks, no evidence of silica or potash alteration
Xenoliths	Biotite, biotite-hblende, hblende all abundant in granodiorite, foliated; no xenoliths in microgranodiorites
Classification	Granodiorite, microgranodiorite

Distribution and exposure

Egn_5 crops out extensively in the Hedleys Creek 1:100 000 Sheet area; Egn_6 and Egn_7 form part of the small body of granite centred near HC980420. In the Seigal 1:100 000 Sheet area Egn_5 and Egn_6 form most of the north-central part of the MTR, and Egn_6 forms two bodies in the western part of the Sheet area (Fig. 3c). Egn_7 occurs as aplite dykes and microgranite within Egn_5 and Egn_6. Egn_5 is more extensively exposed than Egn_1 and Egn_2 because of structural controls: it crops out as series of low dome-like hills or ridges along lineaments, fault zones, or quartz veins (Fig. 6). Continuous outcrop occurs where structural zones and dykes of quartz, aplite, or feldspar porphyry are especially dense - e.g., north of the Calvert Fault, granite is exposed in a reticulate framework of quartz-feldspar porphyry dykes.

Egn_5 and Egn_6 are characterised by a more open drainage system than are Egn_1 and Egn_2.

Lithology and field occurrence

Egn_5 is a red or pink even-grained or rarely sparsely porphyritic medium to coarse massive granite. Quartz content is variable, and pink or red K-feldspar is about twice as abundant as green or pink plagioclase. Clots of fine-grained biotite and hornblende are up to 1-2 cm across; these minerals are not dispersed through the rock as they are in Egn_1 and Egn_2. Egn_6 is similar to Egn_5, but is free of mafic minerals. Quartz is commonly microporphyritic in Egn_6.

The initial weathering effects on Egn_5 and Egn_6 are the chloritisation of biotite, where present, and the sericitisation of plagioclase. Secondary effects are the oxidation of both feldspars and subsequent removal of these minerals to leave a concentrate of residual quartz. This contrasts with the K-feldspar concentrate produced by weathering of Egn_1 or Egn_2. Most of the exposed Egn_5 comprises rusty-weathered feldspars, quartz, and chloritised biotite.
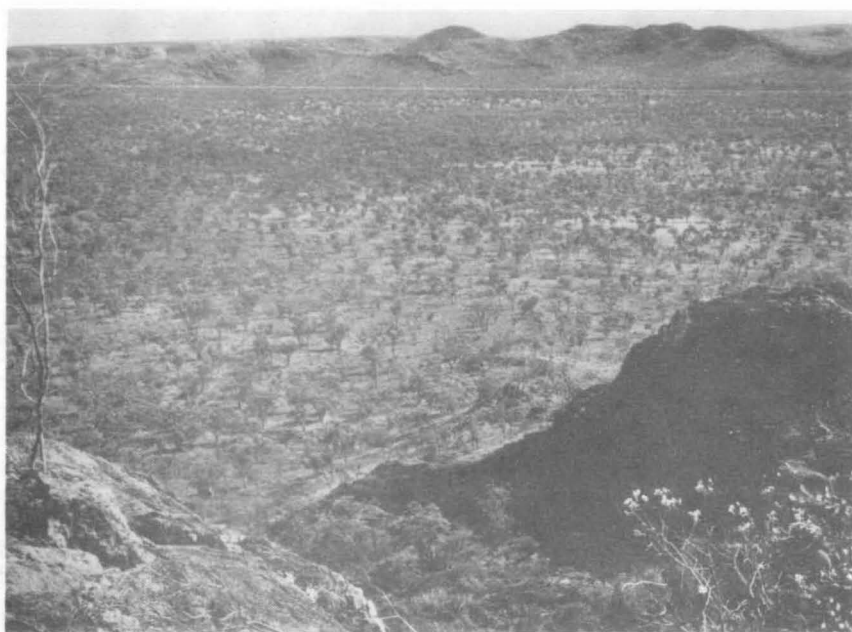
Fig. 6a. Fault ridge outcrop of Bgn_5 (foreground) projects above the adjacent Bgn_5 plain; the Cliffdale volcanics are in the background.
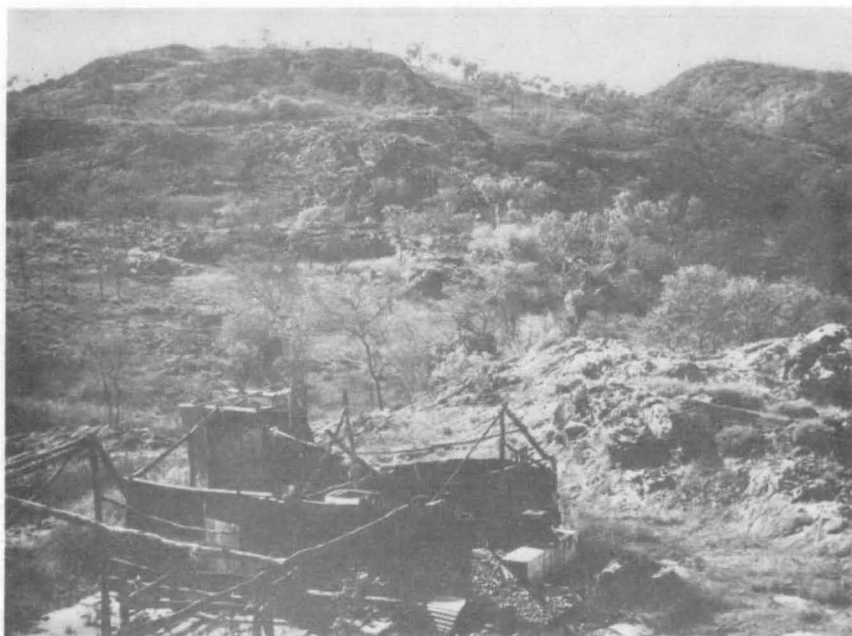
Fig. 6b. Crystal Hill tin-processing plant, with low hills of Bgn_5 in the background.

45

Egn$_7$ is pink or red, dark red or purple weathering, aplitic leuco-microgranite, rarely carrying traces of biotite, hornblende, or muscovite, and invariably fresher than the host granite. The fine, dense quartz veining in many aplites is a result of their localisation near contacts or in fault zones.

In the Hedleys Creek 1:100 000 Sheet area, contacts between Egn$_5$ and Ecc are forceful and steeply-dipping. Xenoliths of grey medium-grained porphyritic acid volcanic rocks in the granite near these contacts have been recrystallised to hornfels. Farther west, however, contacts are passive and subhorizontal and characterised by only slight recrystallisation of the country rock volcanics and decrease in grainsize of the granite. Quartz veins, greisen dykes, zones of greisenised granite, and microgranites are particularly dense in the strip of Egn$_5$ between S970360 and S890330. Quartz veins mostly trend northwards, but the greisens fill northeasterly trending joints parallel to the northern margin of the complex.

Microgranite of Egn$_7$ occurs as dyke-like masses from a few centimetres to several meters wide. Their contacts with the host granite are sharp and follow irregular non-linear paths unrelated to the regional or local structural trends. The Egn$_7$ veins are darker than the granite owing to the greater abundance of iron oxide in the microgranite, and comprise up to about 40 percent of the volume of the total rock; they are broadly contemporaneous with the granite, as the joints and narrow 'ptygmatic' quartz veins cutting the granite continue unaffected through the microgranites. There is a marked increase in the proportion of microgranite in the total rock adjacent to the China Wall contact with the Westmoreland Conglomerate, as has already been noted in Egn$_2$ west of the Fish River. The localisation of microgranite indicates a high intrusive level and proximity to the original margin of the complex. Jointing is related to the northeast-trending structural system.

Egn$_6$ intrudes the Murphy Metamorphics along a gradational contact 0.5 to 1 km wide, which consists of pink microgranite rich in muscovite, greisenised granite, and muscovite granite gneiss. These rocks are similar to rocks along the southeastern contact of the Metamorphics, but distinct from the foliated hornblende-biotite granite along the contact of the Metamorphics with Egn$_1$ and Egn$_2$.

46

The area of Egn$_6$ straddling the Fish River is cut diagonally by
a dolerite dyke (see Section VI, 'Dyke rocks') anastomosing at its western end.
The dyke parallels the east-northeast-trending structures, and runs semi-
continuously from S680225 to S060430, a distance of nearly 50 km.

Most of the area marked as Egn$_6$ west of Tin Hole Creek (Plate 1) is
covered by Cainozoic gravel and soil. The granite here is typically even-
grained medium to fine leucogranite, commonly brecciated and silicified. At
S797200 muscovite gneiss and aplite form lit-par-lit injections into muscovite-
biotite schists of the Murphy Metamorphics. The contact of Egn$_6$ with Egn$_8$ in
the west is defined on the basis of overall increase in grainsize, the occurr-
ence of biotite, and particularly, the occurrence of porphyritic muscovite. It
is likely that there are unexposed remnants of Murphy Metamorphics in this area.

Petrography (Table 6)

Egn$_5$ is medium-grained, even-grained, and sparsely porphyritic. K-
feldspar and plagioclase are equally anhedral and intergrown with quartz in
a coarse allotriomorphic granular interlobate texture (Fig. 7a). The larger
K-feldspar grains are rimmed by myrmekitic quartz-K-feldspar intergrowths
which are coarser away from the phenocrysts (Fig. 7b). The myrmekite grades
into the groundmass, a blebby interlobate intergrowth of quartz, feldspar and
plagioclase, in which inclusions of K-feldspar in quartz and of quartz in K-
feldspar are equally abundant, and are up to 0.4 mm across. Many of the
K-feldspar grains are rimmed by albite.

Optical continuity of quartz and K-feldspar is maintained over
areas several times the local grainsize (K-feldspar 0.5 - 3 mm diameter;
quartz up to 0.6 mm diameter); in particular, discrete linear, bow-shaped
and cuspate quartz inclusions are continuous within their host K-feldspar
(Fig. 7c). Areas of intergrowth are free from inclusions of other minerals.
The intergrowth texture is similar to textures described by Tuttle & Bowen
(1958) as having been produced by exsolution of sodic and potassic feldspars
from a single alkali feldspar. Thus the crystallisation sequence is:
simultaneous crystallisation of quartz and alkali feldspar, followed by
exsolution of albite, some of which migrated to the grain boundaries of
K-feldspar to form clear albite rims. Postmagmatic deposition of secondary
quartz is indicated by the occurrence of quartz veins and the replacement of

47

(a)
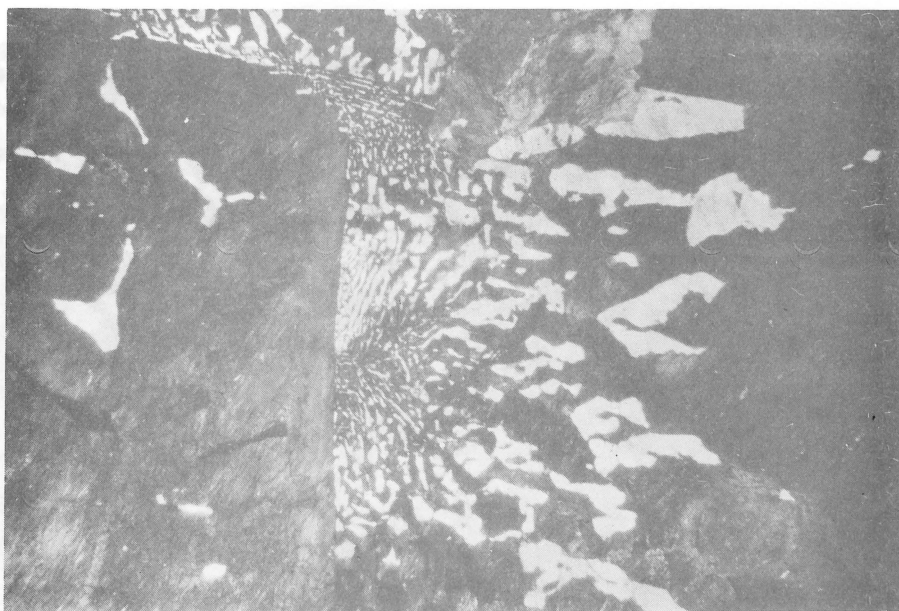
(b)

Fig. 7. Typical petrographic textures of Bgn_5 and Bgn_7.

    (a) Bgn_5: Allotriomorphic granular K-feldspar (grey, lower left, with central quartz inclusions); plagioclase (partly altered to sericite, right); biotite (dark, upper centre); and quartz (pale, right of centre). X20, crossed nicols.

    (b) Bgn_5: K-feldspar phenocryst rimmed by granophyric quartz-K-feldspar intergrowth which becomes coarsed-grained away from phenocryst. X20, crossed nicols.
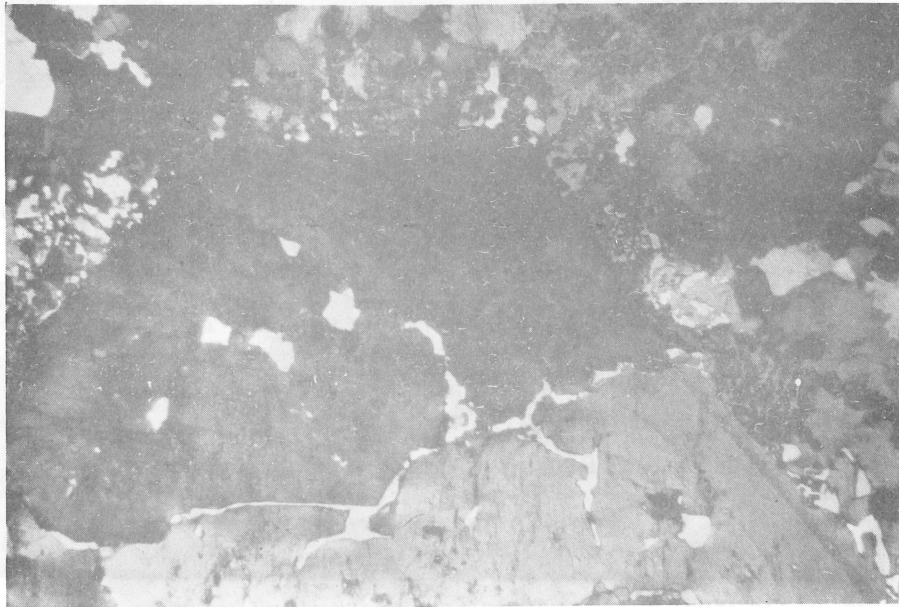
(c)
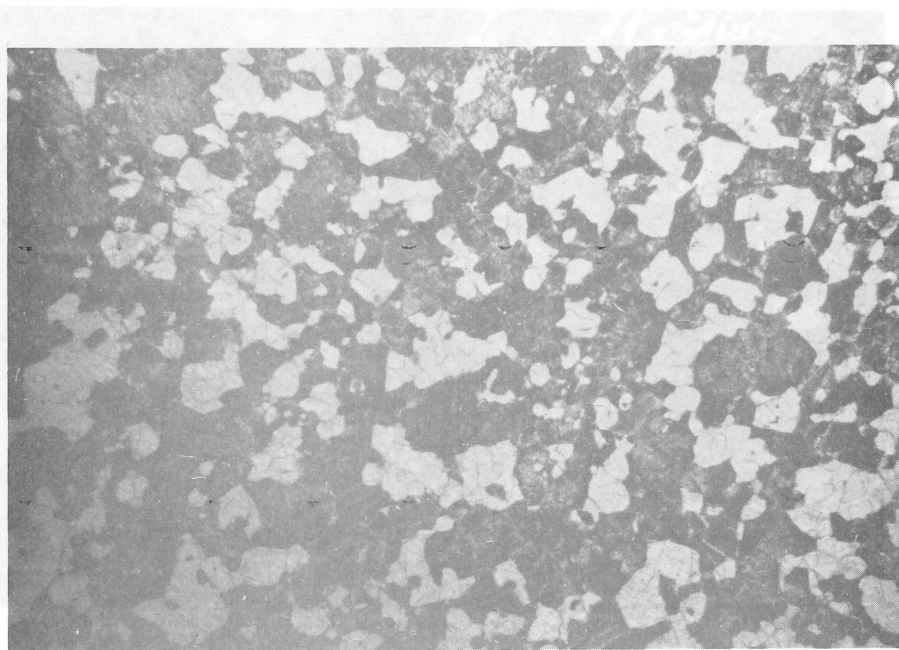
(d)

Fig. 7. (c) Bgn$_5$: K-feldspar phenocryst rimmed by recrystallised **matrix**.
Note linear and cuspate quartz inclusions in K-feldspar;
note also discontinuity within phenocryst. X20, crossed **micols.**

(d) Bgn$_7$: allotriomorphic intergrowth of quartz (pale), K-feldspar
(grey), and albite (dark grey) - the so-called 'web **structure.'**
X20, crossed nicols.

biotite by quartz. Postmagmatic overgrowth of K-feldspar at the expense of quartz may also have occurred; this possibility is discussed in the section 'Origin of the K-feldspar phenocrysts'.

K-feldspar (35%) is zoned, perthitic, intermediate or maximum microcline. Euhedral plagioclase (20%, 1-3 mm diameter) is slightly sericitised but not clouded, and carries rare hornblende and quartz inclusions. Quartz (30%) is unstrained but not recrystallised. Roughly equal amounts of fresh brown subhedral biotite and hornblende (both 0.3 - 1 mm diameter) comprise the mafic clots. Hornblende is altered to yellow-green mossy iron-rich chlorite and yellow-brown amphibole. Accessory minerals are apatite, magnetite, zircon, and monazite.

The xenoliths of Cliffdale Volcanics in Pgn_5 near forceful contacts display petrographic textures consistent with low-grade contact metamorphism. Thin-section evidence of thermal metamorphism is provided by complete recrystallisation of the groundmass to a granoblastic-polygonal texture in which metamorphic biotite marks the triple-point junctions of the quartzofeldspathic minerals (Spry, 1969). The xenoliths contain blastoporphyritic quartz, orthoclase, and sericitised plagioclase, as well as rhyolite clasts in a fine-grained recrystallised granoblastic groundmass. Incipient recrystallisation has re-formed some of the quartz phenocrysts, but embayed margins are preserved on others. The groundmass consists of roughly equal amounts of mosaic quartz, sericitised plagioclase, clear albite, and cloudy anhedral orthoclase carrying inclusions of quartz and feldspar aggregates, and is peppered with subidioblastic flakes of green and brown biotite and minor muscovite. Zircon, chlorite, sphene, and granular opaque oxides are accessory.

The rhyolite clasts are petrographically identical to, though finer-grained than, the groundmass of their host.

Pgn_6 is generally even-grained but very coarse, average grain diameter being 5 mm. Plagioclase (25%) and K-feldspar (40%) present subhedral boundaries to aggregates of polygonal quartz (25%); there is negligible intergrowth of quartz with feldspar. Alkali feldspar carries alternating coarse and fine strings of exsolved albite, rarely expanded to patches. Pgn_6 shows the same features of high-level crystallisation as Pgn_5. Both granites fall in the class of hypersolvus or one-feldspar granites (Tuttle & Bowen, 1958), in which rapid cooling favours growth of a single feldspar.

Subsequent exsolution produces perthite and a separate plagioclase. In Bgn_6 it is likely that most of the plagioclase was originally in solution in K-feldspar. The crystallisation sequence was: K-feldspar and quartz together, followed by exsolution of albite. Narrow veins of secondary quartz are abundant, and some feldspar has been replaced by quartz. Plagioclase was less susceptible to replacement by silica, but has been extensively sericitised or chloritised. Rare zircon is accessory.

In contrast to Bgn_1 and Bgn_2, Bgn_5 and Bgn_6 show evidence of having crystallised under minimal cover-rock pressure from a relatively hot magma. Intrusions contain no cognate xenoliths, and a variety of hypabyssal rocks - including granodiorite and microgranodiorite ring dykes, quartz-feldspar porphyry dykes, aplites, and microgranites - are associated with them. Unfaulted contacts are discordant, commonly chilled, and bordered by narrow metamorphic aureoles. Textures are allotriomorphic - i.e., quartz and feldspar grains are equally anhedral - indicating contemporaneous crystallisation of quartz and feldspar; had the feldspar grains crystallised earlier than the quartz, they would have developed better crystal faces. Bgn_5 and Bgn_6 are epizonal granites of Buddington's (1959) scheme.

$\underline{Bgn_7}$ (microgranite) is fine-grained, even-grained (average grain-size 1 mm), and characterised by the scarcity of mafic minerals and low accessory mineral content. It exhibits the same allotriomorphic granular interlobate intergrowth as Bgn_5: the texture is one of webs of anhedral K-feldspar (35%, 0.5-2 mm diameter) enclosing quartz (40%, 0.5-1.5 mm diameter) and albite (20%, 0.5-2 mm diameter) (Fig. 7d), indicating simultaneous crystallisation of K-feldspar and quartz, followed by exsolution of albite. K-feldspar is rarely simply twinned, carries patchily distributed string perthite, and is heavily clouded with minute inclusions of goethite, hematite, and apatite. Albite exhibits the same habit and degree of oxidation as K-feldspar; quartz shows incipient undulose extinction, and carries abundant fine K-feldspar inclusions. Accessory minerals are 2-3 percent of chlorite and one percent of opaque oxides. Replacement features are not obvious in Bgn_7.

Table 6

Estimated volume percent of minerals and summary of salient

petrographic features of Pgn_5 Pgn_6, and Pgn_7

	Pgn_5		Pgn_6		Pgn_7	
	0883	0888	0870	0816	0824	0813
Kspar	40	35	40	40	35	35
	Int- max microcline, cts medium-grained perthite		Int- max microcline, cts coarse and fine perthite		Int microcline, coarse ribbon perthite	
Plag	10	20; Ab	30; Ab	25	20; Ab	15
Qtz	30	35	30	35	40	45
Biotite	4	5	-	-	tr	3
Hblende	6	3	-	-	-	-
Muscovite	-	tr	-	-	tr	tr
Access	Zircon, fluorite, apatite, opaques, and sphene		Tr opaques, zircon		Opaques, epidote, zircon, chlorite, and apatite	
Grainsize Scheme	Medium even-grained or with porphyritic Kspar; $Kspar_p >$ $Kspar_g$ = plag $\geqslant$ qtz		Coarse ($>$ 4 mm av.) even-grained; Kspar $\geqslant$ qtz $\geqslant$ plag		Fine-grained, even-grained; quartz $\geqslant$ plag = Kspar	
Texture	Allotriomorphic granular, dominated by coarse to granophyric qtz-Kspar intergrowth surrounding phenocrysts		Allotriomorphic granular; coarsely interlobate; Kspar, plag, qtz equally anhedral; Kspar, qtz invade each other.		Allotriomorphic granular; inter-locking qtz-feldspars; both feldspars equally subhedral, oxidised, sericitised	
Inclusion Scheme	Plug-shaped Kspar aggregates carry cuspate qtz incl; qtz carries Kspar; Kspar carries biotite, plag, hblende		Kspar rarely carries qtz, plag inclusions		Kspar carries rare plag, qtz. Qtz carries rare Kspar, plag	
Replacement Scheme	Plag → sericite; biotite → qtz		Kspar → qtz; plag → sericite		Kspar, plag → sericite + opaques; Kspar, plag → qtz (not extensive)	
Other features and comments	Myremekitic qtz-plag intergrowth commonly invades Kspar; extensive potash metasomatism, also silica alteration		Isochronous crystallisation of Kspar, qtz, plag. Some silica, potash alteration			
Xenoliths	-		Country rock xenoliths near contacts		-	
Classification	Albite-microcline granite		Albite-microcline leucogranite		Albite-microcline microgranite	

$$\underline{Pgn}_8$$

Field relations

Pgn_8 is white aplitic muscovite-bearing microcline-albite leuco-
granite. It crops out in small fault-bound blocks in marginal areas between
intrusions of the other phases. Although occurring within the area pre-
viously mapped as Nicholson Granite, it is lithologically and chronologi-
cally more closely related to the younger granites Pgn_5 and Pgn_6.

Pgn_8 represents the last stage of intrusive activity, as it
intrudes Pgn_2, Pgn_5, and Pgn_6. Several samples of Pgn_8 from S805255 have
been dated by the whole-rock Rb-Sr method at 1773 $\pm$ 56 m.y. (Webb, 1975).

Distribution and exposure

Pgn_8 crops out in four large areas and two (or more, but undifferen-
tiated) small ones (Fig. 3d; Plate 1): an irregular partly fault-bound
block centred on S964312; a similar-sized block centred on the Fish River
fork, S858295; a belt crossing the Fish River near its confluence with Tin
Hole Creek at S890200; and an irregular block in the southwestern corner of
the Seigal 1:100 000 Sheet area.

Lithology and field occurrence

Pgn_8 shows local differences in lithology - the largely
fault-bound block centred on the Fish River fork is medium or very coarse
even-grained granular white granite with or without minor clotted biotite,
in places carrying small basic xenoliths. Both feldspars are white, or
plagioclase is pale pink, and euhedral; quartz forms more than 35 percent,
commonly 45 percent of the rock. The leucogranite grades locally into pale
pink finer-grained granite with minor biotite, and westwards into coarser
white granite with minor biotite and into white aplitic leucomicrogranite.
Quartz-biotite and quartz-muscovite pegmatites are commonly associated with
Pgn_8. Outcrop is usually fresh, or, if oxidised, orange-brown instead of
white. Biotite alters to a pale golden pseudomorph identified by XRD as
vermiculite.

54

Fig. 8. Typical petrographic texture of Bgn$_\emptyset$: typical allotriomorphic
granular intergrowth of K-feldspar (centre, white or dark grey);
plagioclase (dark, white-spotted); muscovite (mottled left of
centre); and quartz (white, upper right of centre, or black,
interstitial). X20, crossed nicols.

The block of Egn_8 centred on the Fish River fork grades southwards into Egn_6. Aplite, greisen, basalt, and diorite dykes are abundant, and cut Egn_8 and Egn_2 between the fault zone through S858207 and the Egn_8/Egn_2 contact through S785280. Pods of coarse-grained biotite granite, porphyritic hornblende-biotite granite, and a probable Elm remnant have been exposed through faulting in this area.

The eastern part of the irregular block centred on S964312 is composed of pink, even-grained medium biotite granite. The predominant rock type in the southern and western parts of this area is massive white microgranite rarely carrying hornblende-plagioclase xenoliths. Sheared and silicified granite and quartz-feldspar porphyry, granodiorite, and aplite dykes are found near contacts with Egn_2.

The small stock of Egn_8 intruding Egn_2 at S807250 carries about 40 percent quartz, biotite, muscovite, and accessory garnet.

Egn_8 is poorly exposed in the areas near the confluence of the Fish River and Tin Hole Creek and in the western corner of the MTR, where it is a dense aplitic white or pink muscovite microgranite commonly greisenised and locally extensively brecciated and silicified. The microgranite is in contact with coarse muscovite gneiss of the Murphy Metamorphics at S903222. Pegmatitic muscovite veins up to 0.5 m wide are abundant near the contact, and are common up to several kilometres away from it. The concentration of muscovite pegmatites near the metamorphics suggests that the veins were produced by mixing of metamorphics with microgranite.

Petrography (Table 7)

Egn_8 is distinguished from the other granites by its generally finer and more even grainsize, the presence of muscovite rather than biotite or hornblende, and its higher quartz content. Except for Egn_1, Egn_8 has a higher plagioclase/K-feldspar ratio than the other granites. Grainsize is slightly variable up to about 1 mm, but the rock is everywhere even-grained. Anhedral quartz and microcline are intergrown with subhedral plagioclase in a coarse blebby interlocking mosaic (Fig. 8). The order of crystallisation appears to have been: plagioclase and quartz simultaneously, followed by K-feldspar. In medium-grained Egn_8, perthite is generally poorly developed - fine perthitic albite has exsolved along the microcline twin planes only. Compared with Egn_1 and Egn_2, K-feldspar has fewer inclusions, and plagioclase, muscovite, and K-feldspar are more extensively replaced by quartz.

Muscovite is usually present to the exclusion of mafic minerals, but it may be accompanied by minor biotite. Both are finer-grained than the quartzofeldspathic minerals - muscovite ranging from 0.5-1.0 mm diameter, and biotite from 0.3-0.4 mm diameter. Crystallisation of the two was apparently simultaneous, as both possible cross-cutting relations are seen. Both micas are replaced by quartz. Up to 10 percent cordierite occurs in one sample.

The microgranites are aplitic, with rectangular subhedral microcline (30%, 0.5-1.5 mm diameter), equant subhedral albite (20%,, 0.5 mm diameter), and quartz (40%, 0.2-1.0 mm diameter) interlocking in jigsaw fashion. Microcline generally includes sharply bounded, coarse strings of exsolved albite which in the larger K-feldspar grains have coalesced to form patches separated from their host by a transitional boundary. Rounded or cuspate quartz inclusions, often mantled by plagioclase, are common in the K-feldspar, and biotite and small plagioclase inclusions occur sparsely. Quartz and microcline commonly replace each other. Slightly sericitised albite is irregularly twinned and commonly mantled by quartz, and carries quartz inclusions; the reverse relation is also observed. About 5 percent of dark green-brown biotite and slightly less abundant muscovite (1.0-1.5 mm diameter) generally lie parallel to adjacent feldspar grain boundaries. The abundant accessory minerals comprise apatite, fluorite, calcite, monazite, and zircon. Pegmatites of Pgn_8 consist of white medium to coarse granite with about 10 percent of porphyritic muscovite.

Weathering of the pegmatites has been extensive, and roughly 30 percent each of the K-feldspar and plagioclase (albite?) can now be distinguished only by the smaller average grainsize - 1.0 mm vs 2-3 mm - and greater degree of sericitisation and oxidation of the plagioclase. Both feldspars are anhedral to subhedral, but albite grains tend to be connected in web-like chains. Perthitic albite was not observed. Quartz (30%, 1 mm diameter) is free from inclusions. Euhedral but penetrated muscovite (up to 3 mm diameter) is primary but only rarely partly altered to mossy brown iron-rich chlorite. The muscovite displays slight pleochroism (colourless-beige) reflecting high iron content, although no opaque oxides or any other accessory minerals are found.

Table 7

Estimated volume percent of minerals and summary of salient

petrographic features of Pgn_8

	0855C	0853	0926	0858	0864A
Kspar	30	25	28	15	20
	Microcline, and coarse microcline perthite				
Plag	25	25: Ab	30	15	25
Quartz	40	35	35	35	30
Hblende	-	3	-	-	-
Biotite	1.5	-	tr	-	-
Muscovite %	3.5	7	7	7	20
Cordierite	-	-	-	10	-
Access	Apatite, zircon, fluorite, opaques, calcite, geothite, monazite, sphene, and garnet				
Grainsize Scheme	Medium fine- or coarse-grained, even-grained; Kspar $\geqslant$ plag $\geqslant$ qtz, but variable, depending on abundance				
Texture	Distinctive granophyric intergrowth of branching qtz & feldspar grains; Kspar invaded by groundmass				
Inclusion Scheme	Kspar carries qtz, plag, muscovite, biotite; plag carries qtz, muscovite; qtz carries plag				
Replacement Scheme	Kspar→qtz; muscovite→qtz; plag→qtz, sericite				
Other features and comments	Myrmekite common; silica alteration more extensive than potash metasomatism.				
Xenoliths	-				
Classification	Microcline-albite granite				

57

The greisenised granites show textures intermediate between the original granite and the quartz-sericite greisens. They are slightly gneissic fine to medium rocks consisting of ill-defined bands of which alternate ones are richer in micaceous minerals. These bands also show a vague foliation. The thin section texture is similar to that of Egn_8. K-feldspar (20%, 0.5-1.2 mm diameter), plagioclase (20%, 0.5-1.0 mm diameter), and quartz (30%, 0.5-1.0 mm diameter) are interlocked in jigsaw fashion, and grain junctions are marked by mafic clots (20%). K-feldspar is anhedral or subhedral and invaded by other minerals. It is distinctive in its excellent cross-hatched twinning pattern and in its replacement relation with quartz: larger coalesced K-feldspar grains carry bow-shaped or U-shaped blebs and stringers of quartz which merge with a coarse intergrowth of quartz and K-feldspar surrounding the larger grains. Subhedral plagioclase is barely recognisable as it is oxidised and completely sericitised; the sericite has partly recrystallised into coarser grains. The mafic clots consist of ragged muscovite, sericite, biotite (partly altered to aluminous chlorite), opaques, and sphene; most of these minerals are more or less sericitised. Apatite and zircon are accessory.

The presence of muscovite in Egn_8 and the association of greisen with Egn_8 suggest a high-level, late-stage, residual-melt origin for this granite (Marmo, 1971).

ORIGIN OF THE K-FELDSPAR PHENOCRYSTS

Granite crystallisation takes place under decreasing temperature and pressure; thus the completion of crystallisation occurs at a lower temperature and pressure than did the start of crystallisation. There will thus be a strong tendency during crystallisation for minerals to recrystallise and be resorbed in an attempt to maintain equilibrium under changing pressure-temperature regimes. Granites which have been uplifted since they solidified are moved to an even lower-temperature, lower-pressure regime than that under which they are crystallised, and will undergo a series of secondary reactions. Various replacement and recrystallisation reactions that may have occurred during or after initial crystallisation must be considered when deducing the sequence of crystallisation of minerals in a granite.

The simplest order of crystallisation of the quartzofeldspathic minerals for the porphyritic granites Pgn_1, Pgn_2, and Pgn_{3-4}, based on the relative sizes of the minerals and their boundary relationships, is: K-feldspar phenocrysts, joined by interstitial albite, then joined by interstitial quartz. Following Sheraton & Labonne (1978), however, the nature of the inclusions within the K-feldspar phenocrysts is taken to suggest an alternative sequence: some K-feldspar, crystallising as even-grained subhedral or anhedral crystals, joined by albite and quartz. When crystallisation was complete, the small K-feldspars recrystallised and reoriented themselves at the expense of neighbouring minerals, and formed porphyryblasts. Under magmatic conditions, K-feldspar has a very low force of crystallisation, and does not form phenocrysts even if the K_2O activity is high; under metasomatic - i.e., deuteric - conditions, however, euhedral crystal faces tend to develop on K-feldspar (Marmo, 1971).

Figure 9a shows a single K-feldspar phenocryst carrying inclusions of quartz, albite, hornblende, and biotite. This is not an intergrowth texture, and suggests that the crystallisation of the host K-feldspar postdated crystallisation of the inclusions.

The most common mineral included in K-feldspar is quartz, which occurs in linear, cuspate (Fig. 9b), or bow-shaped grains, always in optical continuity. The cuspate form of the quartz inclusions is produced by the inwardly concave boundaries of the grains, as if the quartz is interstitial to two or more inward-pointing plug-shaped subgrains, as in Figure 9b. The quartz is unlikely to be an exsolution or replacement product, as isolated grains are randomly oriented with respect to the crystallographic planes of the host, and are in optical continuity. The texture indicates replacement of quartz by K-feldspar after initial intergrown crystallisation of quartz and K-feldspar from the magma.

The suggested crystallisation sequence for these grains, following Marmo (1971) and Orville (1962) is: 1. magmatic precipitation of K-feldspar albite, and quartz; 2. redistribution of alkalis on a small scale via a fluid phase, which is still present in the closing stages of crystallisation: transferral of K from the fluid phase to the feldspar boundaries so that they grow at the expense of surrounding quartz and albite grains, and removal of Na from the crystals to the fluid; 3. growth of adjacent K-feldspar grains towards each other to reduce grain boundary stress by eliminating grain boundaries; grains form plug-ghaped protrusions into each

Fig. 9. Petrography of K-feldspar phenocrysts.
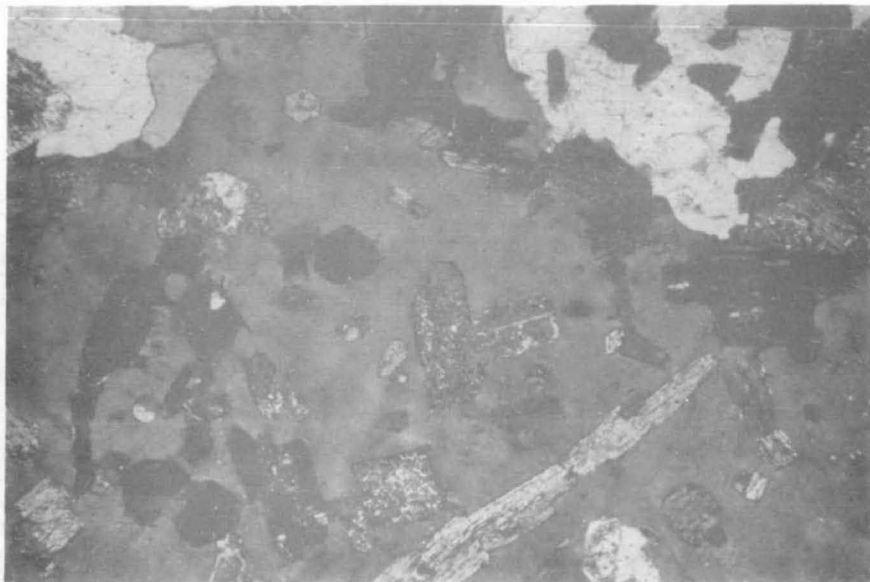
Fig. 9a. Inclusions of albite (mottled), quartz (white),
          biotite (grey, lathlike), hornblende (black, pseudo
          hexagonal) in poikilitic K-feldspar phenocryst.
          X35, cross nicols

Fig. 9b. Linear and cuspate quartz inclusions (white) in
          K-feldspar phenocryst. X35, cross nicols

60

Fig. 9c. Granite groundmass included in perthitic K-feldspar
phenocryst. X35 cross nicols

Fig. 9d. Irregular boundary between adjacent K-feldspar
phenocrysts; groundmass inclusion within lower
phenocryst. X35, cross nicols.

Fig. 9e. Cross-hatched twinned K-feldspar phenocryst carries
          stellate groundmass inclusion - phenocryst is made
          up of inward-pointing plug-shaped areas, relic
          grains. X35, cross nicols.

Fig. 9f. Recrystallised groundmass adjacent to K-feldspar
          phenocryst. Edge of inclusion-free part of pheno-
          cryst is relict grain boundary. X35, cross nicols.

other (Fig. 9d); 4. small-scale recrystallisation of adjacent grains pro-
duces an euhedral crystallographically continuous K-feldspar phenocryst
(Fig. 9e); 5. the groundmass often recrystallises under the stress induced
by the growing phenocrysts (Fig. 9f).

DISCUSSION

Intrusions within the Nicholson Granite Complex follow a pattern
observed in many igneous complexes: that of a series of related intrusions
emplaced at successively higher crustal levels with time. Buddington (1959)
refers the formation of such complexes to three levels of emplacement: the
epizone, which lies above the level of greenschist facies metamorphism; the
mesozone, which corresponds to the zones of greenschist and lower amphibolite
facies metamorphism; and the catazone, which corresponds to the zone of
upper amphibolite and granulite facies metamorphism. Anatectic granite melts
are generated in the catazone, and may crystallise in situ or may migrate to
the mesozone or epizone before solidifying. Volatile-saturated or near-
saturated melts will crystallise within the catazone as concordant elongate
foliated bodies surrounded by a regional aureole with associated migmatites,
granite gneisses, and pegmatites. Melts that reach the epizone produce vol-
canics initially, but the sudden release of pressure accompanying extrusion
causes the remaining magma to crystallise rapidly. This produces subvolcanic

discordant circular intrusions surrounded by narrow contact aureoles and acc-
ompanied by porphyry dykes, ring dykes, granophyres, and chill zones. Epi-
zonal granites are distinguished from deeper granites by field, petrographic,
and chemical evidence of high-level pressure-quenched isochronous crystalli-
sation. The mesozonal granites are intermediate between epizonal and cata-
zonal granites - they are not associated with metamorphic rocks from the
source area of the granites, neither are they associated with volcanic or
subvolcanic rocks.(Buddington, 1959).

The microcline-albite and albite-microcline granites Pgn_1, Pgn_2,
and the older granodiorite stocks of Pgn_{3-4} are the oldest exposed rocks of
the complex, and show features characteristic of mesozonal intrusions. If
they were catazonal granites they would be enveloped by higher-grade rocks
than the greenschist-grade Murphy Metamorphics. Contacts with the metamor-
phics are partly conformable, and consist of a zone of migmatitic and lit-
par-lit rocks grading from mica schists and gneisses into foliated hornblende-

63

biotite granites. Apart from schlieren derived from the metamorphics, Bgn_1 carries few xenoliths. Bgn_2 carries a higher proportion of basic xenoliths but is more acid than Bgn_1 -- i.e., it has lower mafic content, lower hornblende/biotite ratio, and lower plagioclase/total feldspar ratio than Bgn_1. The close spatial and temporal relations between Bgn_1 and Bgn_2 have already been described. The field relations and petrographic features of Bgn_2 are consistent with its having crystallised as a high-level differentiate of Bgn_1.

Bgn_5, Bgn_6, and Bgn_8 are high-level epizonal granites, whose intrusion was preceded and accompanied by emplacement of quartz-feldspar porphyry dykes and the younger granodiorite ring of dykes of Bgn_{3-4}. Contacts between Bgn_5 and the Cliffdale Volcanics are generally discordant. The abundant aplites, chill zones, and greisens; the scarcity of cognate xenoliths; and the petrographic evidence of isochronous crystallisation of quartz and feldspars -- are further indicators of the shallow depth of crystallisation of Bgn_5, Bgn_6, and Bgn_8.

DYKE ROCKS

        Dyke rocks within the granites include the following:-
  i)   (quartz-) feldspar porphyry
 ii)   aplite and microgranite
iii)   dolerite and basalt
 iv)   greisen
  v)   quartz

Porphyry dykes

        The porphyry dykes range in composition from granodiorite to granite. The proportion of phenocrysts to groundmass and the relative amounts and sizes of phenocrystic minerals differ from dyke to dyke. The phenocrysts may comprise any or all of the following: plagioclase, K-feldspar, quartz, biotite, and hornblende. The K-feldspar phenocrysts are euhedral and white or pink, and commonly reach 6 cm in length; the plagioclase phenocrysts are euhedral, pale green, and up to 1.5 cm long; the quartz phenocrysts are subhedral and up to 1 cm long; and the biotite and hornblende

phenocrysts are subhedral and invariably smaller than the quartz and feldspar phenocrysts, and are mostly about 0.5 cm long. Dykes cut by Pgn_5 carry phenocrystic quartz, plagioclase, K-feldspar, biotite, and hornblende; dykes which cut Pgn_5 do not carry quartz phenocrysts. Basic xenoliths are common. The phenocrysts and xenoliths are randomly set in a pale grey or dark greyish pink aphanitic groundmass. Porphyry dykes cut all units of the Cliffdale Volcanics, Pgn_2, and Pgn_5. In the Hedleys Creek 1:100 000 Sheet area and between the Calvert Fault and the fault between the Cliffdale Volcanics and Westmoreland Conglomerate in the Seigal 1:100 000 Sheet area, porphyry dykes cut Cliffdale Volcanics in a dense reticulate pattern; some occur as offshoots of Pgn_5. Dykes are less plentiful in the granites than in the volcanics. The distribution of the dykes provides evidence that dyke emplacement largely preceded but also accompanied and followed intrusion of Pgn_5 and Pgn_6. South of the Calvert Fault, porphyry dykes cut Pgn_5 and Pgn_2 at several localities: SO34414, S975347, S845309, and S028388. Outcrop is generally very good, and takes the form of fresh rounded boulders with distinctive pitted surfaces produced by preferential weathering of plagioclase and hornblende. The dykes have positive topographic relief relative to the granite they cut. Airphoto-pattern is characteristic, and differs with lithology: dykes of granitic composition (e.g., at SO34414) have a white and red mottled pattern reflecting the sparse vegetation they support, and those of granodioritic composition have a smooth, darker, green airphoto-expression. The porphyries weather reddish white or greyish white, and produce a dark red soil. They fill linear and sublinear joints and faults, and are from several hundred metres to 4-5 km long, though most are between 0.5 and 2 km. Maximum width is about 20 m; short dykes are much narrower - from 3 to 4 m. Wider dykes are commonly zoned from a narrow outer margin in which quartz and feldspar phenocrysts are set in a dark aphanitic groundmass, to a central core in which the same phenocryst minerals (same composition, grainsize, and density) are set in a lighter-coloured coarser-grained granophyric groundmass. The contact between the outer margin and the core is sharp. Some of the larger acid dykes contain basic xenoliths up to 50 cm across. Contact aureoles were not observed in the granite adjacent to dykes.

The dyke at S034414 is about 20 m wide, and cuts volcanics and granite for 2.5 km parallel to the Calvert Fault, but is slightly deflected at the granite/volcanic contact. The rock is a massive granodiorite composed of 20 percent plagioclase phenocrysts (average 5 cm across), 15 percent hornblende-biotite clots (average 3 cm across), 10 percent K-feldspar microphenocrysts* (average 0.1 cm diameter), commonly associated with mafic clots, set in a pinkish-brown aphanitic groundmass. No zonation was observed. The groundmass is a structureless microcrystalline intergrowth of quartz, groundmass is a structureless microcrystalline intergrowth of quartz, alkali feldspar, and opaques, sphene, biotite, chlorite, and epidote. Zircon, apatite, and zoisite are accessory.

The dyke through S975347 is 12 m wide, and extends for 1.5 km parallel to the northern margin of the complex. The granite shows not contact effects, and the dyke is not zoned. Although of similar composition to that at S034414, this dyke carries fewer phenocrysts in a dark grey microcrystalline groundmass.

Small plugs of porphyry at S845309 intrude Egn_5; similar plugs are associated with basalt at S843305 and with microgranite dykes and granodiorite ring dykes, indicating that this area is part of a zone of localisation of late-stage magmatic activity.

Petrography

Phenocrysts constitute up to half of the section of the dyke at S034414. Plagioclase (15-20%,,up to 7 mm across) is simply-twinned, usually sericitised, and contains inclusions of biotite, hornblende, and epidote. K-feldspar (7-15%, up to 2 mm across) is also sericitised and commonly inter-grown with biotite and amphibole. Deep red biotite (12%, up to 4 mm across) is altered in lenses or at its ends to green chlorite. Amphibole (7%, up to 0.5 mm across) is replaced by aluminous chlorite and epidote. Clinopyroxene (5%, up to 0.5 mm across) is also chloritised. The groundmass comprises

---

* Many of the dykes are made up of minerals of three distinct grainsizes, which are referred to as phenocrysts, microphenocrysts, and groundmass. The term 'microphenocryst' is used qualitatively to indicate the middle grainsize group of a trimodal distribution of grainsizes, and does not have any quantitative significance.

quartz, alkali feldspar, opaque oxides, biotite, sphene, epidote, and accessory zircon, apatite, and zoisite. Grain boundaries are vaguely defined, as if the quartz and feldspar were formed by the devitrification of glass. The extensive replacement of the mafic minerals by chlorite and epidote and of the feldspars by sericite suggests hydrothermal alteration. K-feldspar phenocryst-bearing dykes commonly contain microphenocrysts of plagioclase or biotite. Apart from size differences between the phenocrysts, the texture of these dykes is similar to that described above.

The porphyry dykes may be divided into two groups on the basis of field relations and petrography. Dykes of the first group intrude Egn_2, are of granitic composition, and carry phenocrysts of quartz and K-feldspar only. Dykes of the second group intrude the Cliffdale Volcanics and Egn_5, are of granodioritic composition, and do not carry phenocrystic quartz. The order of phenocryst formation in the second group is plagioclase, followed by biotite accompanied by hornblende, followed by K-feldspar. The change in the proportions of the phenocryst minerals in the second group of dykes is accompanied by an overall decrease in the size of the phenocrysts relative to the first group. The smaller grainsize of the phenocrysts, coupled with the absence of quartz, suggests that the second group of dykes was derived from shallower levels than was the first group of dykes - levels where quartz was no longer a liquidus phase (Green & Ringwood, 1968). The inferred shallower level of derivation of dykes of the second group suggests that they are younger than dykes of the first group.

Chemical analyses of the dykes at S034414 (not listed in Table 9) and S975347 (Table 9, No. 36) show that these rocks are similar in composition to several of the granodiorite ring dykes (Table 9, Nos. 10, 11, 13, 14) and to the xenolith in Egn_2 (Table 9, No. 9).

Aplite and microgranite dykes

The microgranites have been described as Egn_7, and summaries only are given here.

Microgranite is abundant as chill zones within Egn_5, and as dykes and chilled margins, mainly near contacts - e.g., in the areas between S940340 and S960360, and between S020365 and S060374 (Fig. 3c); aplite dykes occur throughout the complex, but more commonly in Egn_2, Egn_5, and Egn_6 - e.g.,

67

at S932315, S851312, S920250, S854271, S866234, and S031283. Silicified aplite is abundant along fault zones - e.g., at S982360, S016378, S031361, and S010350.

The microgranite is invariably fresher than the granite host, and crops out as regular jointed blocks (Fig. 10a, b) with finely etched weathered surfaces. Because the microgranite is less susceptible to weathering than its granite host, the percentage of total outcrop is higher in areas where microgranite is abundant.

Contacts of dykes and chilled margins with granite are sharp and vertical. The microgranite dykes are unzoned, range from 10 to 20 m wide, and are of various lengths though most are less than 60 m long. Dykes away from contacts of granite with country rock tend to be longer and narrower and more aplitic in that they are free from mafic minerals. On weathering, plagioclase turns purple as it is replaced by sericite and hematite. Biotite in the microgranite weathers to chlorite or yellow clay. This is commonly removed, and secondary quartz deposited in the spaces.

Texture as seen in thin section is described under Pgn_7. The microgranites are generally even-grained and medium-grained and granular. Roughly equal proportions of anhedral K-feldspar, plagioclase, and quartz are coarsely interlocked, and each mineral contains inclusions of the other two. Phenocrysts of K-feldspar and quartz are rare. High iron content and high oxidation state are reflected by the abundance of hematite and goethite. Minute rounded goethite grains frequently form nuclei in quartz grains.

Dolerite and basalt dykes

One major dolerite dyke and four smaller ones occur in the basement. The oldest basalts in the area are the Peters Creek Volcanics.

The longest dolerite dyke can be traced from near the western edge of the Seigal Sheet area (at S680225) eastwards almost continuously for 50 km, intersecting the Calvert Fault at S043414. Dolerite collinear with this dyke can be traced on the northern side of the fault. Although the faulting post-dated dolerite emplacement, the dyke is not displaced laterally by the fault, indicating that movement was restricted to vertical displacement. Three of the smaller dykes are restricted to the Cliffdale Volcanics. The fourth intrudes Pgn_1 at S100313, and is 2 km long and 30 m wide.

The dolerite crops out poorly as rounded, etched, red-weathering boulders in dark red soil, which in many places has crept so that it does not coincide with the original location of the dyke.

The longest dyke is fine to medium, even-grained tholeiitic dolerite. It is deuterically altered, but not metamorphosed. The average width of this dyke is about 50 m; small offshoots are much narrower. Over most of its extent it forms a linear vertical intrusion parallel to the east-northeast structural trends except where the dyke is offset or locally coincides with cross-faults. The dolerite is displaced along faults parallel to the Calvert Fault, east of the Fish River. The dyke becomes irregular and anastomoses west of this locality, trending east-west rather than east-northeast.

At S028397, the dolerite is apparently cut by granite belonging to Egn_{3-4}, although the two were not actually seen in contact.

Small basalt dykes occur at S843309.

Relatively fresh samples of the longest dyke from S000380 (0876), S039410 (0916), and S954343 are medium, even-grained tholeiitic dolerites in which plagioclase laths, pyroxene prisms, and opaque oxide subhedra form a subidiomorphic groundmass carrying sporadic plagioclase phenocrysts. The estimated volume percentage of minerals in two of these rocks is given in Table 8. The plagioclase is unzoned and almost completely replaced by a fine-grained aggregate of sericite, opaque oxides, and epidote. Alteration of the clinopyroxene is variable. Small grains are usually fresh or only corroded along their margins, the marginal minerals being a mixture of pale brown amphibole and epidote; these grains display simple twinning and ex-solution traces. Larger clinopyroxene grains are completely replaced by dark yellow-green chlorite and opaque oxides. Small subhedral brown unaltered orthopyroxene grains are associated with the coarser-grained clinopyroxene. Quartz is present as primary interstitial polygonal grains and also in myrme-kitic intergrowths surrounding plagioclase. Secondary dark brown fine-grained biotite is also interstitial. Accessory apatite forms minute inclusions in quartz.

Near the western margin of the Seigal Sheet area, the longest dyke is basaltic and lithologically similar to nearby outcrops of Seigal Volcanics (Sweet & Slater, 1975). From this, it is considered that the dolerites may belong to the same basic igneous activity which produced the Seigal and Peters Creek Volcanics.

Table 8

Estimated volume percent of minerals in dolerites

	0876	0916
Plagioclase (An$_{70}$)	30	36
Orthopyroxene	7	7
Clinopyroxene	33	23
Amphibole	10	10
Biotite	5	5
Quartz	5	5
Opaque oxides	3	7
Chlorite	5	5
Epidote	2	2
Apatite	tr	tr

Greisen

Hatch, Wells, & Wells (1961) distinguished three types of greisen, i.e., rock formed by the action of the pneumatolytic components of a magma. The pneumatolytic fluid may modify existing granite, and produce the first type of greisen, or it may enter veins or joints and form primary dykes, the second type of greisen. The third group of greisen comprises large apophyses of quartz-white mica rock not related to granite fissuring; these masses may be the product of crystallisation of a late-stage magma fraction driven upwards from the main granite by filter-press action (Hatch and others, 1961).

Greisens of all three of these types are associated with the Nicholson Granite Complex. The first are described as greisenised granite, the second as greisen dykes; the greisen at Crystal Hill falls in the third group. Outcrop of the greisens is usually good.

70

Partly greisenised granite in which feldspars are still recognisable crops out extensively in the southern part of the complex around S940220, within the area mapped as Bgn_8. Aggregates of fine-grained sericite pseudomorphs after feldspar are preserved in some greisenised granite samples, whereas ragged webs of mica enclose granular quartz in others. Complete disaggregation of the sericite is accompanied by recrystallisation of quartz to produce a poikilitic texture in which mosaic quartz includes disseminated sericite. Intermediate stages in the greisenisation of granite are evident at S800205, in which signs of two original feldspar types can still be distinguished, although K-feldspar has been replaced by pale sericite, and plagioclase has been replaced by dark sericite and released opaque oxides; paler, coarser-grained mica has nucleated at cleavage intersections. Feldspar outlines are no longer recognisable in a specimen from S802200; this rock is composed of polygonal quartz and two generations of mica, the dark sericite being partly replaced by pale fine-grained muscovite.

Greisen dykes as fault and joint fillings of quartz-sericite rocks are concentrated in the northern part of the MTR, in an area centred on S010380, and occur less commonly in the fault-bound strip 1.5 km wide which extends southeast of this area, as far as the Fish River. The greisen-filled fault zones are mainly parallel to the northwestern contact of the granite with the Westmoreland Conglomerate, and are most abundant where these fault zones intersect those parallel to the Calvert Fault. The dykes are up to several metres wide and 1 to 2 km long. Frequently dolerite or porphyry is superimposed on a greisen dyke - e.g., at S016389, the photo-pattern and soil are doleritic but outcrop is of the older greisen.

The greisen dykes crop out as fine to medium, green to grey jointed blocks of quartz and sericite, which are tightly intergrown to give the rock a massive structure. They are cut by abundant narrow quartz veins, and are quite distinct in appearance from the unaltered granite. Colour is patchy and variable, depending on the amount of sericite present.

The largest greisen is the Crystal Hill greisen, an area of outcrop 0.5 km in diameter, centred on a ridge parallel to the Calvert Fault, and one of the dominant topographic landmarks in the MTR. It is characterised by the same mineralogy and photo-pattern as the zones of greisenised granite, but is an apparently primary plug. Other smaller plugs consisting of quartz, muscovite, biotite, and minor feldspar intrude Bgn_2 in the Fish River area - e.g.,

at S880220 and S845213; they are less than 5 m across, and carry chalcopyrite.
In hand specimen the Crystal Hill greisen is granular rather than massive:
coarse polygonal quartz and dark iron-rich muscovite occur in hypidiomorphic
granular texture rather than as intergrown grains, but the relative proportions
of each differ from sample to sample. Quartz ranges from 30 to 70 percent.
Where muscovite content is high, the rock is more massive and hand specimen
appearance approaches that of the greisen dykes. Pegmatoidal fractions carrying
cassiterite, fluorite, topaz and wolframite are associated with the greisen.

In thin section the Crystal Hill greisen is seen to consist of a
regular mosaic of unstrained irregular to polygonal quartz (0.5-5 mm dia-
meter), and slightly finer-grained muscovite as separate flakes up to 2 mm
long or as clots, both at triple or double quartz-grain boundary junctions.
Although brown in hand specimen, the mica is iron-rich muscovite, pleochroic
from colourless to pale brown, with a distinctive banded appearance imparted
by inclusions of exsolved goethite lenses. Magnetite inclusions are also
common. Quartz carries inclusions of muscovite, magnetite, and goethite, the
latter usually as a nucleus at the centre of the quartz crystal.

Quartz veins

Quartz is the most abundant dyke rock, occurring as silicification
along faults as well as massive veins probably not controlled by faulting.
The concentration of quartz veins in areas of outcrop of Egn_5 is responsible
for the greater topographic relief of this phase, as these dykes, flanked by
granite, form resistant ridges from a few metres to 5 km long, rising up to
20 m above the local topography (the Calvert Fault is much higher - 60 m).
Although occurring in all orientations, most fault-controlled
quartz veins occur in north-south tensional zones. Goethite, limonite, and
hematite are associated with these veins, and minor copper mineralisation
occurs rarely. Two veins at S885289 and S116337 are amethystine.

VII STRUCTURE

The dominant structure in the Murphy Metamorphics is a west to
northwest-trending foliation; the plane of schistosity is vertical or near-
vertical. The linear form of the intruding Nicholson Granite Complex is east-
northeast - i.e., it is slightly oblique to the foliation in the Murphy

Metamorphics. Secondary foliations in the metamorphics, however, are parallel
to the main east-northeast trends in the granites or to the Fish River Fault
Zone, the southern margin of the Murphy Tectonic Ridge (Sweet & Slater, 1975).

The structure of the MTR is controlled by two intersecting fault
systems: one trending east-northeast, parallel to the northern margin of the
complex - the Tin Hole Hinge Line (Roberts, unpubl. ms); and a younger cross-
cutting northwest system, parallel to the Calvert Fault (Fig. 11).

The older system is expressed by:

i) two major fault zones, in parts silicified, collinear with the
northern and southern margins of the Tawallah Group inlier at the
western end of the ridge. Only a little movement has taken place
along these faults;

ii) the strike direction of the Westmoreland Conglomerate north of
the Tin Hole Hinge Line and within the Tawallah Group inlier.
The older system controlled deposition of the Westmoreland
Conglomerate;

iii) the trend of the dolerite dyke from east of the Fish River to
Crystal Hill. The dolerite was emplaced after the granites, and
is displaced by younger faults;

iv) the joint patterns in Egn_2 and Egn_5 adjacent to the northern
margin of the complex. This system controlled the orientation
and form of intrusion of the younger phases;

v) the trends of abundant short quartz veins, microgranite dykes,
and greisen dykes and zones. The dykes are related to the closing
stages of crystallisation of their host granite;

vi) the faulting of the Murphy Metamorphics at S880230.

Movement along the east-northeast-trending faults was apparently restricted
to vertical block-thrusting. As the effects of the east-northeast fault
system are less evident in the older, southeastern part of the MTR (Egn_1
and Egn_2), it is inferred that the system was initiated after or as the
result of, intrusion of Egn_1 and Egn_2. The parallel alignment of the east-
northeast fault system with the long axis of the MTR suggests that the
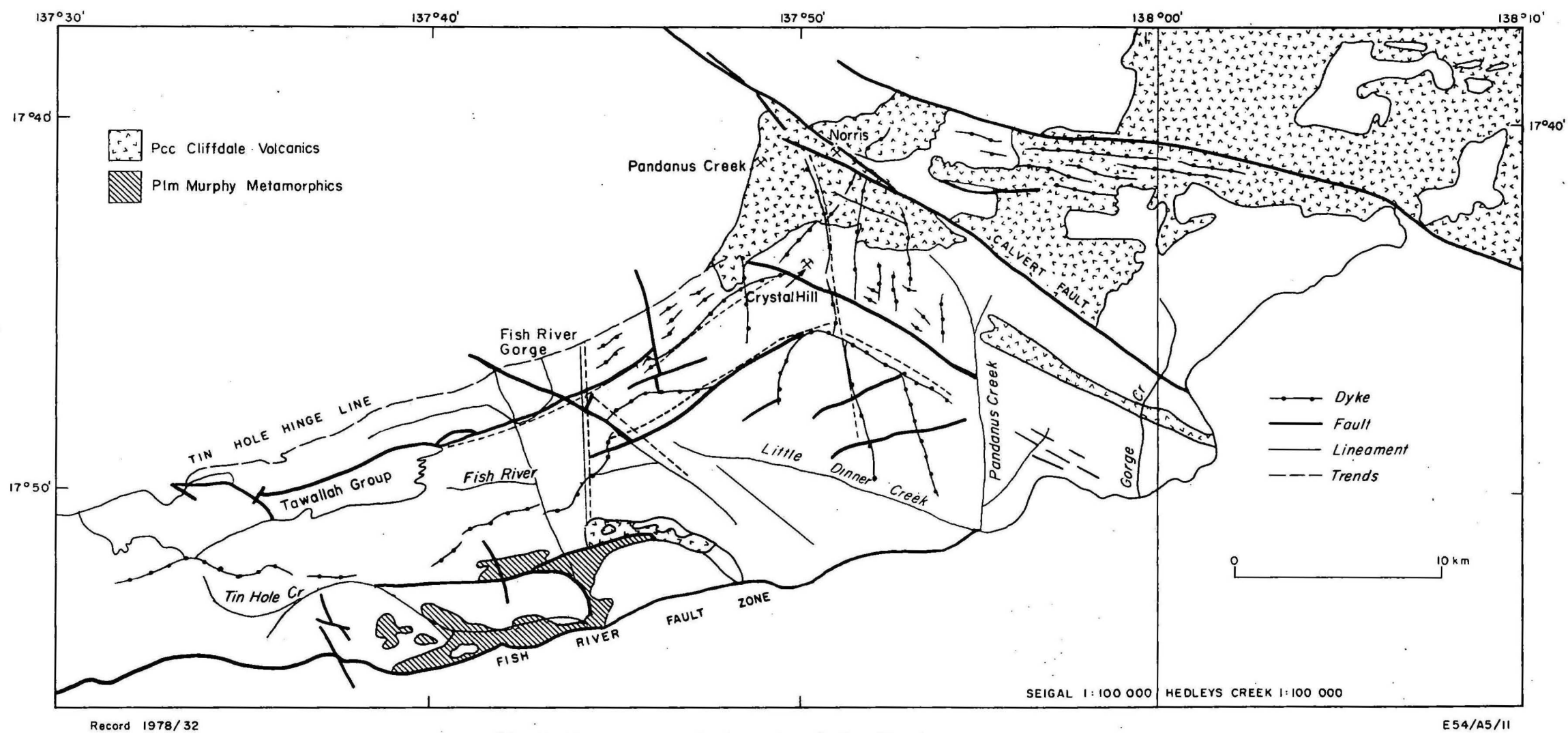
Fig. II Main structural elements of the Murphy Tectonic Ridge
dashed lines show how intersection of northwest and east-northeast
trends produces lineaments striking roughly north-south.

system was produced by stresses normal to the MTR - i.e., normal to the Murphy Metamorphics depositional basin. At first these stresses would have been compressional, as indicated by the tight isoclinal folding in the metamorphics, but, as there are structural features of Bgn_1 also parallel to the fault system, it would seem that the east-northeast faulting on the ridge was initiated by later tensional stresses related to updoming of the geosyncline at the time of intrusion of Bgn_1. The orientation of the faults is consistent with the interpretation that they are the result of tensional failure of rocks arched along an east-northeast axis (cf. Price, 1966).

Conjugate structures to the east-northeast system are well developed, and continue into the lower beds of the Westmoreland Conglomerate. These are expressed by:

    i)   the Fish River and related creek pattern;
    ii) a fault zone entering the Westmoreland Conglomerate 8 km
         west-southwest of Crystal Hill, and deflected at its southern
         end by structures related to the Calvert Fault system;
    iii) two prominent quartz veins striking parallel to the northwest
         branch of Pandanus Creek, passing through S050316 and S040307
         respectively;
    iv) faults south of Tin Hole Creek at S765200 and continuing into the
         Fish River Formation.

The Calvert Fault system reflects structural influences that are younger than the east-northeast structural system that controlled the uplift and shape of the Murphy Tectonic Ridge. The main expression of the Calvert Fault System, the Calvert Fault itself, can be traced northwest to the northern boundary of the Seigal 1:100 000 Sheet area and through the McArthur Basin; it crosses the MTR as a wide silicified ridge 60-70 m above the surrounding country. Other expressions of the Calvert Fault system are:

    i)   the shape and orientation of the two lenses of Cliffdale Volcanics
         west of Gorge Creek and east of the Fish River;
    ii) lineaments in Bgn_5 and Bgn_2 in the area 6-7 km east and southeast
         of Crystal Hill;
    iii) lineaments in Bgn_1 between Pandanus and Gorge Creeks;
    iv) Little Dinner Creek and related creek pattern (including Tin
         Hole Creek);

v)   a major lineament entering the Westmoreland Conglomerate at
     S858318 2.5 km west-southwest of Fish River Gorge, and displacing
     the dolerite dyke and the older faults at S900300.

Whereas conjugate structures are as well developed as the major
structures in the older east-northeast system, there is almost no expression
of a system conjugate to the Calvert Fault trend. Possible conjugate struc-
tures are occupied by the two tributaries of Pandanus Creek, through S100270
and S093340, and another may determine the orientation of a lens of Ecc_g at
S090270.

The intersections of trends of the two structural systems of the
MTR define a locus of subsidiary structures running roughly north-south. The
main line of intersection is defined by a pair of prominent quartz veins and
smaller parallel veins connecting Norris copper mine with Crystal Hill and
continuing southwards to S011330 and S033332 respectively. Faults connecting
the intersection points are generally more extensively and more continuously
silicified and greisenised than faults of the two original systems. The
main intersection is the major zone of known mineralisation in the MTR - copper
at Norris and tin at Crystal Hill.

Two less prominent zones of intersection are also sites of minerali-
sation, greisenisation, and silicification. The first lies roughly along the
contact between the Westmoreland Conglomerate and the Cliffdale Volcanics
through Pandanus Creek uranium mine and a hut at S986377, and is defined by
a series of quartz veins, microgranite, and feldspar porphyry dykes.

The second line is a broader zone of short lineaments and faults,
which intersects the contact of the MTR with the Westmoreland Conglomerate
at S888330, 1 km east of Fish River Gorge, and continues south to the sou-
thern margin of the MTR. Between S890220 and S888194 it is occupied by the
Fish River. Granodiorite ring dykes between Egn_2 and Egn_6 are emplaced along
this zone. It is the site of amethyst development in some of the quartz
veins and of localisation of small quartz-mica plugs.

Many variably oriented barren joint systems are represented in
the complex. Some, including joints in Egn_5 between the Fish River and Crystal
Hill, are parallel to zones of greisenised granite, greisen dykes, or major
east-northeast faults, and were therefore produced by stresses related to
granite emplacement and cooling. Joints in the roughly circular mass of
Egn_6 centred on the Fish River are developed radially and concentrically

with respect to the intrusion's boundaries and were produced by cooling contraction stresses (Price, 1966). Structural controls in the western part of the MTR are not obvious, but the dominant trend is apparently east-west.

Trends are dominantly east-west north of the Calvert Fault, where they are defined by a dense conjugate pattern of porphyry dykes and quartz veins. There is a preference for north-south trends for the latter, and for east-west trends for the former. Tin and copper mineralisation around Tracey's Table (S066440) is associated with the intersection of this east-west system with the Calvert Fault system.

VIII GEOCHEMISTRY

Forty-one rocks from the Seigal 1:100 000 Sheet have been analysed for major and minor elements. The analysed samples are 26 granites, nine Cliffdale Volcanics, two greisens, two feldspar porphyry dykes, and two dolerite dykes. Thirty-one of the analyses are listed in Table 9, along with six analyses of average granitoids for comparison.

Major elements

The forty-one analyses and six averages are referred to the following variation diagrams and triangular plots:

  (i)   Niggli variation diagrams: alk, c, fm, al vs si (Fig. 12)
  (ii) $\%K_2O$ vs $\%SiO_2$; $\%K_2O$ vs $\%Na_2O + \%K2_0$; $\%Na_2O + \%K_2O$ vs $\%SiO_2$ (Fig. 13)
  (iii) F-M-A (Fig. 14)
  (iv)   Q-Ab-Or (Fig.15)
  (v)   An-Ab-Or (Fig. 16)

(i) Niggli variation diagrams (Fig. 12)

Major-element trends are more concisely represented by Niggli si value-based variation diagrams than by SiO_2-based variation diagrams (Burri, 1964) because the abscissa si value is a function of the ratio of SiO_2 to the total of the other oxides, and exaggerates the horizontal axis of the variation diagram, thus giving better-defined trends. The Niggli si value is thus an indicator of the degree of fractionation - i.e., a rock with

77

higher si value is more fractionated than one with a lower si value. Where straight line trends are normal in SiO_2 variation diagrams, si variation trends are curved. On the Niggli plots, different suites of rocks can be expected to define unique curves. A consanguineous suite will define a single smooth variation trend on each of the diagrams. In Figure 12, some average granites (Buddington, 1959; Turekian & Wedepohl, 1961; Harme, 1965; Taylor, 1968; Sheraton & Labonne, 1978) are plotted for comparison with the Westmoreland rocks.

The following features of the Niggli diagrams are apparent.

1.   With few exceptions, the intrusive rocks fall on normal smooth variation trends.

The greisenised granite (Table 9, No. 22) is the most highly fractionated granite, probably due to metasomatism. The greisen dyke, No. 31, falls away from the trend towards a field of iron enrichment and alkali depletion. The Crystal Hill greisen, No. 30, shows silica enrichment as well as iron enrichment and alkali depletion.

2.   The acid intrusive rocks form a fractionation sequence, with Bgn_{3-4} and the feldspar porphyry dykes being the least fractionated, and Bgn_1, Bgn_2, Bgn_5 and Bgn_7 being successively more fractionated. Thus fractionation increased with time. The departure of the greisens from the main trend is due to the fact that the source of the greisens was a late-stage magmatic fluid rich in iron and silica.

3.   The porphyry dykes and Bgn_{3-4} are chemically close in composition although lithologically dissimilar. The field and chemical relations of Bgn_{3-4} with the other granites suggest that it is the nearest in composition to the source rock of Bgn_1 and Bgn_2 - i.e., Bgn_1 and Bgn_2 could have been derived by partial melting of a rock of the composition of Bgn_{3-4}.

4.   The Cliffdale Volcanics lie on the same trend as the granites; unit 4a of the volcanics corresponds to Bgn_1 or Bgn_2 in composition and is classified as rhyodacite (Irvine & Baragar, 1971), and unit 4b corresponds to Bgn_5 in composition (rhyolite). The more basic volcanic, No. 32, shows slightly increased al and depleted fm relative to granites of similar si.

Table 9
Chemical Analysis of Nicholson Granite Complex

Analysis no.	1 łgn₁	2	3	4	5	6 łgn₂	7	8	9	10	11	12 łgn₃₋₄	13	14	15	16 łgn₅	17
Spec. no.	0889	0924	0859A	0875	0882	0923A	0925	0927	0923B	0860	0862A	0862B	0827	0850	0812	0885	0888
SiO_2	70.24	67.03	69.01	72.47	74.78	70.42	66.78	73.18	62.25	63.58	63.59	56.82	58.80	61.37	73.64	70.86	75.16
Al_2O_3	14.36	14.35	13.34	12.89	12.27	13.54	14.47	13.38	15.15	14.57	14.52	13.82	13.87	16.05	12.92	13.77	12.23
Fe_2O_3	.99	1.13	1.02	1.09	.61	.69	1.09	.67	.47	1.09	.84	.93	1.76	1.36	.62	1.03	.66
FeO	2.04	2.63	4.09	1.56	1.26	3.15	3.60	1.56	5.56	3.97	4.33	6.41	5.00	4.85	1.34	1.78	1.07
CaO	2.13	2.70	1.29	1.20	.84	2.24	2.29	.92	2.21	3.09	3.33	5.03	4.21	3.99	.70	1.63	.78
MgO	1.06	1.56	.89	.35	.17	.73	.83	.46	1.92	3.71	3.65	6.27	6.70	2.52	.38	.54	.18
Na_2O	3.28	2.70	2.10	2.84	2.96	2.76	2.70	3.18	2.82	2.12	2.22	1.84	2.08	2.72	2.24	2.26	2.46
K_2O	4.55	5.09	5.91	5.33	5.28	4.63	5.38	4.89	6.01	5.46	5.07	5.59	3.93	4.72	6.57	6.14	5.84
TiO_2	.32	.45	.58	.28	.15	.41	.56	.20	.65	.63	.65	.76	.62	.71	.22	.36	.18
MnO	.06	.06	.07	.06	.05	.05	.06	.05	.08	.06	.07	.12	.09	.09	.04	.05	.03
P_2O_5	.01	.16	.21	.09	.03	.09	.18	.09	.14	.22	.23	.27	.16	.22	.04	.08	.03
H_2O+	.92	1.13	1.14	.77	.76	1.33	1.31	.71	1.53	1.34	1.33	1.38	1.88	1.02	.72	1.03	.54
H_2O-	.06	.03	.04	.03	.04	.01	.03	.05	.05	.04	.03	.04	.06	.04	.12	.05	.04
Total	100.02	99.03	99.68	98.95	99.20	100.05	99.29	99.34	98.85	99.87	99.86	99.28	99.16	99.67	99.55	99.57	99.20
Pb	22	24	34	40	50	30	32	34	32	30	22	34	18	32	28	30	42
U	10	10	8	14	22	8	8	6	6	6	6	<4	<4	6	4	6	6
Th	32	28	24	40	50	22	24	26	20	24	22	16	10	20	24	24	30
W	<10	<10	10	<10	<10	<10	<10	<10	<10	40	<10	<10	<10	<10	<10	<10	<10
Sn	<4	<4	4	12	14	6	4	4	<4	6	<4	18	<4	<4	8	<4	<4
Mo	<10	<10	12	10	<10	<10	<10	<10	<10	<10	<10	<10	10	<10	<10	<10	10
Zr	170	190	340	150	140	230	320	170	220	260	270	230	160	270	190	210	160
Sr	380	500	130	100	44	120	240	160	150	500	500	410	330	390	125	230	85
Ba	480	980	1350	480	240	650	1400	600	920	1300	1150	1300	1050	1850	1000	1050	300
Nb	15	10	20	15	35	10	20	15	10	15	15	15	5	15	10	10	10
Rb	170	180	250	310	500	210	190	190	300	210	190	240	160	165	280	200	270
Ce	90	100	140	100	100	90	160	80	100	110	130	130	70	130	110	110	150
Y	25	20	45	35	80	45	45	25	50	30	25	35	20	25	30	30	50
Bi	<8	10	<8	<8	<8	<8	<8	<8	<8	<8	8	10	<8	<8	<8	<8	<8
Co	11	10	13	8	4	9	10	5	14	23	18	30	36	23	4	8	4
Cu	3	3	15	3	2	37	18	3	220	16	10	134	48	16	6	7	1
Li	16	19	24	26	39	26	27	18	32	19	24	20	18	25	6	12	10
Ni	8	12	4	<2	<2	6	4	2	18	46	44	81	83	12	<2	2	<2
Pb	25	32	38	51	54	30	40	57	47	29	27	44	24	38	43	66	48
Rb/Sr	.45	.36	1.92	3.10	11.36	1.75	.79	2.50	2.00	.42	.38	.59	.48	.42	2.24	.87	3.18
K/Rb	222	235	196	143	88	183	235	214	166	215	222	193	204	237	195	255	180
Ba/Sr	1.26	1.96	10.38	4.80	5.45	5.42	5.83	3.75	6.13	2.60	2.30	3.17	3.18	4.74	8	4.57	3.53
Ba/Rb	2.80	5.44	5.44	1.55	.48	3.10	7.63	1.50	3.07	6.14	6.05	5.37	6.58	11.29	3.55	5.25	1.11
K/Ba	79	43	36	92	183	59	32	68	54	35	37	36	31	21	55	49	162
Th/U	3.20	2.8	3	2.86	2.27	2.75	3	4.33	3.33	4	3.67	>4	>2.5	3.33	6	4	5

Table 9 (cont'd)

	egn7			egn8									Greisen		Cliffdale Volcanics			QFP dyke		Dol. dyke
Analysis no.	18	19	20	21	22	23	24	25	26	27	28	29	30	31	32	33	34	35	36	37
Spec. no.	0824	0855C	0858	0864A	0868	0926							0805	0809	Ecc_{4a} (0828)	Ecc_{4b} (0845)	Ecc_{4c} (0893)	Ecc_5 (630) 0815A		0916
SiO_2	74.76	74.35	75.58	72.51	76.27	74.37	74.2	71.2	66.9	73.4	77.04	70.11	85.69	73.88	65.53	73.67	79.05	74.66	63.63	52.13
Al_2O_3	12.58	13.75	13.18	13.27	12.29	13.68	13.6	14.7	15.7	13.42	12.89	14.11	6.74	13.70	15.85	13.31	10.28	12.73	14.36	13.59
Fe_2O_3	1.19	.67	.82	1.29	.67	.80	1.83	3.24	3.78	.54	.15	1.14	.93	1.71	2.34	.79	1.16	1.62	.82	1.77
FeO	.77	.67	.30	.67	.41	.89				1.59	.27	2.62	1.96	1.18	2.52	1.48	1.07	.52	3.90	10.35
CaO	.65	.53	.29	.21	.25	.39	.71	2.00	3.56	1.66	.22	1.66	.36	.30	2.95	.58	.25	.19	3.85	6.50
MgO	.33	.35	.18	.43	.07	.29	.27	.55	1.57	.56	.17	.24	.04	.70	1.18	.26	.42	.37	2.75	4.87
Na_2O	2.84	2.70	2.14	.02	2.86	2.80	3.48	3.54	3.84	3.47	1.96	3.03	.13	.15	3.19	3.00	1.30	1.32	2.38	2.08
K_2O	5.57	6.24	6.59	8.78	6.09	5.67	5.05	4.18	3.07	4.22	6.91	6.03	2.93	5.62	4.39	6.09	4.21	6.75	4.80	3.08
TiO_2	.15	.10	.07	.46	.07	.11	.20	.40	.57	.24	.05	.42	.11	.34	.61	.14	.16	.18	.62	1.77
MnO	.03	.04	.03	.04	.03	.05	.05	.05	.08	.05	.01	.06	.07	.03	.07	.06	.04	.02	.06	.18
P_2O_5	.03	.07	.05	.14	.02	.12	.14	.16	.21	.06	.12	.09	.04	.06	.15	.03	.02	.03	.24	.23
H_2O+	.41	.84	.77	1.13	.40	.86				.72	.41	.23	.97	1.75	.93	.59	1.36	1.11	1.59	2.55
H_2O-	.17	.04	.09	.15	.04	.06					.06	.07	.07	.05	.05	.05	.10	.15	.07	.17
Total	99.48	100.15	100.09	99.10	99.46	100.10				99.93	99.76	99.81	100.04	99.48	99.76	100.05	99.35	99.66	99.09	99.27
Pb	26	36	34	20	28	36	19	30	15	26			14	10	28	32	10	18	26	18
U	14	6	8	4	18	1.2	3.0	4.8	2.7	7			<4	4	6	14	8	6	8	4
Th	42	12	4	24	14	12	17	17	10	30			18	20	22	34	16	26	28	8
W	<10	<10	<10	<10	<10	<10							15	25	<10	<10	<10	<10	10	10
Sn	4	<4	<4	12	<4	10	3	3	2	5			50	170	<4	6	<4	<4	4	4
Mo	<10	<10	<10	<10	<10	<10							<10	<10	<10	<10	<10	<10		
Zr	150	60	45	310	60	60	175	180	140	134			90	240	290	230	250	26	266	210
Sr	70	140	60	65	55	65	100	285	440	88			40	50	340	110	60	60	500	270
Ba	230	720	300	1500	170	400	840	600	500	311			140	600	1750	820	1200	1250	1000	650
Nb	15	5	5	20	15	5							80	10	10	20	15	15	15	15
Rb	370	200	350	290	270	280	170	145	110	301			1000	840	170	310	150	280	210	110
Ce	60	30	20	140	30	30	92	57	47	67			30	30	130	120	90	90	140	80
Y	50	15	25	45	15	30	40	40	30	57			80	25	30	30	35	35	25	50
Bi	<8	<8	<8	<8	<8	8							<8	<8	<8	<8	10	8		
Co	2	6	5	5	3	2	1.0	2	10	5			2	5	12	3	4	4		
Cu	42	<1	21	79	115	3	10	10	25	6			1	4	20	3	29	7		
Li	3	8	4	9	1	14	40	30	25	34			433	82	10	5	4	3	16	21
Ni	<2	<2	4	<2	<2	<2	4.5	4	15	3			<2	<2	4	<2	<2	2		
Pb	31	43	42	28	30	35	19	30	15	26			5	41	76	42	15	22		
Rb/Sr	5.29	1.43	5.83	4.46	4.91	4.31	1.7	.51	.25	3.42			25	16.80	.50	2.82	2.50	4.67	.42	.41
K/Rb	125	259	156	251	187	168	250	240	230	116			24	56	214	163	233	200	190	232
Ba/Sr	3.29	5.14	5	20	3.09	6.15	.4	2.1	1.14	3.5			3.50	12	5.15	7.45	20	20.8		
Ba/Rb	.62	3.60	.86	4.48	.63	1.43	4.9	4.1	4.5	1.03			.14	.72	10.19	2.63	8.00	4.44		
K/Ba	201	72	182	56	297	118	50	58	51	113			174	78	21	62	29	45	3.5	2.00
Th/U	3	2	.5	6	.78	1	5.7	3.5	3.7	4.3			>4.5	5	3.67	2.43	2.00	4.33		

9. mafic xenolith in Egn_2

12. mafic xenolith in Egn_{3-4}

24. Average low Ca-granite (Turekian & Wedepohl, 1961)

25. Average granite (Taylor, 1968)

26. Average granodiorite (Taylor, 1968)

27. Average Upper Palaeozoic granite, Northeast Queensland (Sheraton & Labonne, 1978)

28. Precambrian potassic granite, Helsinki (Harme, 1965)

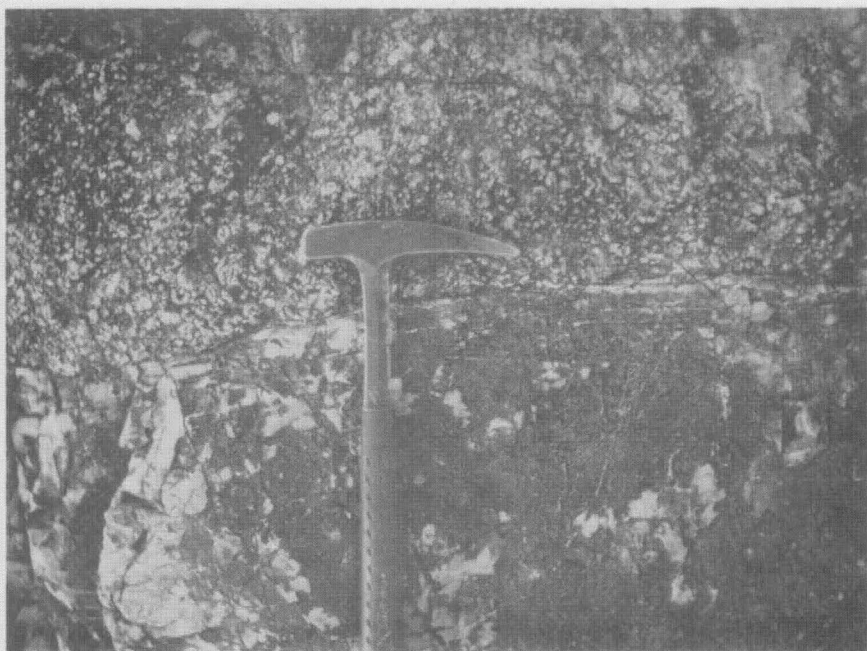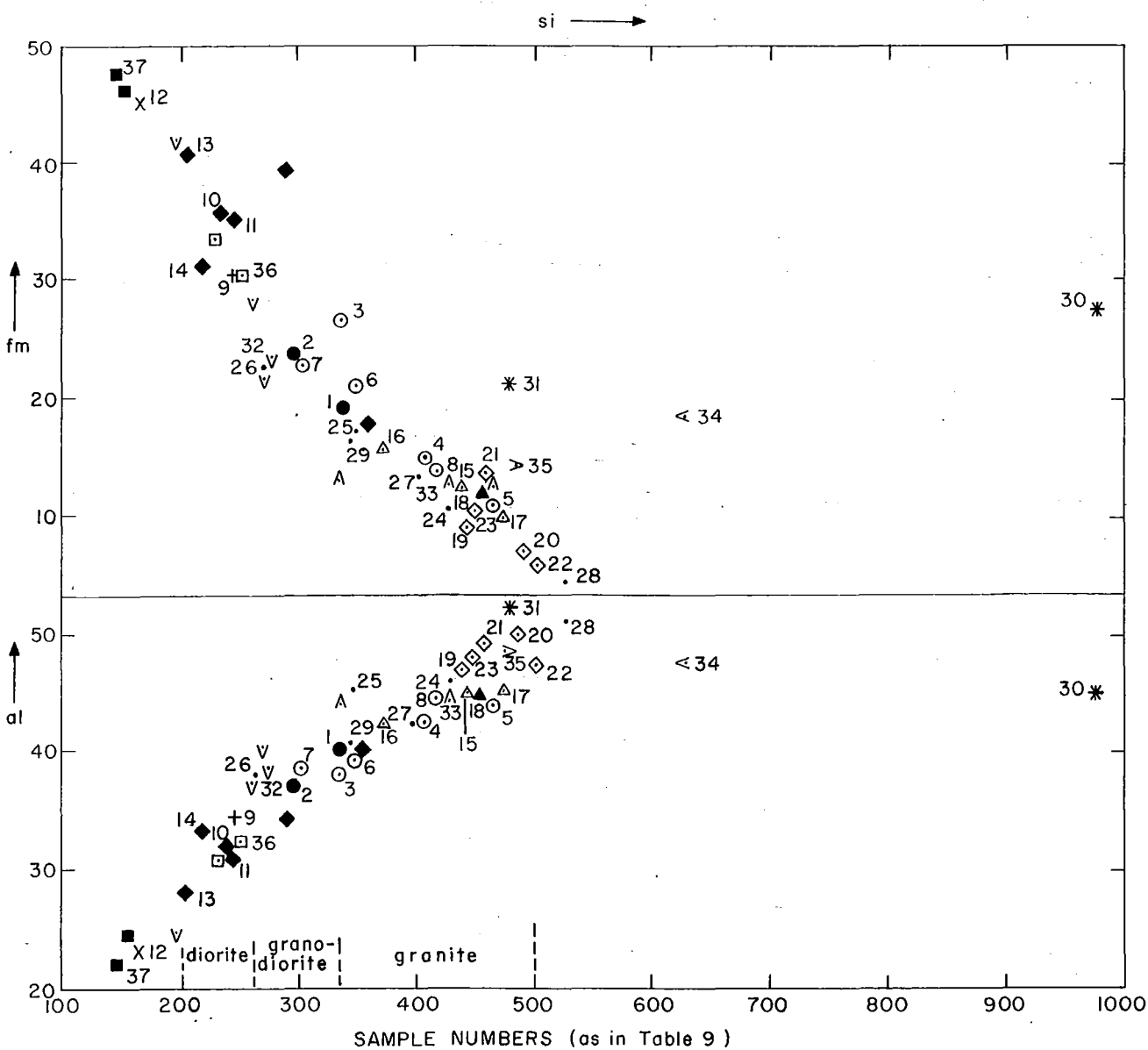29. Precambrian potassic hornblende granite (Buddington, 1959)
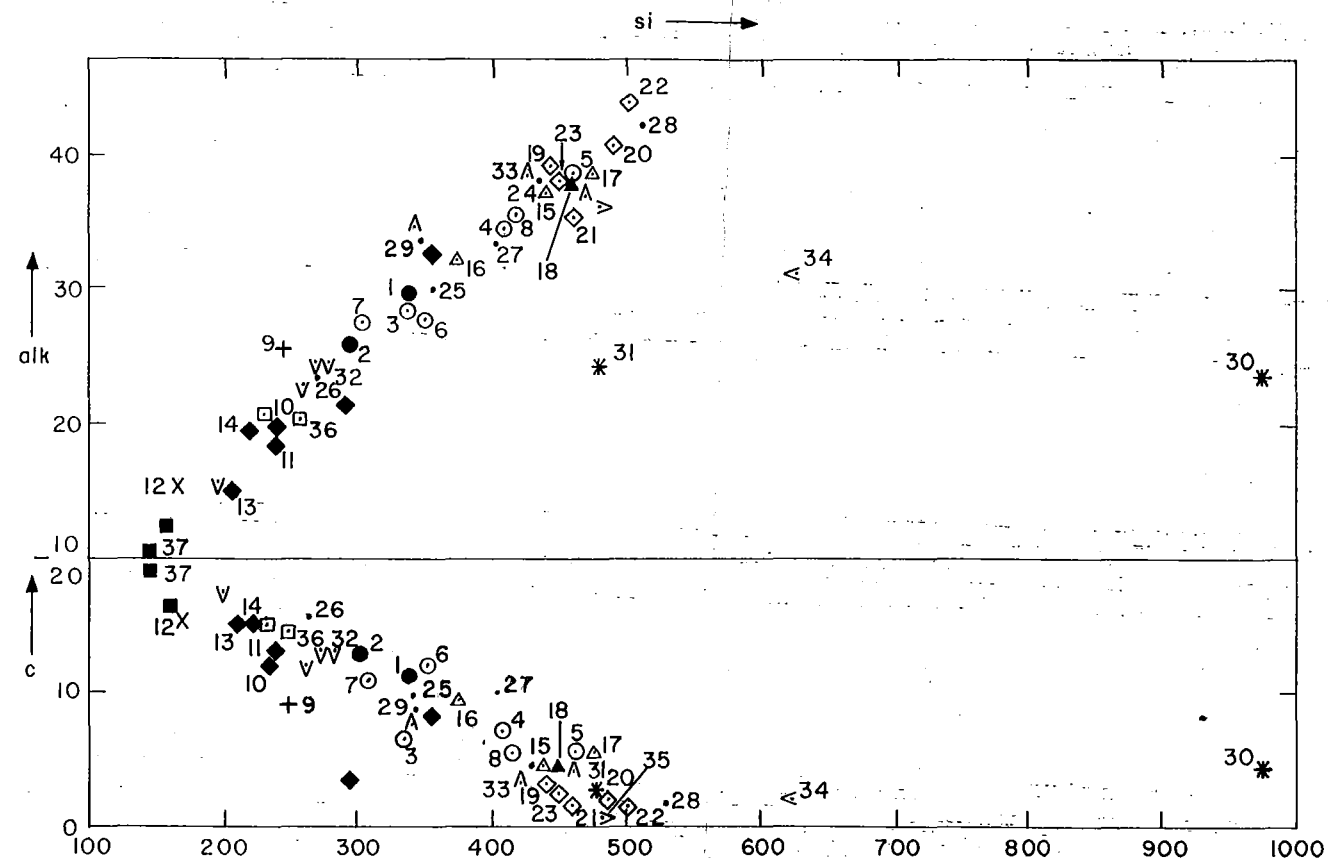
81

Fig. 10a. Quartz-veined microgranite dyke cutting Bgn$_5$.

Fig. 10b. Microgranite chill zone in Bgn$_5$

82

The Niggli values si, al, fm, c, and alk are used to summarise the geochemistry of the Nicholson Granite Complex. The values are calculated from the chemical analyses as follows

$$si = \frac{100}{T} \cdot 1000 \left(\frac{wt\% \ SiO_2}{MW \ SiO_2} \right) \quad ; \quad al = \frac{100}{T} \cdot 1000 \left(\frac{wt\% \ Al_2O_3}{MW \ Al_2O_3} \right)$$

$$fm = \frac{100}{T} \cdot 1000 \left(\frac{2 \cdot wt\% \ Fe_2O_3}{MW \ Fe_2O_3} + \frac{wt\% \ FeO}{MW \ FeO} + \frac{wt\% \ MgO}{MW \ MgO} \right)$$
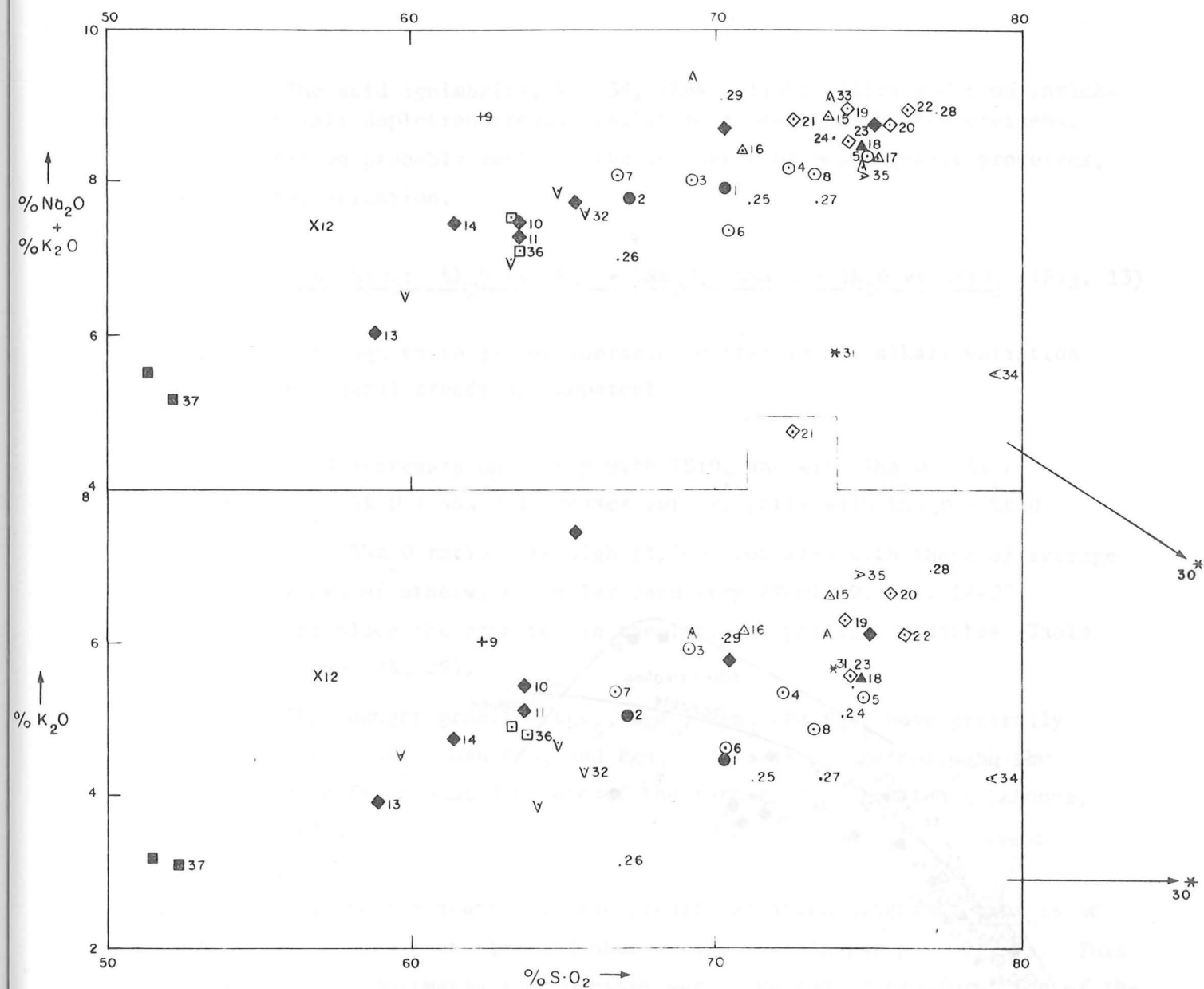
$$c = \frac{100}{T} \cdot 1000 \left(\frac{wt\% \ CaO}{MW \ CaO} \right) \quad ; \quad alk = \frac{100}{T} \cdot 1000 \left(\frac{wt\% \ Na_2O}{MW \ Na_2O} + \frac{wt\% \ K_2O}{MW \ K_2O} \right)$$

$$where \ T = 1000 \left(\frac{wt\% \ Al_2O_3}{MW \ Al_2O_3} + \frac{2 \cdot wt\% \ Fe_2O_3}{MW \ Fe_2O_3} + \frac{wt\% \ FeO}{MW \ FeO} + \frac{wt\% \ MgO}{MW \ MgO} + \frac{wt\% \ CaO}{MW \ CaO} + \frac{wt\% \ Na_2O}{MW \ Na_2O} + \right.$$

$$\left. + \frac{wt\% \ K_2O}{MW \ K_2O} \right)$$

MW= Molecular Weight

Legend

- ● 1, 2 Pgn$_1$
- ⊙ 3,4,5,6,7,8 Pgn$_2$
- ◆ 10,11,13,14. Pgn$_{3-4}$
- △ 15,16,17 Pgn$_5$
- ▲ 18 Pgn$_7$
- ◇ 19,20,21,22,23 Pgn$_8$
- + 9 Xenolith in Pgn$_2$
- X 12 Xenolith in Pgn$_{3-4}$

- · 24,25,26,27,28,29 average Granites, see Table 9
- ✳ 30,31 greisen
- V 32 Pcc$_{4a}$
- Λ 33 Pcc$_{4b}$
- ◁ 34 Pcc$_{4c}$
- ▷ 35 Pcc$_5$
- ⊡ 36 quartz-feldspar porphyry dyke
- ■ 37 dolerite dyke

SAMPLE NUMBERS (as in Table 9)
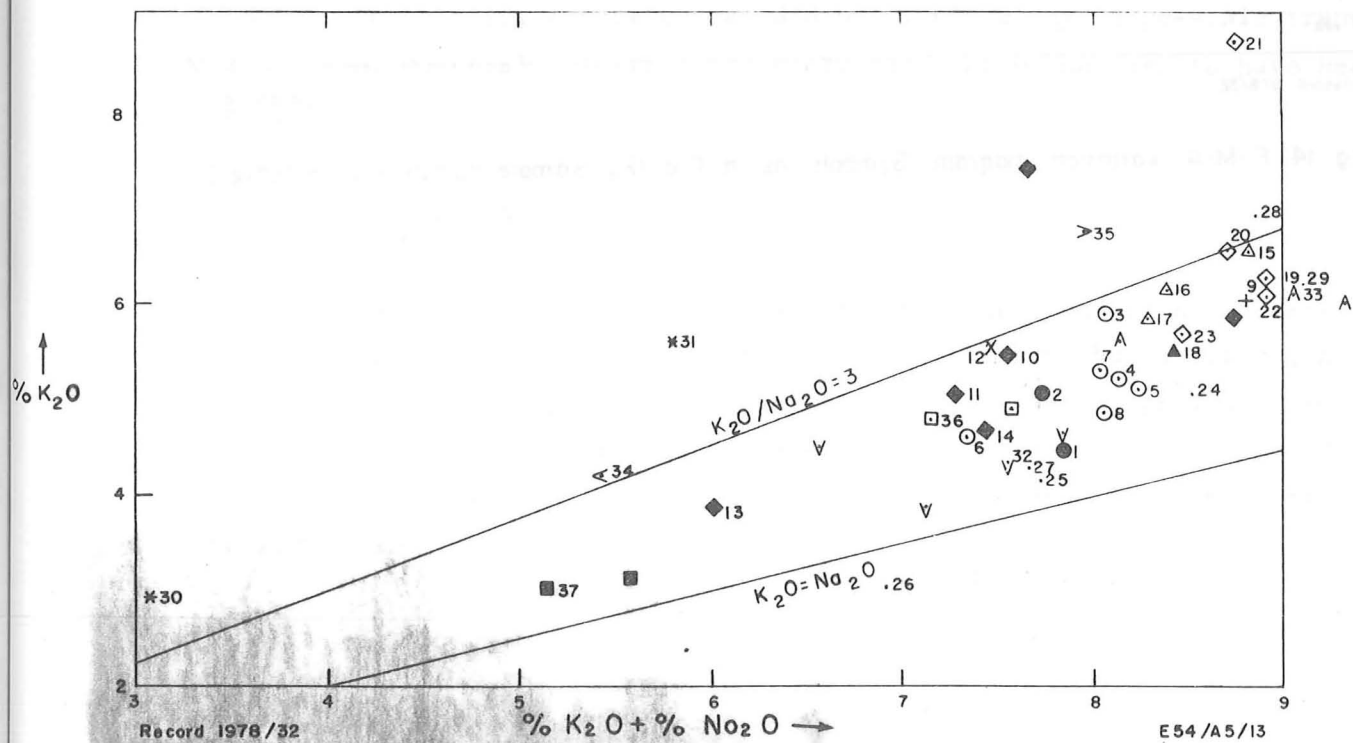
Fig. 12 Niggli variation diagrams

Fig. 13. Alkali variation diagrams. Symbols as in Fig. 12; sample numbers as in Table 9.
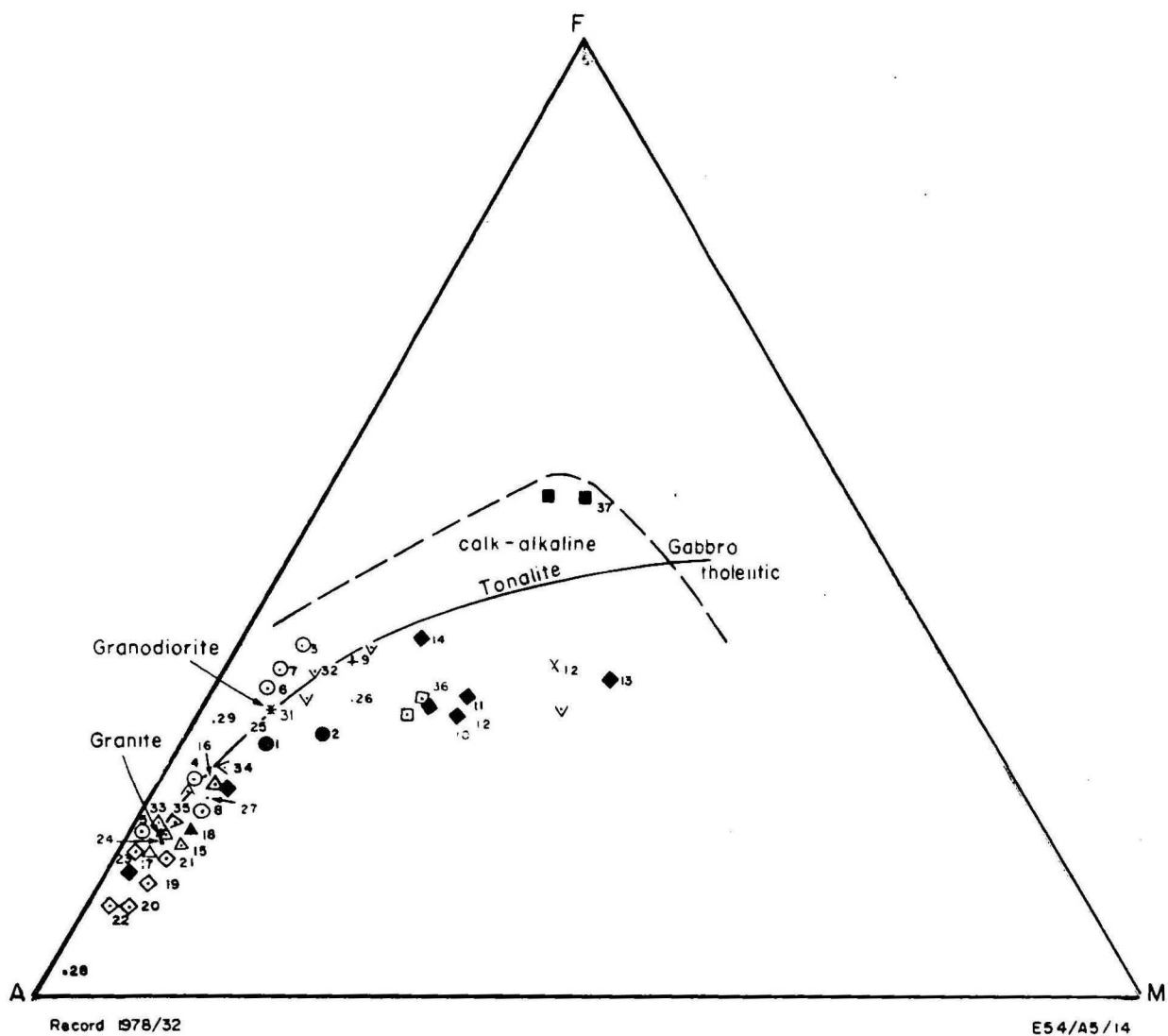
Fig 14. F-M-A variation diagram. Symbols as in Fig 12; Sample numbers as in Table 9.

5.   The acid ignimbrite, No. 34, shows slight silica and iron enrich-ment and alkali depletion trends similar to those shown by the greisens. Its composition probably reflects the influence of postmagmatic processes, such as greisenisation.

(ii) $\%K_2O$ vs $\%SiO_2$; $\%K_2O$ vs $\%K_2O + \%Na_2O$; $\%Na_2O + \%K_2O$ vs $\%SiO_2$ (Fig. 13)

1.   Although there is considerable scatter in the alkali variation plots, some general trends are apparent:

(i) $\%K_2O$ increases uniformly with $\%SiO_2$ and with $\%Na_2O + \%K_2O$

(ii) $\%K_2O/\%K_2O + \%Na_2O$ increases very slightly with $\%Na_2O + \%K_2O$

(iii) $\%K_2O/\%Na_2O$ ratios are high (1.5-3) compared with those of average rocks of otherwise similar chemistry (Table 9, Nos. 24-27) and place the granites in the field of potassic granites (Table 9, Nos 28, 29).

(iv)   The younger granites Egn_5, Egn_6, Egn_7 and Egn_8 have generally higher $\%K_2O$ than Egn_1 and Egn_2. This is consistent with the more fractionated nature of the former (cf. Sheraton & Labonne, 1976).

2.   Despite the scatter in the alkali variation diagrams, ther is no correlation between chemistry and abundance of K-feldspar phenocrysts. This suggests that if postmagmatic processes were involved in the formation of the feldspar phenocrysts, the processes did not include any large-scale trans-portation of material. Instead the recrystallisation appears to have been isochemical.

iii)   F-M-A (Fig. 14)

1.   The granites fall along the fractionation trend of normal calc-al-kaline granites between granodiorite and granite (Carmichael, Turner, & Verhoogen, 1974), but Egn_8 lies on an alkali-enrichment extension of this trend, closer to the alkali corner than most granites - i.e., simple frac-tionation cannot account for the whole range in the chemical composition of the granites.

2.   The basic end of the trend diverges - the porphyry dykes and Egn_{3-4} fall below the main trend.

3.   The volcanics overlap the granite trend.

iv) <u>Q-Ab-Or</u> (Fig. 15)

1.   The granites are uniformly displaced towards the Or apex relative to the most common granite compositions (Tuttle & Bowen, 1958).

2.   Two broad groups can be distinguished as shown in Fig. 15; the normal granites and the alkali-enriched granites. As the thermal minimum for these rocks in the system Q-Ab-Or is believed to be roughly as shown (the minimum cannot be fixed exactly as it varies with pH_2O and CaO content - see below under 'Discussion') it is possible to produce the range of compositions in the group of normal granites by successively greater degrees of partial melting, or by separating successive residual melts as fractional crystallisation proceeded - i.e., those rocks close to the minimum represent the lowest temperature melts, and those towards the Q-Or base represent greater degrees of anatexis of a source whose composition would lie near the Q-Or edge, as the liquid composition would migrate along the divide with increasing temperatures. The second group, which includes the granodiorite dykes, xenoliths, porphyry dykes, and Egn_1, converges on the minimum but forms a distinct lineage between the postulated source composition and the thermal minimum. Sediments and volcanics from the base of the sequence now represented by the Murphy Metamorphics are postulated as the source material of the granites. This source has a probable average composition within the area shown in Fig. 15. Fractionation of the source material would produce a series of melts with compositions along the lineage defined by the group of alkali-enriched granites.

3.   The divergence described above seems to be reproduced by the volcanics, though more analyses will be needed to confirm this.
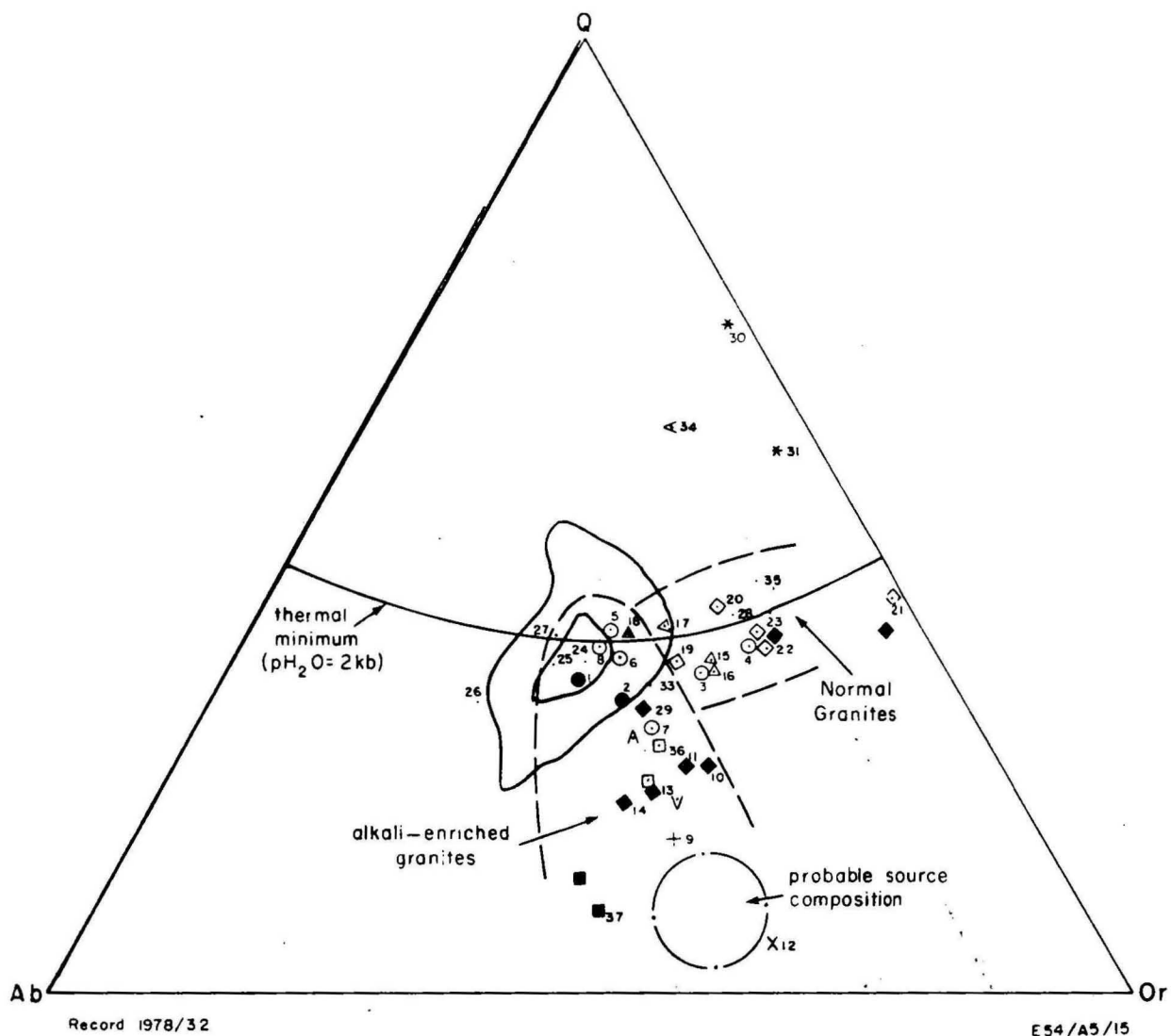
Fig 15. Q-Ab-Or variation diagram. Solid lines are density contours of most granites (Tuttle & Bowen, 1958). Dashed lines outline 2 groups (referred to in text as normal granites and alkali-enriched granites) following different trends in relation to the thermal minimum. Symbols as in Fig 12, sample numbers as in Table 9.
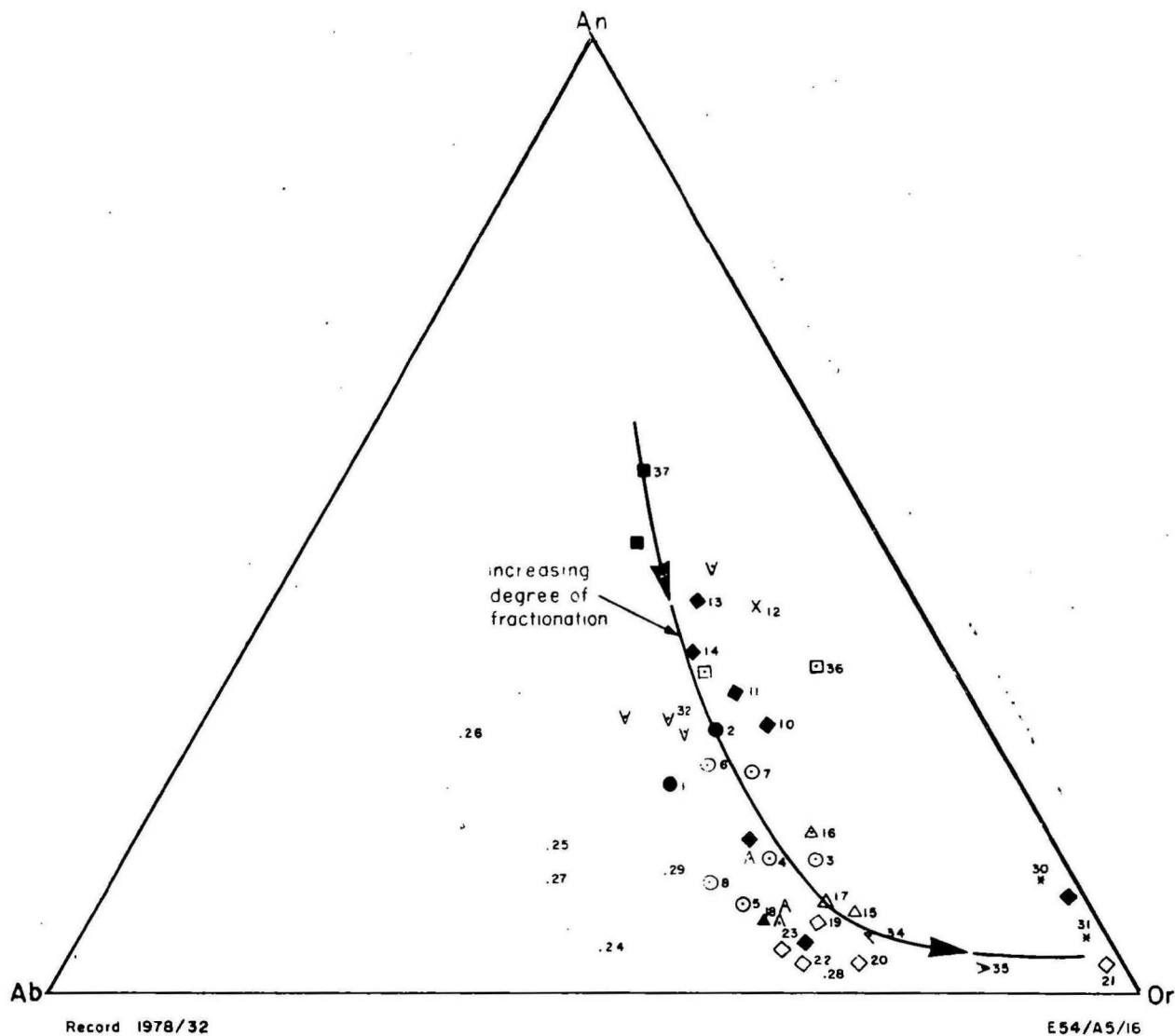
Fig.16. Normative An – Ab – Or compositions of the Nicholson Granite Complex.
Symbols as in Fig.12, numbers as in Table 9.

(v) <u>An-Ab-Or</u> (Fig. 16)

1.   The Nicholson Granite Complex lies on a trend of initial Ab increase
followed by Or increase, consistent with increasing degree of fractionation
towards the Or apex (Carmichael, 1963).

2.   There is a close antipathetic relation between An and Or, while
Ab increases slightly, then decreases sharply. K_2O is slightly higher and
CaO slightly lower than for average rocks with the same silica contents
(Table 9, Nos. 24-29). This confirms that the K_2O content of these granites
is a primary feature, and that any postmagmatic chemical alteration proceeded
isochemically.

        The smooth trends defined by the Nicholson Granite Complex on all
of the major-element plots suggest that the two age groups of granites are
comagmatic.

Minor elements

        The analyses are referred to silica variation diagrams (see Fig.
17a-k) (including K/Rb, K/Ba, Rb/Sr, Ba/Rb, Th/U, and Y/Ce vs SiO2) and to
the following systems:

        (i)   K vs Rb (Fig. 18)
        (ii)   Rb vs Sr (Fig. 19)
        (iii)   Ca vs Sr
        (iv)   Sr vs K
        (v)   Ba vs K

Some average granite minor-element abundances (Turekian & Wedepohl, 1961;
Taylor, 1968; Sheraton & Labonne, 1978) are also plotted in Figure 17 for
comparison.

1.   Many of the incompatible trace-element abundances are higher than
average in the Nicholson Granite Complex. From Table 9, it can be seen that
U, Th, Ba, Rb, and Ce are present in greater abundance than the average
(Nos. 24, 25, 26) by factors of up to 2.

90

2.   Th concentrates at 20-30 ppm, which is higher than for average granites, and reaches 50 ppm in one Egn_2 sample. U values are consistently higher than the average (Nos. 24, 25, 26) by a factor of about 2, and Th/U clusters at about 3.0-4.0. Although U often concentrates in residual magmas (Taylor, 1965), there is no concentration of U or Th in the greisens or microgranites, but it is possible that these elements have been leached.

3.   Many of the granites have higher than average Ba. K/Ba shows the trend characteristic of increasing differentiation: initially constant, then sharply increasing with increasing SiO_2 (Fig. 17k). Ba follows Th in its enrichment in Egn_8, and depletion in the greisen rocks.

4.   Rb is generally high, and increases with SiO_2 and with K. K/Rb values fall within, but on the low side of, the range of normal K/Rb ratios as defined by Taylor (1965), and shown in Fig. 18. The K/Rb ratios of the Nicholson Granite Complex follow a decreasing trend parallel with differentiation. The Crystal Hill greisen lies in the zone of Rb enrichment.

5.   Sr follow Ca in its smooth decrease with SiO_2. Rb/Sr also follows the characteristic differentiation trend - constant values, then sharp increase at high SiO_2 from 0.5 to 25 in the greisen.

6.   Y/Ce follows the same pattern with differentiation as Rb/Sr and K/Ba.

7.   Li is low in Egn_5, Egn_6, Egn_7, and Egn_8 compared with average granites (Nos 24, 25), but is greatly enriched in the greisen dykes. It is not enriched in the greisenised granites. As for other trace elements, enrichment occurs sharply.

8.   Compared with average granites (Nos. 24, 25, and 26) Ni and Co show normal concentration except for Ni depletion in Egn_5, Egn_6, Egn_7, and Egn_8. This depletion corresponds to decreasing Ni/Co ratio in these granites, indicating that they are more fractionated than Egn_1, Egn_2, and Egn_{3-4} (Taylor, 1968).
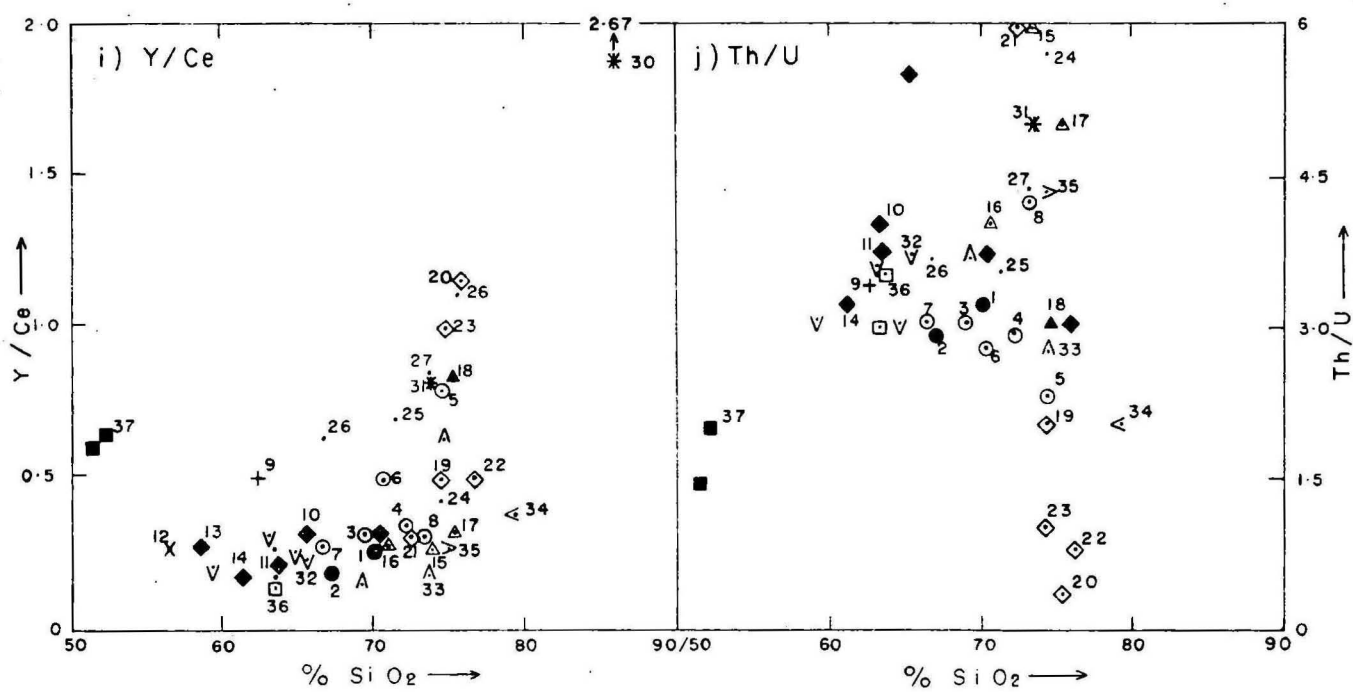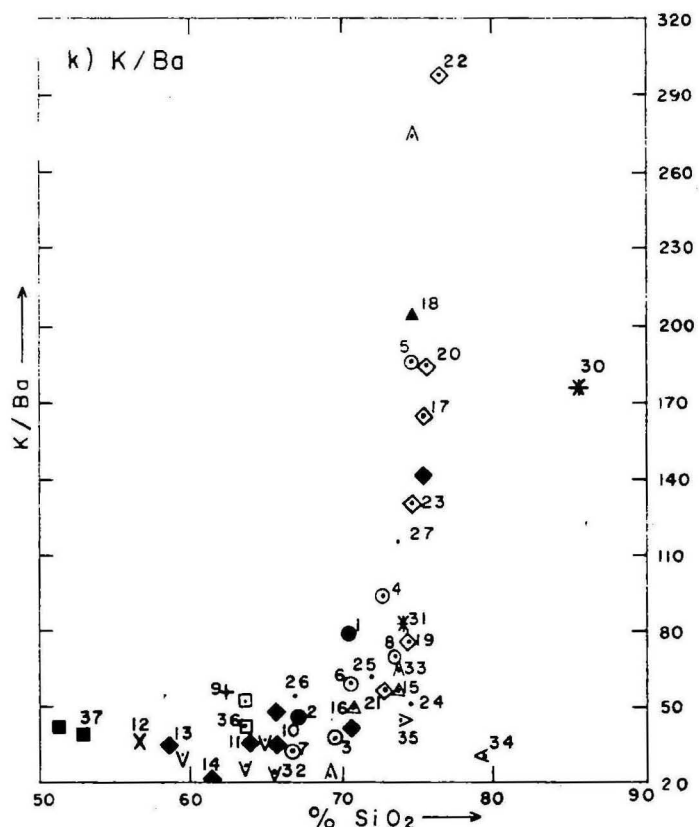
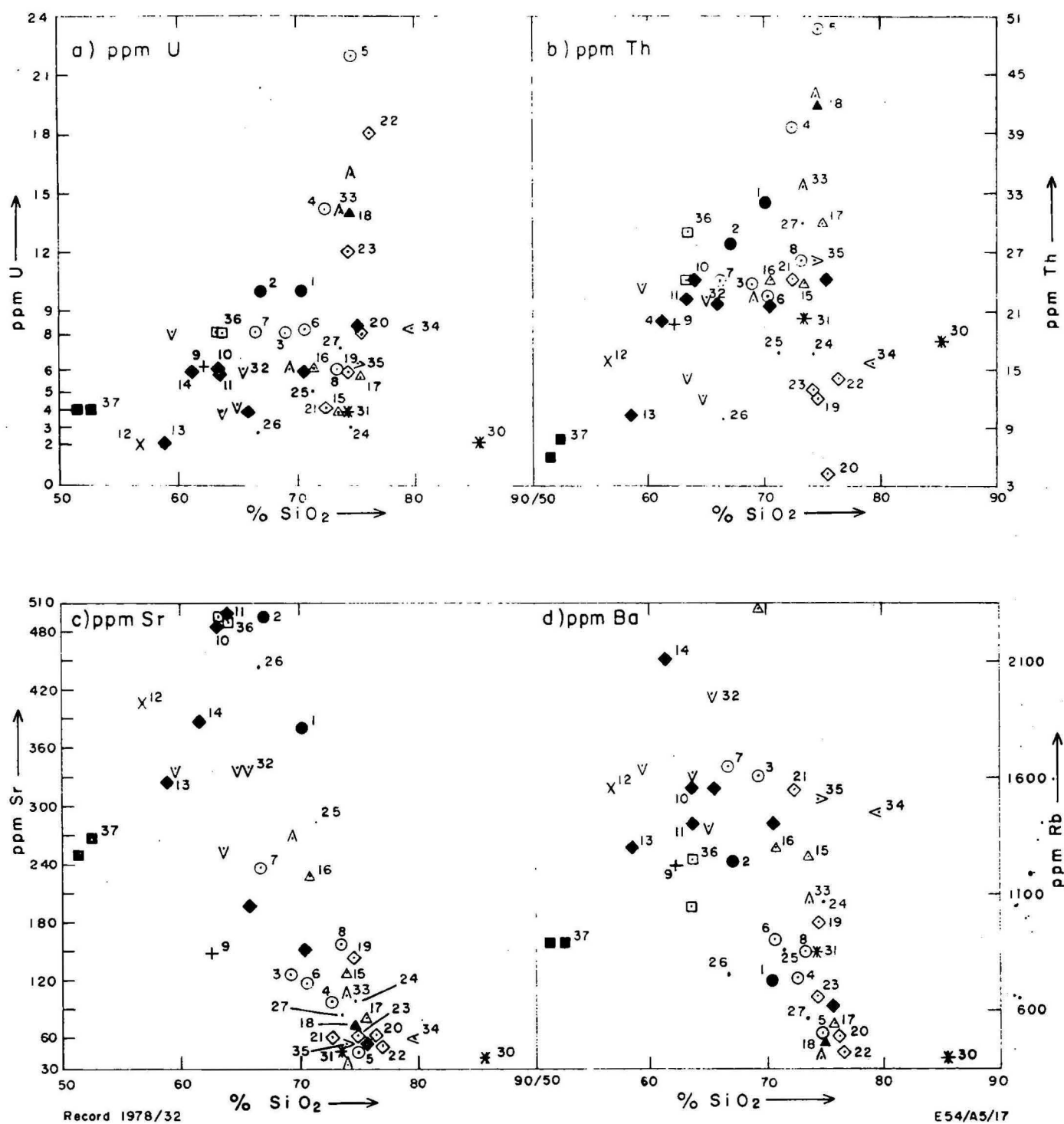Fig. 17 Minor element variation diagrams (sheet 1 of 3)

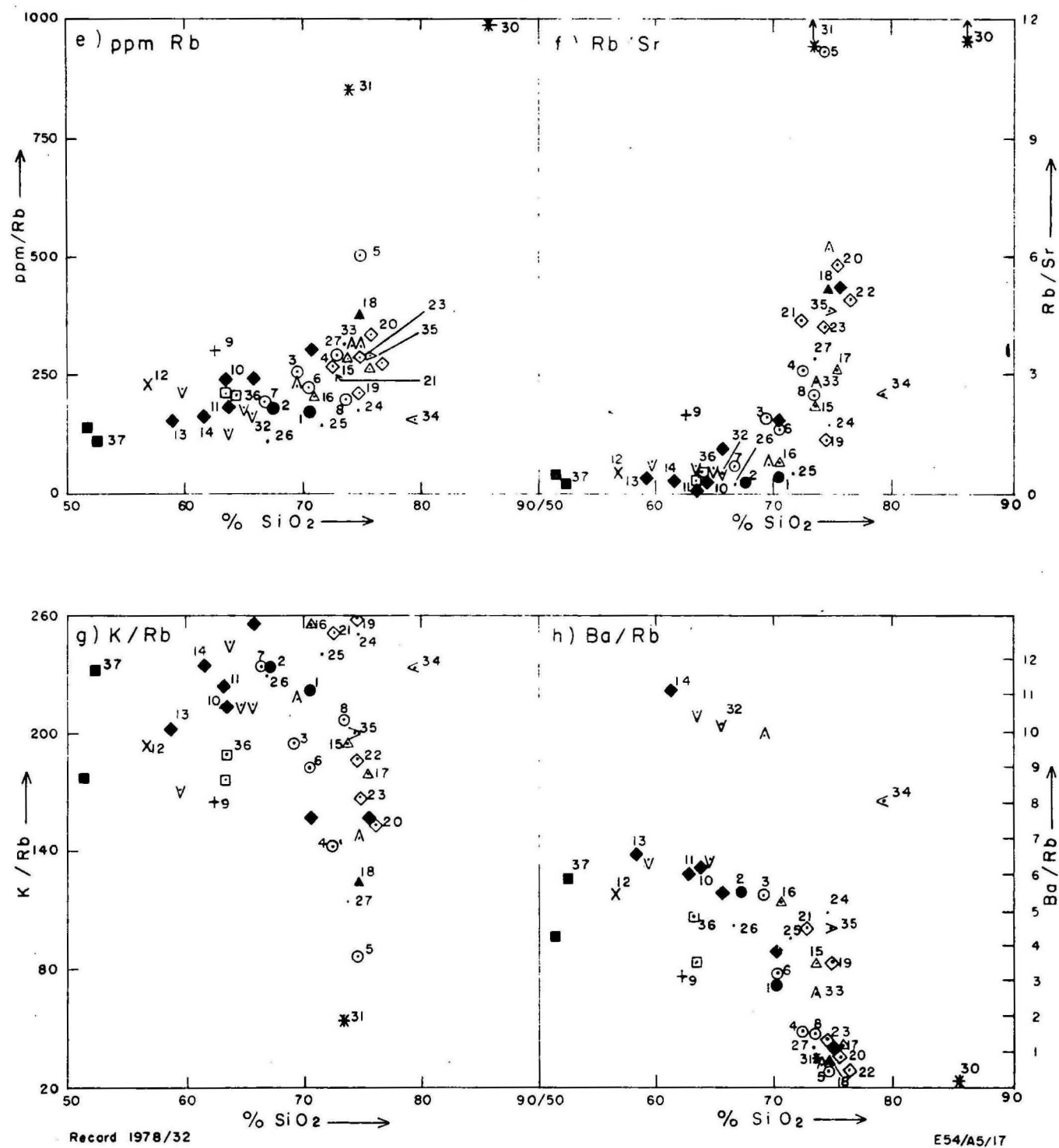Fig. 17 Minor element variation diagrams (sheet 2 of 3)

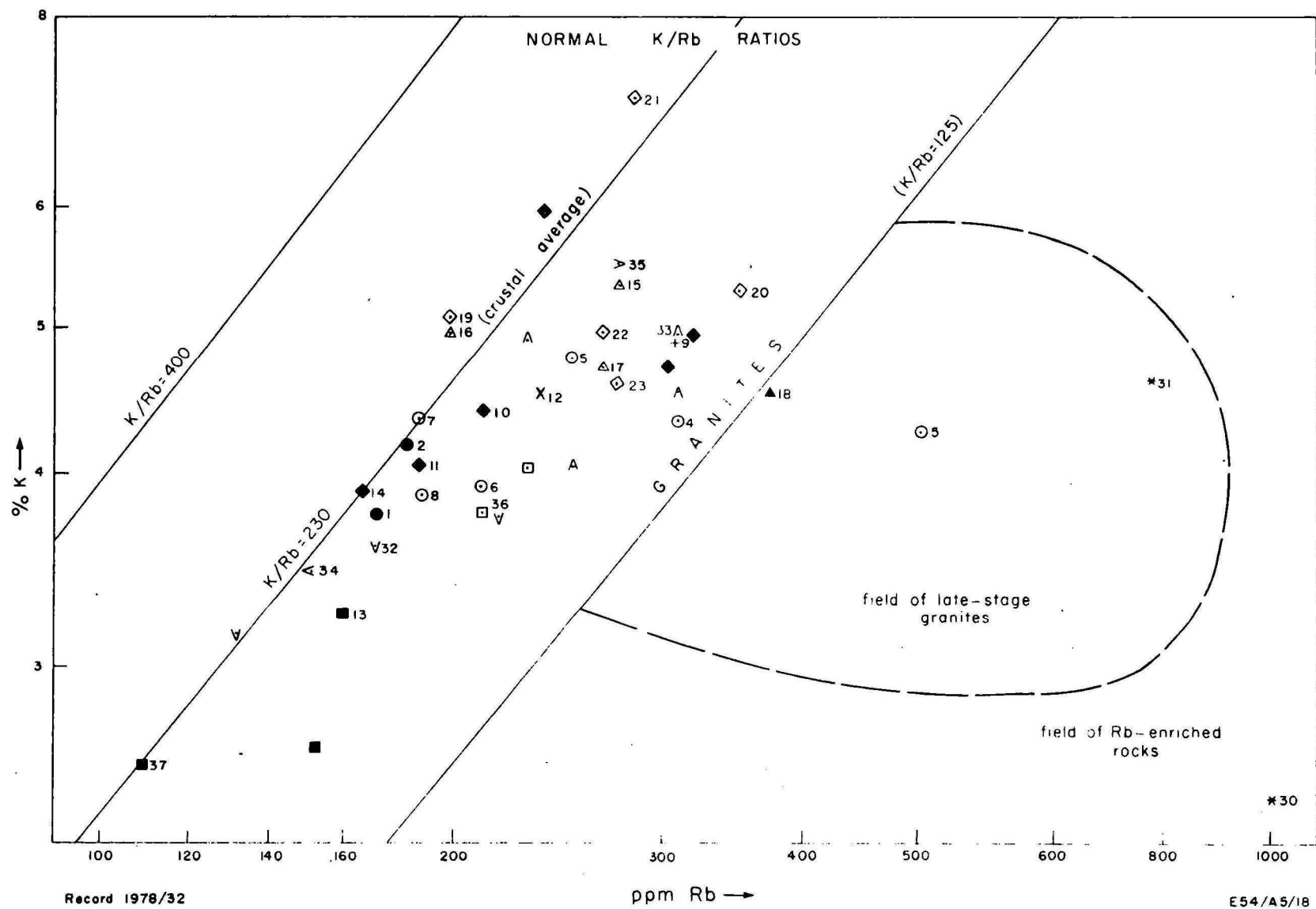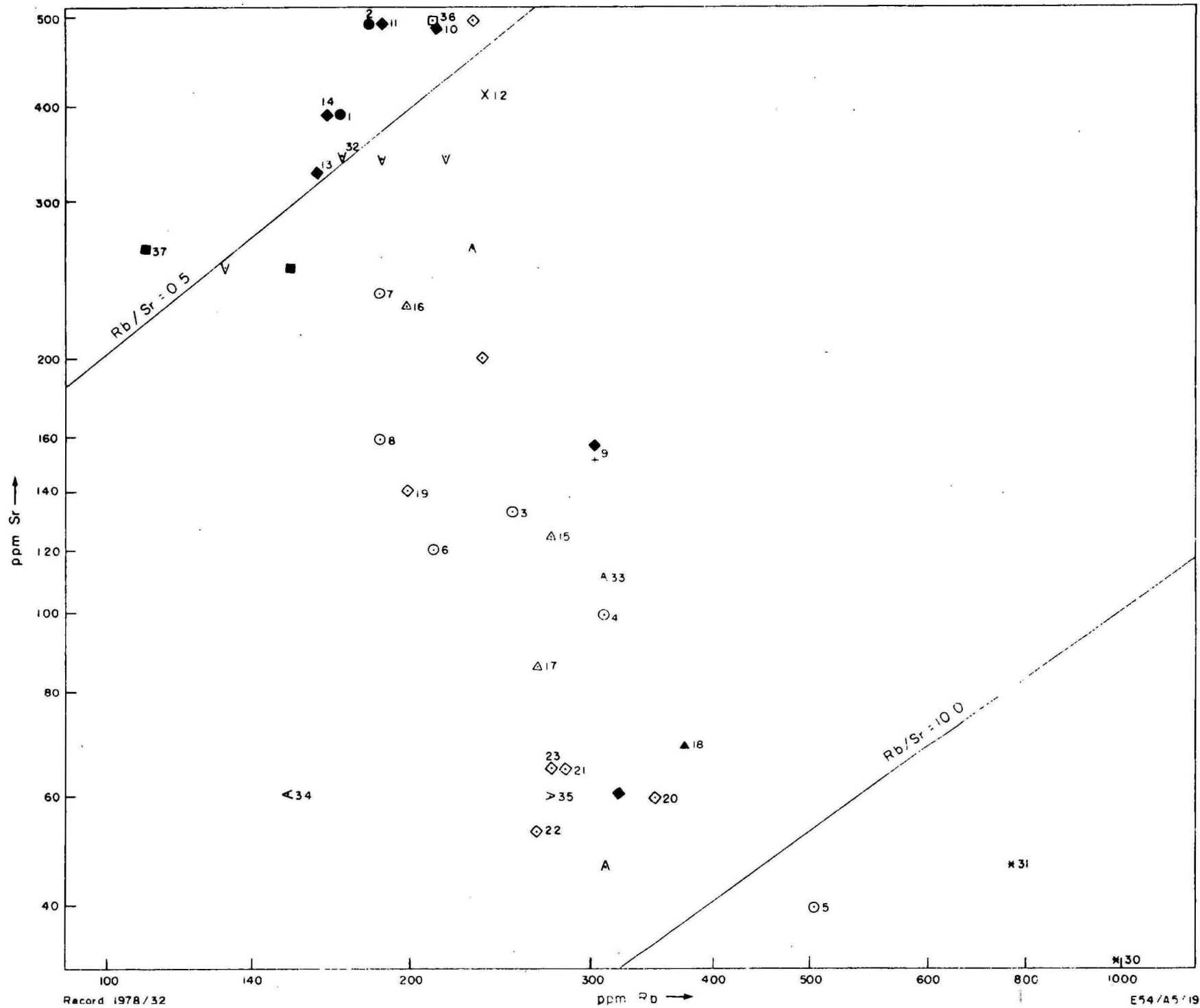Fig. 17 Minor element variation diagrams (sheet 3 of 3)

Fig. 18. K/Rb ratios in the Nicholson Granite Complex. Symbols as in Fig. 12; numbers as in Table 9

Fig. 19. Rb v Sr in the Nicholson Granite Complex. Symbols as in Fig. 12; numbers as in Table 9.

9.   Co, Ni, and Cu are all characteristically enriched in basic rocks, and depleted in acid rocks (Taylor, 1965). In the Nicholson Granite Complex, Co and Ni are concentrated normally, with a partitioning which parallels fractionation as described above (8.). Cu is normal except that it is enriched in Bgn_8 and some of the leucogranites - an anomalous enrichment, as these are residual rocks which are normally depleted in Cu (Taylor, 1968). Cu is higher in the volcanics than in the granites of otherwise similar composition.

10.   Sn shows normal concentration in the granites, and displays relative enrichment in all the greisens.

11.   The greisenised granites and greisen dykes are generally more successively enriched in incompatible elements than the unaltered granites, with the Crystal Hill greisen showing the most extreme enrichment.

DISCUSSION

Major-element chemical variation trends of granites younger than the Cliffdale Volcanics are indistinguishable from those of the older granites. Trace elements show wide variation for both groups. Thus the chemical data are inconclusive as to whether all the granites of the complex are comagmatic. The similarity in major-element and minor-element chemistry between the older ring dykes Bgn_{3-4} and the younger feldspar porphyry dykes suggests a genetic relation among the granite dykes of the complex. Regardless of the source of the major intrusions, it seems that the granodiorite dykes emplaced at various times throughout the history of the complex were all derived from the same magma source.

Initial Sr^{87}/Sr^{86} ratios vary widely both between and within the two groups of granites. The younger granites are characterised by generally higher initial ratios (from 0.710 to 0.718) than the older granites, for which the ratios range from 0.705 to 0.710. As initial Sr ratios of a granite are inherited from its source material, then the the enrichment of the younger intrusions in radiogenic Sr implies a history involving more than single-stage fractionation from the same parent material as the older granites. In interpreting the Sr isotope data, the following considerations (Faure & Powell, 1972) are taken into account.

97

It is well established that the continental crust has with time become enriched in Rb relative to the upper mantle. Granitic rocks derived from the crust are therefore characterised by higher initial Sr^{87}/Sr^{86} ratios than are basalts derived from the upper mantle. Crustally derived rocks show also a greater spread in initial Sr^{87}/Sr^{86} ratios than do rocks of direct mantle origin, because the former include rocks that have undergone reworking by means of metamorphism, partial melting, fractional crystallisation, mixing, etc. Such processes produce diverse ratios spanning the range between basaltic and high crustal ratios. Faure & Powell (1972) give as the general range of basaltic ratios 0.702 to 0.706. Rocks with ratios higher than 0.706 are thought to have been derived from a source with a significant sialic component.

A graphical representation of the evolution of Sr^{87}/Sr^{86} ratios in the upper mantle and in the continental crust is reproduced from Faure & Powell (1972) in Figure 20. The field of ratios of the source regions of basaltic rocks and a postulated continental crust development line are based on a compilation of whole-rock analyses from the literature, and on a crustal system model in which the crust is 2500 million years old and has an initial Sr^{87}/Sr^{86} ratio within the basaltic range. The positions of the two Nicholson Granite Complex isochrons and the Cliffdale Volcanics isochron are superimposed on the plot.

The plot is used to place constraints on the genesis of a particular granitic suite as follows. Granites with initial ratios within the basaltic field were derived by fractionation of a mantle-derived magma with negligible incorporation of Sr from older crustal rocks. Granites with initial Sr^{87}/Sr^{86} ratios on or above the continental crust line formed from magma whose generation involved the reconstitution of significant amounts of older, presumably sialic, material. Granites with ratios intermediate between continental and basaltic could have formed through one or more of several processes: mantle derivation and subsequent contamination with radiogenic strontium at crustal levels; derivation from source rocks of appropriate ratio - i.e., a multistage process; or bulk mixing of mantle and crustal material. The last process is commonly applied to granites thought to have been generated by partial melting of basic volcanic and sedimentary eugeosynclinal sequences.

98

Keeping within the general limits outlined above, and bearing in mind the point made by Faure & Powell that the position of the continental crust line in Figure 20 is subject to some assumptions and could be re-positioned, especially for the Precambrian, the following interpretation of the Nicholson Granite Complex and Cliffdale Volcanics data is suggested.

The older granite, Egn_1, and the Cliffdale Volcanics fall almost coincidentally within the range of intermediate to high initial Sr^{87}/Sr^{86} ratios. This coincidence, combined with the chemical similarity between the volcanics and the older granite, strongly suggests that the Cliffdale Volcanics and Egn_1 are cogenetic. From their positions on the plot in Figure 20 we may deduce that they were derived by anatexis of predominantly crustal material. In view of the field association and the probable chemical fractionation lineage between Egn_1 and the Murphy Metamorphics (see Figure 15), it seems reasonable to further suggest that basal sequences of the metamorphics formed the source rocks of Egn_1 and the volcanics, and that a mechanism involving mixing of basic and sialic material produced their initial isotopic Sr ratios.

The higher initial Sr^{87}/Sr^{86} ratios of the younger granites suggest a history of extensive reworking of predominantly sialic material. This suggestion is consistent with the chemical indications of extreme fractionation of Egn_5, Egn_6, Egn_7, and Egn_8. Postulation of a source material for the younger granites is made difficult by the evidence of their multistage histories, but the simplest theory, that of an origin comagmatic with the volcanics - as suggested by close spatial, temporal, and chemical relations - is not precluded by the isotopic data.

Different initial Sr^{87}/Sr^{86} ratios from within a suite of other-wise apparently cogenetic rocks may arise in several ways, most involving some form of source rock inhomogeneity, contamination through wall-rock reaction, or postcrystallisation activity (Faure & Powell, 1972).

It seems unlikely that postcrystallisation activity in the younger granites could have effected such a large increase in initial Sr^{87}/Sr^{86} ratio. Wall-rock interaction also seems unlikely, as the effect of contamination of the younger granites with strontium from country rock compositionally similar to the Murphy Metamorphics would have been towards a lowering of the Sr^{87}/Sr^{86} ratio. The highly fractionated chemistry and the Sr isotope ratios of the younger granites suggest instead that they are, at least partly, the products of remelted, previously fractionated material, namely remelted Egn_1. The
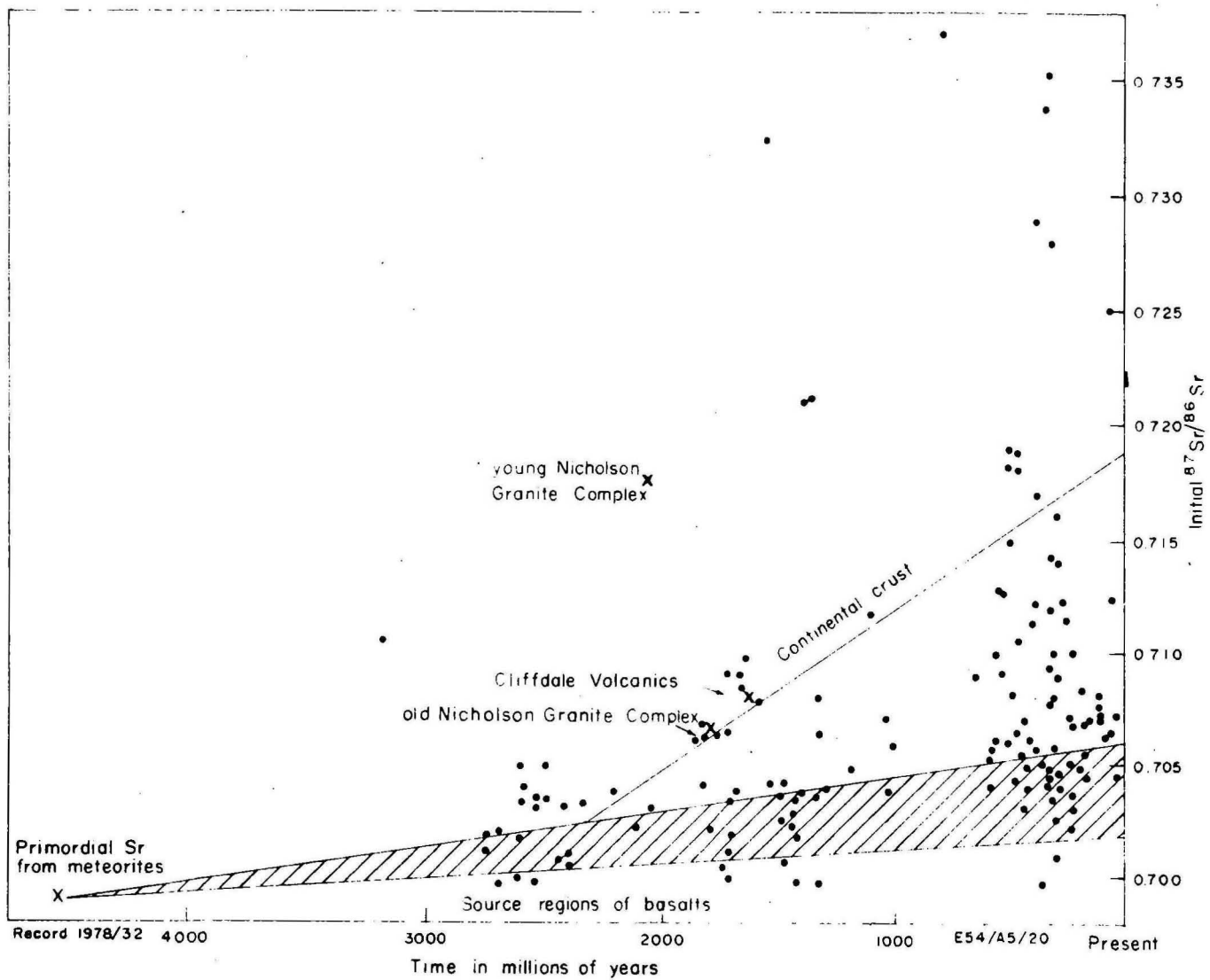
Fig 20. Initial $^{87}Sr/^{86}Sr$ ratios v age for analysed granitic rocks
(from Faure & Powell, 1972)
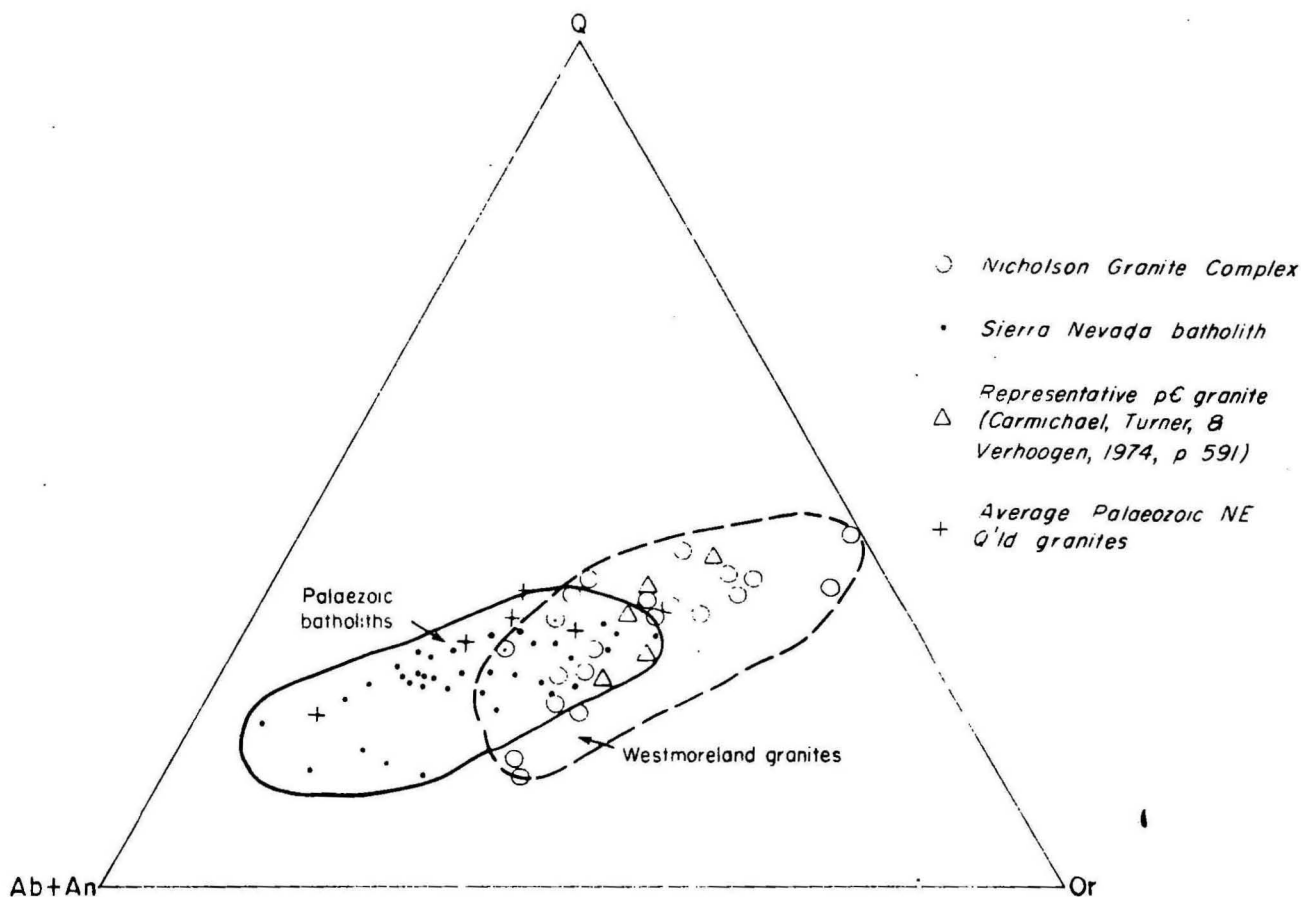
Fig 21 Comparison of Westmoreland granites with Palaeozoic batholiths
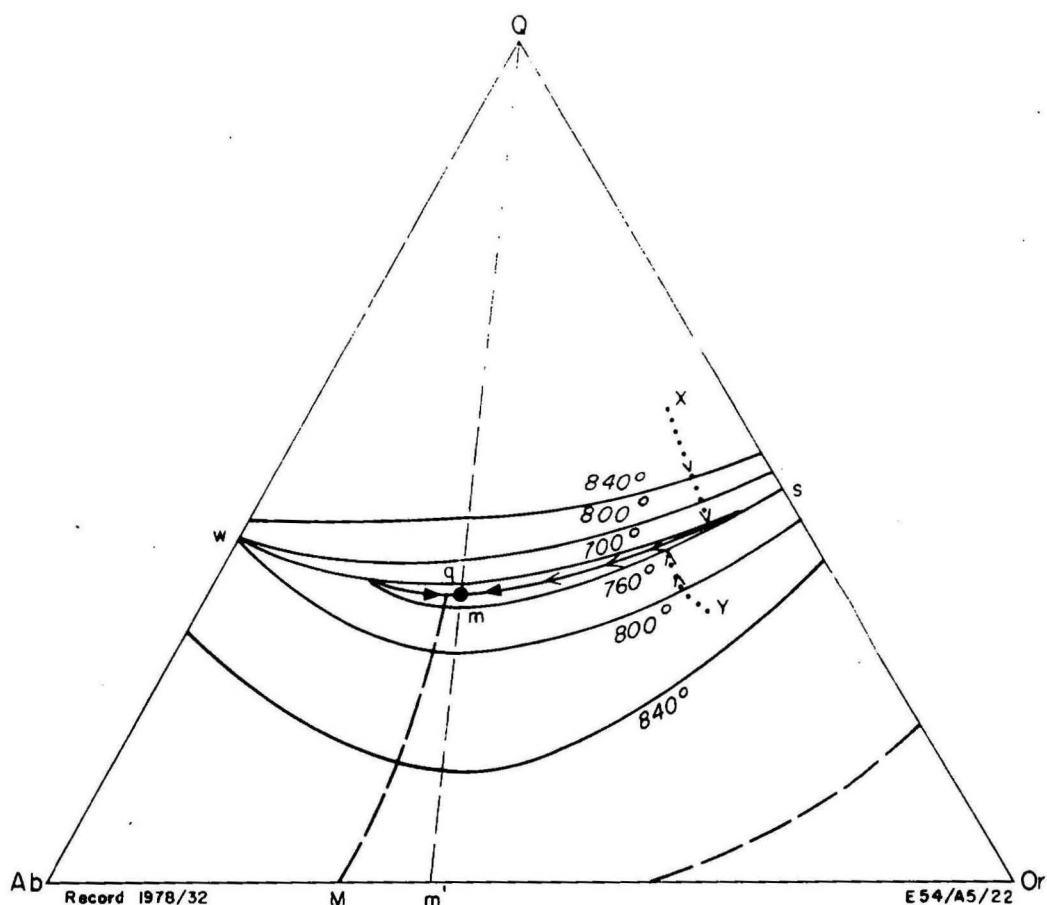
Fig 22 Crystallisation in the system Q-Ab-Or. The liquidus surface is shown
for 1000 bars confining pressure. The curve wqms separates quartz from
feldspar crystallisation fields; qM separates sodic from potassic feldspar
fields. m, m' are minima. Fractionation paths from starting compositions X, Y
are shown thus ....>.. Both paths proceed along the curve sm towards m.
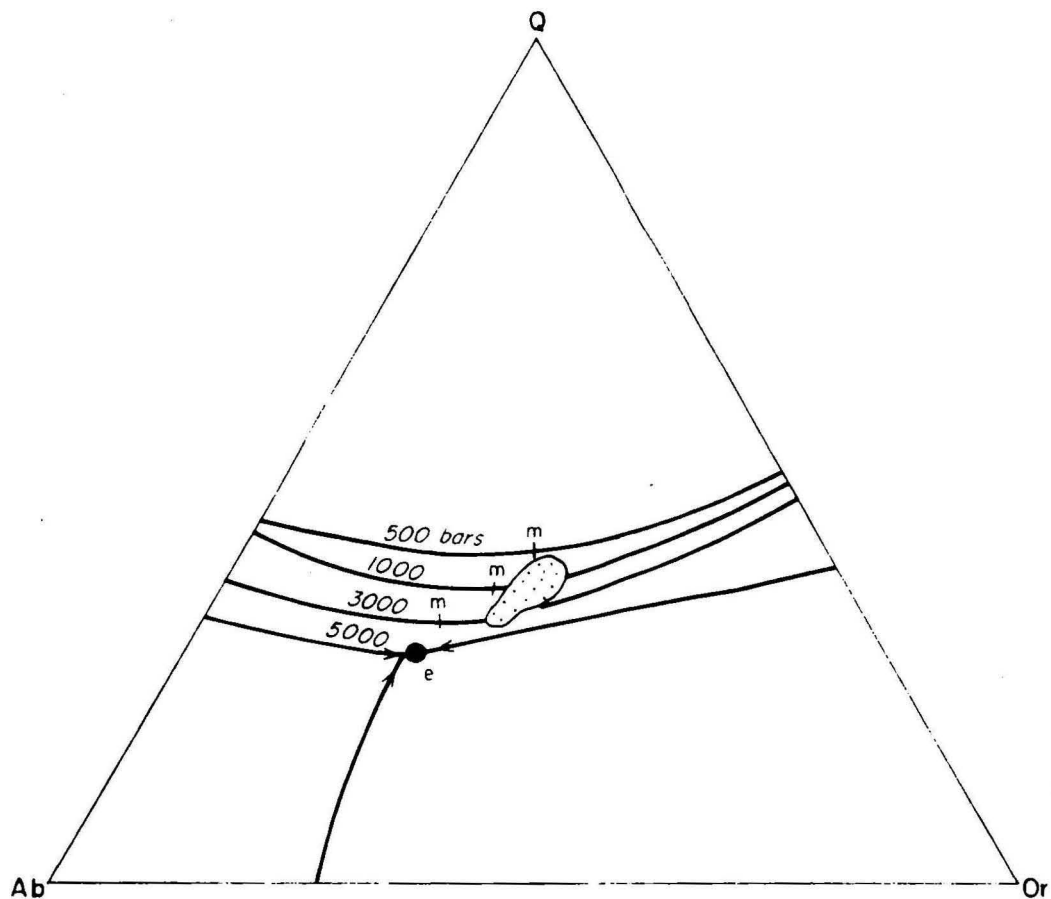
Fig 23a Variation in position of cotectic minimum with pH_2O. m indicates isobaric minima; e is ternary eutectic. Analysed rocks concentrate in the stippled area. (from Tuttle & Bowen, 1958)

E54/A5/23
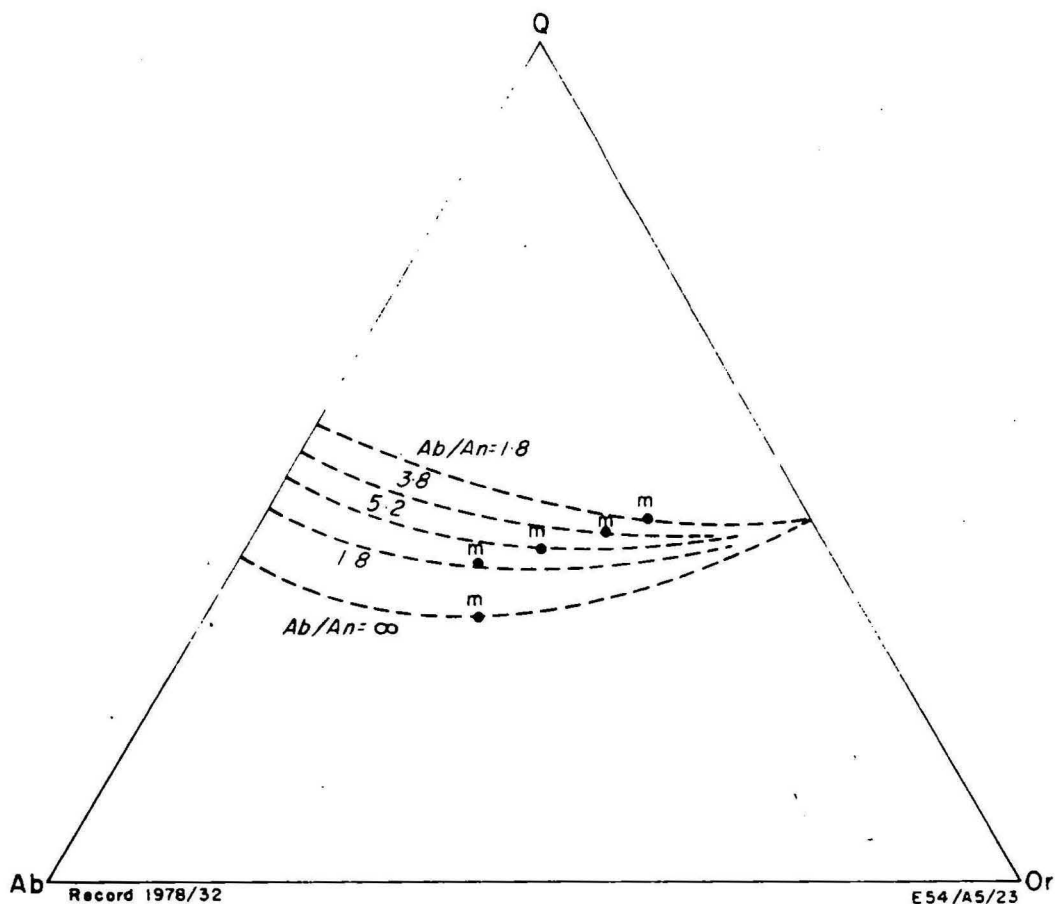
Fig 23b Variation in position of cotectic minimum for 2kb pH_2O with Ab/An. m indicates isobaric minima. (from von Platen, 1965)

102
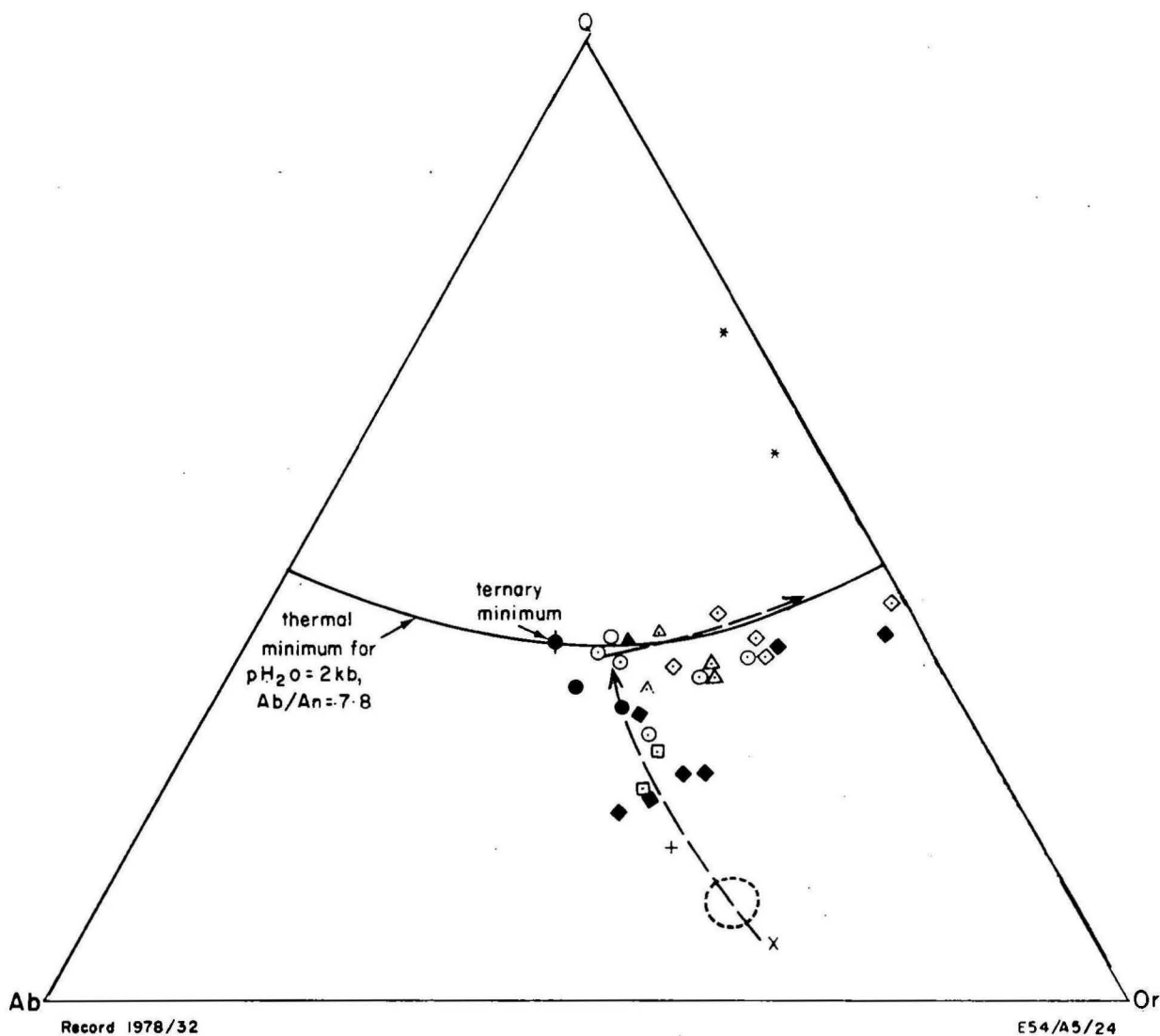
Fig 24 Relation between Nicholson Granite Complex and its inferred cotectic minimum curve. Initial fractionation towards the minimum followed by metasomatic addition of Q and Or and/or depletion of Ab can explain the two arrowed trends. Symbols as in Fig. 12

E54/A5/24

103

suggested process is one of reactive assimilation of Egn_1 by granitic magma at high crustal levels; the extent of the mixing is difficult to assess.

The Nicholson Granite Complex is compared with two Palaeozoic granite suites in Figure 21. The Westmoreland granites are distinguished from the Palaeozoic batholiths by their higher K_2O and $SiO2$ contents. This feature is characteristic of some groups of Precambrian granites; several other Precambrian plutons (Carmichael, Turner & Verhoogen, 1974, p. 591) are also plotted in Figure 20, and can be seen to fall within the high K_2O, high SiO_2 field defined by the Westmoreland granites. The higher potash and silica contents of Precambrian granites relative to younger granites is probably related to elevated geothermal gradients in the Precambrian, as anatexis at low pressures favours relatively potassic minimum-melt compositions (Burnham, 1967; Carmichael, Turner, & Verhoogen, 1974).

A cotectic curve (W-S, Fig. 22) divides the Q-Ab-Or system into two crystallisation fields, so that granites crystallising from the same source material can all be expected to lie on the one side of the cotectic curve. Rocks whose compositions fall on opposite sides of the curve cannot be related by simple fractionation (Tuttle & Bowen, 1958). The position of the cotectic curve is not fixed, however; it is influenced by the activity of other components, principally pH_2O and CaO. Figure 23 shows the expansion of the quartz field at the expense of the feldspar field under high water pressure or high Ab/An ratio. Thus the appropriate minimum curve should be found for each group of granites referred to this system. Ab/An can be calculated directly from the norms but pH_2O can only be estimated. The 2kb curve (Fig. 24) is used for the Nicholson Granite Complex - the position of the microgranite (Egn_7) near the curve is consistent with petrographic evidence of isochronous crystallisation, indicating that the microgranites crystallised on or close to the cotectic minimum.

The relatively SiO_2-rich, K_2O-rich nature of the granites of the Nicholson Granite Complex indicates that they were generated at relatively low pressures (Burnham, 1967). As Buddington (1959) gives 10-15 km as the depth range of generation of mesozonal granites, it is suggested that Egn_1 and Egn_2 were generated at a depth of about 10 km and emplaced at a slightly higher level. The younger granites were emplaced at shallower crustal levels than was Egn_1, as evidenced by the abundance of aplites, chill zones, etc., associated with Egn_5. In order to reach shallow crustal levels, however, the Egn_5 magma must have been strongly water-undersaturated, otherwise water

would have reached saturation level in the melt during ascent and exsolved as a separate phase (Burnham, 1967). The consequent sudden increase in the melting point of the remaining melt would have forced it to crystallise at depth. The absence of evidence of exsolution of an aqueous phase - e.g., pegmatites - indicates that Bgn_5 crystallised before becomming water-saturated. Therefore P_t must have been in excess of 2 kb - this corresponds to a depth of generation of 7 km. It is therefore suggested that the Nicholson Granite Complex was generated and emplaced between about 10 and 7 km depth, the younger granites having been formed within the zone of emplacement of the older granites.

Bgn_1, Bgn_2, and Bgn_5 plot in the potash feldspar field close to the minimum curve, but Bgn_8 and the greisenised granites have moved 'up' the thermal valley towards the Q-Or edge. From the preceding discussions, it follows that the younger granites are not differentiation products of the Bgn_2 magma.

However, the thermal barrier of this system applies only to magmatic crystallisation, and does not exist for metasomatic processes. This is because the barrier is a phenomenon related to the temperature-dependent processes of incongruent melting and fractional crystallisation. The compositional range of products of these processes is limited by the melting points of the various source minerals. The extent of addition or removal of material metasomatically, however, depends on the nature of solid-solution reactions that are possible under the prevailing physical conditions. Rock composition is altered proportionately with the mixing of fluid material with crystalline phases. In particular, leaching of alkalis resulting in depletion of the Ab and/or Or component can cause the composition of a rock to move from the feldspar field into the quartz field. Addition of Or accompanied or followed by removal of Ab can cause a minimum-melt composition to move along the thermal valley towards the Q-Or edge. The suggestion that these processes operated in the younger granites is supported by the petrographic evidence of extensive deuteric potash and silica alteration in the Nicholson Granite Complex. The data do not,however, preclude the existence of different source materials for the granites of the two age groups, although as these granites are highly fractionated the source composition cannot be estimated. Given this possibility, the generation of the younger granites probably involved a shift in magmatic activity to a part of the crust poorer in K_2O and H_2O and richer in SiO_2 In view of the extensive

greisenisation and occurrence of greisen dykes associated with the younger granites, however, the first hypothesis is favoured.

IX GEOLOGICAL HISTORY

Pelitic and quartzofeldspathic sediments were deposited in a geosyncline probably trending roughly east-west. Subsequent folding, accompanied by regional metamorphism, compressed the sediments along their geosynclinal axis. Towards the close of orogenic activity, about 1860 m.y., the basin was domed and intruded by magma generated by anatexis at the base of the pile, at a depth of about 10 km.

The adamellitic, volatile-rich magma (Egn_1) intruded along tensional zones which opened in response to the arching of the rocks in the geosyncline. The east-northeast fault system thus initiated remained active throughout most of the history of the complex, especially along its northern side.

As the Egn_1 magma was derived by anatexis of geosynclinal sediments, it would have been relatively hydrous (Harris, Kennedy, & Scarfe, 1970), and would not have risen far in the crust before starting to crystallise. Fractional crystallisation of the Egn_1 magma left a residual melt, which was subsequently extruded as a series of ignimbrites and lavas - the Cliffdale Volcanics. The release of volatiles accompanying extrusion resulted in decreased pH_2O in the magma chamber, enabling the remaining melt to rise further in the crust before solidifying as Egn_2. In response to the volatile release accompanying crystallisation, there was a shift to subvolcanic activity, with the intrusion of the quartz-feldspar porphyry dykes and the fractionated high-level granites Egn_5, Egn_6, and Egn_7.

Evidence for the higher temperatures of Egn_5, Egn_6, and Egn_7 relative to Egn_1 and Egn_2 has already been described (red feldspars in the former as opposed to white feldspars in the latter). The increased heat flow inferred from the higher temperatures of the younger granites was probably responsible for activation of the residue from the granite source region and its intrusion as granodiorite ring dykes (Egn_{3-4}) along the contacts of the roughly circular, or fault-bound, Egn_5 and Egn_6 plutons, with the older granites.

Volcanic activity was in its closing stages by the time muscovite granite, probably derived from the metasediments, was emplaced as Egn_8 at about 1750 m.y. Late-stage fluids from the source region had been circulating since intrusion of Egn_2, effecting the growth of K-feldspar phenocrysts

and deposition of secondary silica soon after crystallisation of the various granites. As the fluids moved to higher levels, alteration became localised in zones of structural weakness, and was accompanied by emplacement of greisen dykes. Further uplift and tilting towards the northeast was accompanied by block faulting along the northern side of the MTR. A 50 to 100 m.y. period of erosion separated magmatic activity on the MTR from the commencement of deposition of sediments in the basins on its northern and southern margins.

X MINERALISATION

Minor Cu, Sn, and W mineralisation has been found along faults and alteration zones within the granites, mainly near contacts between granite and Westmoreland Conglomerate or Cliffdale Volcanics.

1. The mass of Egn_2, Egn_6 and Egn_7 at HC975420 includes an area of altered Egn_2 (Egn_{2a}) cut by massive limonite-stained milky quartz veins which contain thin irregular veins and fracture coatings of malachite and azurite. The Motor Car (HC965412) and Jennifer Ann (HC967434) prospects are of this type. At the latter locality malachite and azurite form films and fracture coatings on a jointed vein 2 m wide striking 075° for over 30 m; limonite and hematite form a patchy gossan and surface staining. The Jennifer Ann prospect lies 200 m south of the contact of granite with unit 2 of the Cliffdale Volcanics (ignimbrite), and about the same distance north of a small mass of Egn_7, which has been costeaned along a quartz vein without discovery of mineralisation.

Mineralised quartz veins collinear with the Jennifer Ann veins occur in soil plains 500 m east of the hills of Egn_{2a} at HC990425. Weathered coarse-grained, partly greisenised granite is cut by north-trending veins displaced en echelon to the northeast, bearing fine-grained Sn mineralisation. The veins are about 1 m wide, and contain scattered boxwork structures containing occasional druses lined with books of mica or quartz crystals.

2. Cu-stained quartz veins occur in Cliffdale Volcanics near contacts with granite at several localities. These were described by Roberts and others (1963), and include the Norris orebody, Chapmans prospect, two localities near the Calvert Fault, Tracey's Table, and the hut at S986377. At all these localities traces of malachite occur in quartz-impregnated Cliffdale Volcanics where

these are adjacent to Pgn_5. The Norris deposit is a metre-wide lode of massive chalcopyrite brecciated and altered along fractures, in an east-striking quartz vein branching from the Calvert Fault.

3.   Chalcopyrite occurs in quartz-biotite plugs associated with Pgn_8 around the Fish River.

4.   ·   Cassiterite is associated with quartz veins and greisen at Tracey's Table and Crystal Hill. At Crystal Hill, cassiterite occurs at the base of the hill in a micaceous pegmatoidal vein, along with topaz, fluorite, and wolframite.

5.   At Pandanus Creek mine, uranium occurs in shear zones in altered volcanics adjacent to their contacts with Westmoreland Conglomerate and a small pod of granite.

6.   Wolframite is fairly widespread in quartz veins associated with granite/volcanic contacts; it has been mined 2 km south of Chapmans prospect.

7.   Subsurface zoned amethyst occurs at S880290. The host quartz vein is about 10 m wide, and the amethyst occurs in a 1 m wide zone increasing in intensity and continuity of colour with depth. The amethyst has not been mined.

The interaction of chemical and structural controls has produced a pattern of mineralisation related to four factors: rock chemistry; the north-south trending structural system produced by the intersection of east-northeast and northwest trends; contacts; and alteration and late-crystallising rocks.

Cu   Although most of the Cu mineralisation occurs in the volcanics, and Cu is usually concentrated in a basic environment, (Taylor, 1965), abnormally high Cu values were found in one greisenised granite (73760864A) and a muscovite microgranite (73760868); also chalcopyrite occurs in two quartz-biotite dykes. This suggests that the Cu mineralisation in quartz veins cutting altered granites is related to migration of Cu, along with late-stage greisening fluids, into low-pressure zones - i.e., tensional structures formed by the two intersecting trends.

108

Sn   The concentration of Sn in residual melts is reflected by high Sn values for a greisenised granite (73760864A), a greisen dyke (73760809), and the Crystal Hill greisen (73760805). Hence Sn is also introduced by late-stage fluids in low-pressure zones.

U   U values are high in the granites and the greisen dykes relative to average granites (Taylor, 1965, also Table 9, Nos. 24, 25, 26) and are even higher in the volcanics of similar SiO_2 content. This distribution pattern suggests that U migrated from the granite into the volcanics along granite/volcanic contacts.

W   W behaves similarly to Sn, and is also, but to a lesser extent, enriched in greisen dykes and greisenised granite. Its occurrence is apparently more closely related to granite/volcanic contacts than to low-pressure zones - one sample of slightly altered Bgn_{3-4} has a high W content.

In summary, mineralisation appears to be restricted to granite/volcanic contacts or to late-crystallising rocks emplaced in north-south tensional zones. If, as seems likely from the high-level nature of the younger granites, there had been widespread mineralisation throughout the original upper levels of the complex, it has been removed by the extensive erosion that has taken place before and since the deposition of the Westmoreland Conglomerate and equivalents.

XI REFERENCES

AGI, 1972 - GLOSSARY OF GEOLOGY. American Geological Institute, Washington, DC.

BUDDINGTON, A.F., 1959 - Granite emplacement with special reference to North America. Bulletin of the Geological Society of America, 70, 671-747.

BURNHAM, C.W., 1967 - Hydrothermal fluids at the magmatic stage; in BARNES, H.L. (Editor) - GEOCHEMISTRY OF HYDROTHERMAL ORE DEPOSITS. Holt, New York, 34-76.

BURRI, C., 1964 - PETROCHEMICAL CALCULATIONS BASED ON EQUIVALENTS (METHODS OF PAUL NIGGLI). Program for Scientific Translations, Jerusalem.

CARMICHAEL, I.S.E., 1963 - The crystallization of feldspar in volcanic acid liquids. Quarterly Journal of the Geological Society of London, 119, 95-131.

CARMICHAEL, I.S.E., TURNER, F.J., & VERHOOGEN, J., 1974 - IGNEOUS PETROLOGY. McGraw-Hill, New York.

CARTER, E.K., BROOKS, J.H., & WALKER, K.R., 1961 - The Precambrian mineral belt of north-western Queensland. Bureau of Mineral Resources, Australia, Bulletin 51.

FAURE, G., & POWELL, J.L., 1972 - STRONTIUM ISOTOPE GEOLOGY. Springer-Verlag, Berlin.

FIRMAN, J.B., 1959 - Notes on the Calvert Hills 4-mile geological sheet ES3/8. Bureau of Mineral Resources, Australia, Record 1959/50 (unpublished).

GREEN, T.H., & RINGWOOD, A.E., 1968 - Genesis of the calc-alkaline igneous rock suite. Contributions to Mineralogy and Petrology, 18, 105-62.

GREGORY, A.C., 1861 - North Australian Expedition. South Australian Parliamentary Paper 3(170).

HARME, M., 1965 - On the potassium migmatites of southern Finland. Bulletin Commission Geologique de Finlande, 219.

HARRIS, P.G., KENNEDY, W.Q., & SCARFE, C.M., 1970 - Volcanism vs. plutonism - the effect of chemical composition; in NEWELL, G., & RAST, N., (Editors) - MECHANISM OF IGNEOUS INTRUSION. Gallery Press, Liverpool, 187-200.

HATCH, F.H., WELLS, A.K., & WELLS, M.K., 1961 - PETROLOGY OF THE IGNEOUS ROCKS. 12th edition. Thomas Murby & Co., London.

IRVINE, T.N., & BARAGAR, W.R.A., 1971 - A guide to the chemical classification of the common volcanic rocks. Canadian Journal of Earth Sciences, 8, 523-48.

JENSEN, H.I., 1941 - Report on portion of north-western Queensland adjacent to the Northern Territory border. Aerial Survey of Northern Australia, Queensland, Report 47 (unpublished).

JOPLIN G.A., 1971 - A PETROGRAPHY OF AUSTRALIAN IGNEOUS ROCKS. Angus & Robertson, Sydney.

McDOUGALL, I., DUNN, P.R., COMPSTON, W., WEBB, A.W., RICHARDS, J.R., BOFINGER, V.M., 1965 - Isotopic age determinations on Precambrian rocks of the Carpentaria region, Northern Territory, Australia. Journal of the Geological Society of Australia 12(1), 67-90.

MARMO, V., 1971 - GRANITE PETROLOGY AND THE GRANITE PROBLEM. Elsevier, Amsterdam.

MEHNERT, K.R., 1968 - MIGMATITES AND THE ORIGIN OF GRANITIC ROCKS. Elsevier, Amsterdam.

MITCHELL, J.E., 1976 - Precambrian Geology of the Westmoreland Region, Northern Australia, Part II - Cliffdale Volcanics. Bureau of Mineral Resources, Australia, Record 1976/34 (unpublished).

NASCA, S.U., 1972 - Project No. 923: Benmara, Northern Territory. Final report. Esso Australia Ltd Report (unpublished).

ORVILLE, P.M., 1962 - Alkali metasomatism and feldspars. Norsk Geologisk Tidsskrift, 42, 283-316.

PLUMB, K.A., & DERRICK, G.M., 1975 - Geology of the Proterozoic rocks of the Kimberley to Mt. Isa region; in KNIGHT, C.L. (Editor) - ECONOMIC GEOLOGY OF AUSTRALIA AND PAPUA NEW GUINEA. VOLUME 1: METALS. Australasian Institute of Mining and Metallurgy Monograph Series 5, 217-252.

PRICE, N.J., 1966 - FAULT AND JOINT DEVELOPMENT IN BRITTLE AND SEMI-BRITTLE ROCKS. Pergamon Press, Sydney.

ROBERTS, H.G., 1963 - Geology of the Carpentaria Proterozoic Province, Northern Territory, Part 1 - Roper River to the Queensland Border. (unpublished).

ROBERTS, H.G., RHODES, J.M., & YATES, K.R., 1963 - Calvert Hills, Queensland-1:250 000 Geological Series. Bureau of Mineral Resources, Australia, Explanatory Notes SE/53-8.

SEN, K.K., 1960 - Some aspects of the distribution of Ba, Sr, Fe and Ti in plagioclase. Journal of Geology, 68, 638-65.

SHERATON, J.W., & LABONNE, B., 1978 - Petrology and geochemistry of acid igneous rocks of northeast Queensland. Bureau of Mineral Resources, Australia, Bulletin 169.

SMITH, J.V., 1974 - FELDSPAR MINERALS. VOLUME 2. Springer-Verlag, Berlin.

SPRY, A., 1969 - METAMORPHIC TEXTURES. Pergamon Press, Sydney.

STRECKEISEN, A., 1967 - Classification & nomenclature of igneous rocks. Neus Jahrbuch fur Mineralogie Abhandlungen, 107, 144-240.

STRECKEISEN, A., 1973 - Plutonic rocks. Classification and nomenclature recommended by the I.U.G.S. Sub-commission on the systematics of igneous rocks. Geotimes, 18, 26-30.

SWEET, I.P., & SLATER, P.J., 1975 - Precambrian Geology of the Westmoreland Region, Northern Australia, Part I - Regional Setting and Cover Rocks. Bureau of Mineral Resources, Australia, Record 1975/88 (unpublished).

TAYLOR, S.R., 1965 - The application of trace element data to problems in petrology. Physics and Chemistry of the Earth, 6, 133-213.

TAYLOR, S.R.,1968 - Geochemistry of andesites; in AHRENS,RL.H., (Editor) - ORIGIN AND DISTRIBUTION OF THE ELEMENTS. International Series of Monographs on the Earth Sciences, 30, 559-83.

TUREKIAN, K.K., & WEDEPOHL, K.H., 1961 - Distribution of the elements in some major units of the earth's crust. Bulletin of the Geological Society of America, 72, 175-92.

TURNER, F.J., & VERHOOGEN, J., 1960 - IGNEOUS & METAMORPHIC PETROLOGY. 2nd ed. McGraw-Hill, New York.

TUTTLE, O.F., & BOWEN, N.L., 1958 - Origin of granite in the light of experimental studies in the system $NaAlSi_3O_8-KAlSi_3O_8-SiO_2-H_2O$. Geological Society of America Memoir 74.

VON PLATTEN, H., 1965 - Experimental anatexis and genesis of migmatites; in PITCHER, W.S., & FLINN, G.W. (Editors) - CONTROLS OF METAMORPHISM, Oliver and Boyd, London, 203-18.

113.

WEBB, A., 1973 - Carpentaria age determination project. AMDEL Report
    AN2/1/0 - 1814/73, Part Report 4 (unpublished).

WEBB, A., 1975 - Geochronology of 22 rock samples from Nicholson Granite
    Complex. AMDEL Report AN2/1/0-2850/75 (unpublished).

114

PLATE I

PLATE I GEOLOGY OF PART OF THE MURPHY TECTONIC RIDGE

Legend:

Symbol	Description
Czs	Quartzitic sandy and silty soils; colluvium
Pt	Tawallah Group (Westmoreland Conglomerate and Seigal Volcanics)
Pgn_8	White medium-coarse muscovite-biotite granite
	Greisen
Pgn_7	Red microgranite
Pgn_6	Pink coarse leucocratic granite
Pgn_5	Red-even grained medium-coarse biotite granite
Pgn_{3-4}	Hornblende granodiorite; porphyritic diorite
Pgn_2	Coarse biotite adamellite with xenoliths
Pgn_1	Coarse porphyritic hornblende-biotite adamellite with xenoliths
Pcc	Cliffdale Volcanics
Plm	Murphy Metamorphics

Grid reference shown at 5000 m intervals; used in text to indicate localities. e.g. Fish River Gorge is approx S 890325 (S=Seigal).

— Fault
— Lineament
↔ Dyke
✕ Mine

McARTHUR BASIN (TAWALLAH GROUP)

SOUTH NICHOLSON BASIN (SOUTH NICHOLSON GROUP)

LAWN HILL PLATFORM (FICKLING GROUP)

N.T.

INDEX TO STANDARD 1:100 000 SHEET AREA

SEIGAL   HEDLEYS CREEK

Crystal Hill
Tracey's Table
Pandanus Creek
Norris
Jennifer Ann
One Hen
Motor Car
Amethyst
Fish River Gorge
Dry Creek
Rocky Creek
Little Dinner Creek
Fish River
Tin Hole Creek
Pandanus Creek
North Road
South Road
Gorge Creek
CALVERT FAULT

0   5 km

Record 1978/32

E53/A8/15